THESIS
3
2002

LIBRARY
Michigan State
University

PLACE IN RETURN BOX to remove this checkout from your record.
TO AVOID FINES return on or before date due.
MAY BE RECALLED with earlier due date if requested.

DATE DUE	DATE DUE	DATE DUE

6/01 c:/CIRC/DateDue.p65-p.15

FUNCTI(

FUNCTIONAL ANALYSIS OF ATVTI1, A FAMILY OF SNARE PROTEINS IN *ARABIDOPSIS*

By

Haiyan Zheng

A DISSERTATION

Submitted to
Michigan State University
in partial fulfillment of the requirements
for the degree of

DOCTOR OF PHILOSOPHY

Genetics Program

2001

FUNCTIONAL A

Most vac

The ones carry

secretory prote

coated transp

vacuolar com

targeting of th

To und

the PVC in m

typical SNAR

Arabidopsis P

and AtVAM3

group SNARE

for accepting

I have

Arabidopsis g

an NTPP car

with SYP2 o

ABSTRACT

FUNCTIONAL ANALYSIS OF ATVTI1, A FAMILY OF SNARE PROTEINS IN *ARABIDOPSIS*

By

Haiyan Zheng

Most vacuolar proteins carry short peptidal sequence as targeting signals. The ones carrying an N-terminal pro-peptide (NTPP) are sorted away from other secretory proteins by NTPP receptors at the TGN and packaged into clathrin-coated transport vesicles. These vesicles are further transported to the pre-vacuolar compartment (PVC) before finally reach the vacuole. The correct targeting of these vesicles to the PVC most likely involves SNARE proteins.

To understand the vacuolar protein trafficking step between the TGN and the PVC in more detail, I have isolated several genes from *Arabidopsis* encoding typical SNARE proteins. First, I identified a SNARE protein called AtPLP, *Arabidopsis* PEP12 Like Protein. Due to its high similarity with AtPEP12 (SYP21) and AtVAM3 (SYP22), it is grouped into SYP2 and renamed as SYP23. SYP2 group SNAREs are located on the PVC membrane. They might be the t-SNAREs for accepting incoming vesicles.

I have also isolated *AtVTI11* and *AtVTI12,* two related SNARE genes from *Arabidopsis* genome. AtVTI11 is localized on the domain of TGN where AtELP, an NTPP cargo receptor and sporamin, an NTPP cargo reside. It also colocalizes with SYP2 on the PVC. AtVTI11 is found in SNARE complexes with SYP2 and

SYP5 group SNA

in directing NTPF

Although

a.a. level), they

and AtVTI12 a

gradient experi

and SYP6 ins

involved in d

between AtV

AtVTI12, altho

observable p

a complex w

Take

SNARE pro

between th

overlapping

SYP5 group SNAREs. All these data suggest that AtVTI11 is a SNARE involved in directing NTPP cargo containing vesicles towards the PVC.

Although AtVTI11 and 12 share high sequence similarity (65% identical at a.a. level), they complement different yeast *vti1* mutants. In *Arabidopsis*, AtVTI11 and AtVTI12 are localized on different membranes based on an Accudenz gradient experiment. The majority of AtVTI12 form SNARE complexes with SYP4 and SYP6 instead of with SYP2 and SYP5. It is likely that AtVTI11 and 12 are involved in different vesicle targeting steps *in vivo*. However, the duty division between AtVTI11 and 12 might not be exclusive. In a T-DNA insertion line of *Atvti12*, although the homozygous mutant plant lacks AtVTI12 protein, it has no observable phenotype because AtVTI11 takes the position of AtVTI12 and forms a complex with SYP4 and SYP6.

Taken together, I have identified and characterized AtVTI1 family of SNARE proteins. AtVTI11 is shown to be involved in NTPP cargo transport between the TGN and the PVC. The closely related AtVTI12 might have overlapping as well as different functions.

I would ha
Ph.D. study the r
feel so much alo
dark. In her lab.
would also like t
Drs. Ken Keegs
to thank Drs. T
collaboration o
Drs. Scott Pe
patience in he
grateful towar
the name of c

My tha
like to thank
and my art re
out the immu
progress so
my research
liked the thin
Thanks to th
particular, Ka
his help on g

ACKNOWLEDGEMENTS

I would have to thank Dr. Natasha Raikhel for making these five years of Ph.D. study the most significant period of my life. She encouraged me when I feel so much alone. She pointed out the sun to me when I felt completely in the dark. In her lab, I learned how to be a good scientist and to be a better person. I would also like to acknowledge the guidance offered by my committee members: Drs. Ken Keegstra, John Wang, Greg Howe, and Michael Garavito. I would like to thank Drs. Tom Stevens and Gabrille Fischer von Mollard for their generous collaboration on yeast complementation of AtVTI1 proteins. Many thanks go to Drs. Scott Peck for introducing me to the new world of proteomics and his patience in helping me with 2-D gel and mass spectrometry. I am especially grateful towards Scott and Antje for their hospitality when I intruded their home in the name of collaboration.

My thanks go to all the past and present numbers of Raikhel lab. I would like to thank Dr. Enrique Rojo for his unselfish help on my science, my English and my art related problems. Dr. Valya Kovaleva for her collaboration in carrying out the immunocytochemistry studies. Without her, my research can not possibly progress so fast. Drs. Diane Bassham and Tony Sanderfoot for their advice on my research and my writing. Dr. Jan Zouhar, for being the only one who always liked the things I wrote. Sharif Ahmed, for being a valuable information source. Thanks to the PRL staff for their help that made my study so much easier. In particular, Kurt and Marlene for their expert on photographic service, and Jim for his help on growth chamber problems.

I woe ever

Tao my most wo

I am mad. Than

them.

Maxi the

angel sent by

assignments as

she thinks it is

writing process

a break.

Finally

will and to ap

I woe everything to my parents who love me without condition. Thanks to Tao, my most wonderful sister, who has the power to make me laugh even when I am mad. Thanks to all my true friends, I feel privileged to have so many of them.

Maxi, the cat who has made an apartment a sweet home, is no doubt an angel sent by God at a difficult time of my life. She has never forgotten her assignments as to stop me whenever I want a snack and to wake me up when she thinks it is time. Besides occasional editing, she slept through the whole writing process on my laps so that I was forced to remain sit even when I wanted a break.

Finally, I believe in God's miracles. My life is a process to understand his will and to appreciate his boundless wisdom.

LIST OF TABLES

LIST OF FIGURES

LIST OF ABBREV

CHAPTER I

Introduction: an O

I. The End

II. SNARE

III. Vacuol

IV. Vacuol

IV-a

IV-b
Sys

V. Conclus

VI. Thesis

Reference

CHAPTER II

The Syntaxin Fa
Shows Polymorp

Abstract

TABLE OF CONTENTS

LIST OF TABLES ix

LIST OF FIGURES x

LIST OF ABBREVIATIONS xii

CHAPTER I

Introduction: an Overview of the Plant Vacuolar Protein Transport Pathways 1

I. The Endomembrane System in Eucaryotic Cells 2

II. SNARE Hypothesis 4

III. Vacuolar Protein Trafficking in Mammalian and Yeast Cells 6

IV. Vacuolar Protein Transport in Plants 9

IV-a. Traffic Routes for Plant Vacuoles 9

IV-b. Components of the Plant Vacuolar Protein Delivery System 13

V. Conclusion 21

VI. Thesis Scheme 24

References 26

CHAPTER II

The Syntaxin Family of Proteins in *Arabidopsis*: a New Syntaxin Homologue Shows Polymorphism Between Two Ecotypes 35

Abstract 36

Introduction

Materials a

Results

Discussio

Reference

CHAPTER III

The Plant v-SN
the PVC

Abstract

Introduc

Materia

Results

Discuss

Refere

CHAPTER IV

Comparison o
Insertion Muta

Abstra

Introdu

Materia

Results

Discus

Introduction 37

Materials and Methods 43

Results 45

Discussion 58

References 62

CHAPTER III

The Plant v-SNARE AtVTI1a Likely Mediates Vesicle Transport from the TGN to the PVC 66

Abstract 67

Introduction 68

Materials and Methods 71

Results 78

Discussion 109

References 114

CHAPTER IV

Comparison of Two AtVTI1 Proteins and Characterization of *Atvti12*, a T-DNA Insertion Mutant of *AtVTI12* 119

Abstract 120

Introduction 121

Materials and Methods 124

Results 129

Discussion 147

Referenc

CHAPTER V

Characterizatio
Columns

Abstract

Introducti

Materials

Results

Discussio

Referenc

CHAPTER VI

Conclusions an

Referen

References 155

CHAPTER V

Characterization of AtVTI1-Containing Vesicles Purified by Immuno-affinity Columns 158

Abstract 159

Introduction 160

Materials and Methods 162

Results 165

Discussion 174

References 180

CHAPTER VI

Conclusions and Future Directions 182

References 194

Table 1-1. T

Table 3-1. R

Table 5-1. e
compartmer

LIST OF TABLES

Table 1-1. The name changes for SNARE proteins used in this dissertation. 23

Table 3-1. Relative sequence identity between Vti1 protein homologues 82

Table 5-1. Relative distribution of T7-AtVTI11 and sporamin in intracellular compartments of transgenic *Arabidopsis* roots. 174

Figure 1-1. Th

Figure 1-2. Th
TGN and the P

Figure 2-1. An
mammalian syn

Figure 2-2. T
ecotypes

Figure 2-3. DN

Figure 2-4. A
ecotype Colum

Figure 2-5. In
AtPLP using a

Figure 2-6. In

Figure 3-1. S
of the family
2497184). H
musculus, a
3213229).

Figure 3-2. I
the absence

Figure 3-3.
traffic to the
biosynthetic

Figure 3-4.

Figure3-5.

Figure 3-6

LIST OF FIGURES

Figure 1-1. The routes for protein transport to the vacuole in plants. 11

Figure 1-2. The likely players involved in the NTPP cargo transport between the TGN and the PVC. 18

Figure 2-1. Amino acid sequence alignment of AtPLP and other plant, yeast and mammalian syntaxins. 47

Figure 2-2. The AtPLP amino acid sequence differs between *Arabidopsis* ecotypes. 48

Figure 2-3. DNA gel blot analysis of the *AtPLP* gene. 51

Figure 2-4. *AtPLP* mRNA distrubution pattern among tissues of *Arabidopsis* ecotype Columbia and RLD. 53

Figure 2-5. Immunoprecipitation of in vitro translation products of AtPEP12 and AtPLP using antiserum against AtPEP12p. 56

Figure 2-6. In vitro membrane assay for AtPLP ± TMD. 57

Figure 3-1. Sequence comparison of AtVTI1a and AtVTI1b with other members of the family including yVti1p (*Saccharomyces cerevisiae*, accession no. 2497184), hVti1p (*Homo sapiens,* accession no. 268740), mVti1a (*Mus musculus,* accession no. 3213227), mVti1b (*Mus musculus*, accession no. 3213229). 80

Figure 3-2. Expression of either AtVTI1a or AtVTI1b allows yeast cells to grow in the absence of Vti1p, but only AtVTI1a functions in TGN-to-PVC traffic. 85

Figure 3-3. AtVTI1b but not AtVTI1a could replace yeast Vti1p in ALP and API traffic to the vacuole, which are transported to the vacuole via two different biosynthetic pathways. 88

Figure 3-4. Northern blot analyses of *AtVTI1a* and *AtVTI1b*. 91

Figure3-5. AtVTI1a is an integral membrane protein. 94

Figure 3-6. Subcellular fractionation of AtVTI1a by step sucrose gradient. 97

Figure 3-7. T
transgenic pla

Figure 3-8. *In*
Arabidopsis ro
localized on th

Figure 3-9. T
Arabidopsis ro

Figure 3-10. A

Figure 4-1. Ch

Figure 4-2. S
Accudenz grad

Figure 4-3. At

Figure 4-4 A

Figure 4-5. P

Figure 4-6. In
plants.

Figure 4-7. S

Figure 5-1. A

Figure 5-2. C

Figure 5-3.
AtVTI11 and

Figure 5-4.
from *Arabido*

Figure 5-5.
AtVTI1 vesicl

Figure 6-1. S

Figure 3-7. T7-tag does not affect AtVTI1a function and is expressed in transgenic plants. 100

Figure 3-8. *In situ* localization of T7-AtVTI1a and AtELP on ultrathin sections of *Arabidopsis* roots from T7-AtVTI1a transgenic plants. T7-AtVTI1a and AtELP are localized on the TGN and on dense vesicles. 104

Figure 3-9. T7-AtVTI1a and AtPEP12p colocalize on the PVC in cryosections of *Arabidopsis* roots from T7-AtVTI1a transgenic plants. 107

Figure 3-10. AtVTI1a associates with AtPEP12p 110

Figure 4-1. Characterization of the specificity of anti-AtVTI11 and anti-AtVTI12. 131

Figure 4-2. Subcellular fractionation of AtVTI11 and AtVTI12 by discontinuous Accudenz gradient. 136

Figure 4-3. *Atvti12* is a null mutant for *AtVTI12.* 139

Figure 4-4. Aleurain processing in *Atvti12* cells. 143

Figure 4-5. Phenotype of *Atvti12.* 144

Figure 4-6. Immunoprecipitation of AtVTI11 from wild type and *Atvti12* mutant plants. 146

Figure 4-7. Summary of results. 148

Figure 5-1. AtVTI1 vesicles were enriched though a step sucrose gradient. 166

Figure 5-2. Characterization of affinity-purified AtVTI1 vesicles. 168

Figure 5-3. The plants crossed between transgeneic plant expressing T7-AtVTI11 and sporamin. 170

Figure 5-4. Immuno-localization of T7-AtVTI11 and sporamin on thin sections from *Arabidopsis* roots. 171

Figure 5-5. Representative 2-D gels showing protein profiles of affinity-purified AtVTI1 vesicles. 175

Figure 6-1. Schematic model for the AtVTI1 protein functions in plant cells. 186

a.a. =
AAP =
ALP =
Ams-1 =
AP =
AP1 =
ARF =
AtPLP =
CCV =
CPY =
CTPP =
ctVSS =
Cvt =
EM =
ER =
ESI =
EST =
FT =
GGA =
GFP =
GST =
ICAT =
LV =
MALDI-TOF =
MS =
M-6-P =
M-6-PR =
nt =
NTPP =
NSF =
ORF =
PBS =
PSV =
psVSS =
PVC =
SNAP =
SNAP-25 =
SNARE =
SD =
SRP =
SYP =
ssVSS =

LIST OF ABBREVIATIONS

a.a.	= amino acid
AAP	= Abridged Anchor Primer (
ALP	= Alkaline phosphatase
Ams-1	=α-manosidase
AP	= adaptor protein
AP1	= aminopeptidase 1
ARF	= ADP-ribosylation factor
AtPLP	= *Arabidopsis thaliana* Pep12 like protein
CCV	=clathrin-coated vesicle
CPY	= carboxy-peptidase Y
CTPP	= C-terminal pro-peptide
ctVSS	= C-terminal sorting signals
Cvt	= =cytoplasm-to-vacuole
EM	= Electron microscopy
ER	= Endoplasmic reticulum
ESI	= electrospray ionization
EST	=expressed sequence tag
FT	= flow through
GGA	=Golgi-localized, γ-ear-containing, ARFs-binding proteins
GFP	= green fluorescence protein
GST	= Glutathione-S-transperase
ICAT	= isotope-coded affinity tags
LV	=lytic vacuole
MALDI-TOF	= matrix-assisted laser desorption ionization- time of flight
MS	= mass spectrometry
M-6-P	= Mannose-6-phosphate
M-6-PR	= Mannose-6-phosphate receptor
nt	= nucleotide
NTPP	= N-terminal pro-peptide
NSF	= N-ethylmaleimide-sensitive factor
ORF	= open reading frame
PBS	= phosphate-buffered saline
PSV	=protein storage vacuole
psVSS	= physical structure signals
PVC	= Pre-vacuolar compartment
SNAP	= Soluble NSF attachment protein
SNAP-25	= 25 kD synaptosomal associated protein
SNARE	= SNAP receptors
SD	= standard medium
SRP	= signal recognition particle
SYP	= syntaxin protein
ssVSS	= sequence-specific vacuolar sorting signals

TBS =
TGN =
TIP =
TMD =
t-SNARE =
v-SANE =
VPE =
VSD =
VSR =
VSS =
VTI =
WT =
YEPD =

TBS	= Tris buffered saline
TGN	= trans-Golgi network
TIP	=tonoplast intrinsic protein
TMD	= Transmembrane domain
t-SNARE	= target-SNARE
v-SANE	= vesicle SNARE
VPE	= vacuolar processing enzyme
VSD	= vacuolar sorting determinant
VSR	= vacuolar sorting receptor
VSS	= Vacuolar sorting signal
VTI	= Vps10 interacting factor
w.t.	= wild type
YEPD	= yeast extract peptone dextose medium

Chapter I

Introduction

An Overview of Plant Vacuolar Protein Transport Pathways

I. The Endom

The en

eukaryotic ce

membrane. tr

enclosed orga

membrane sy

biochemical a

Golgi. endoso

targeted to th

cell biology.

signal peptid

translationall

folding and i

the ER. The

vesicles and

1994; Bar-P

apparatus by

Golgi stacks

Upon arriva

domains of

destinations

cargoes are

I. The Endomembrane System in Eucaryotic Cells

The endomembrane system is an important feature that distinguishes the eukaryotic cell from the prokaryotic cell. Originated as invaginations of the plasma membrane, the endomembrane system has evolved into a series of membrane enclosed organelles in modern eukaryotic cells. Owing to this sophisticated membrane system, cells are organized into compartments featuring different biochemical and biophysical conditions, such as the endoplasmic reticulum (ER), Golgi, endosomes, lysosomes (vacuoles) and plasma membrane. How proteins are targeted to the correct compartment becomes a fundamental question of eukaryotic cell biology. Most lumenal and many membrane proteins have specific N-terminal signal peptides that are recognized by signal recognition particle (SRP) and co-translationally imported into the endoplasmic reticulum (ER) (Rappoport, 1990). The folding and initial modification of newly synthesized protein molecules take place in the ER. The protein molecules ready to leave the ER are sorted into coated vesicles and transported to the next compartment, the Golgi complex (Rothman 1994; Bar-Peled *et al.,* 1996). These cargo proteins further travel through the Golgi apparatus by vesicle transport or maturation (review see Pelham 1998). Along the Golgi stacks, proteins are extensively modified by the resident Golgi enzymes. Upon arrival at the *trans*-Golgi network (TGN), proteins are sorted into different domains of the TGN based on specific sorting signals that indicate their destinations, before eventually packaged into distinct vesicles. Via these vesicles, cargoes are transported to their final destination, such as the extracellular matrix,

endosomes c

system. Con

extracellular n

transported to

forward and r

time allowing t

Homeostas

endomembra

selection me

destination.

and these p

delivered to

cells carry

receptors a

them to the

case, prot

downstrea

delivered

are retaine

the plasm

that in m

plus seie

organelle

endosomes or lysosomes. This forward trafficking system is termed the secretory system. Conversely, proteins localized on the plasma membrane and in the extracellular matrix can be taken back by the clathrin coated vesicles (CCVs) and transported to the endosomes or lysosomes through the endocytic pathway. These forward and retrograde pathways maintain the membrane in balance at the same time allowing transport of proteins between organelles.

Homeostasis of each compartment is important for its proper function. The endomembrane system developed multiple ways to achieve this. One is the active selection mechanism. Many proteins carry peptide signals as the address for their destination. These signals are recognized by membrane anchored signal receptors and these proteins are selectively packaged into coated transport vesicles and delivered to the correct compartment: i.e. many lysosomal proteins in mammalian cells carry a mannose-6 phosphate (M6P) signal that is recognized by M6P receptors at the TGN. These receptors recruit the proteins into CCV that transport them to the lysosome. Some transport pathways or steps are less selective. In that case, proteins are transported forward by bulk flow and selection takes place downstream. The resident proteins belonging to the upstream compartment are delivered back based on the retrieval signal they carry. Many ER resident proteins are retained in the ER by an efficient retrieval system. Some ER proteins can reach the plasma membrane before being delivered back to the ER. It is now believed that in most compartments, the active selection in forward transport and bulk flow plus selective retrieval are combined to maintain the stable composition of the organelle. For example, in the maturation theory, most resident Golgi enzymes are

restricted at c

Golgi apparat

see Allan and

II. SNARE Hy

Both a

selected prote

set of compar

Based on the

(1993) first p

protein comp

attachment

secondary s

are type II m

terminus of t

that in some

SNAREs (R

SNAREs, up

that is impo

specificity o

either Q or

a conserve

of proteins

group of pr

restricted at certain stacks by retrieval from more advanced stacks. Proteins in the Golgi apparatus are matured into the next stack by receiving these vesicles (review see Allan and Balch, 1999).

II. SNARE Hypothesis

Both active selection and selective retrieval require vesicles to deliver the selected proteins. The correct targeting of vesicles is thought to be fulfilled by a set of compartment specific membrane proteins and common soluble factors. Based on their research on neuronal synaptic vesicle secretion, Söllner *et al.*, (1993) first proposed the SNARE hypothesis that specified these membrane protein components to be soluble NSF (N-ethylmaleimide-sensitive factor) attachment protein receptors or SNAREs. SNARE proteins share similar secondary structures. Most SNAREs, with the exception of the SNAP 25 family, are type II membrane proteins with a stretch of hydrophobic residues at the C-terminus of the protein that form a transmembrane domain. It has been shown that in some cases, the transmembrane domain determines the location of the SNAREs (Rayner and Pelham, 1997; Watson and Pessin, 2001). For typical SNAREs, upstream of the transmembrane domain, there is a coiled-coil domain that is important for interacting with other SNAREs and may contribute to the specificity of SNARE interactions (Sutton *et al.* 1998). SNAREs are classified as either Q or R SNAREs based on the presence of either a glutamate or arginine at a conserved position, respectively (Fasshauer *et al.*, 1998a). The SNAP25 family of proteins are a special group of SNAREs with unique structural features. This group of proteins lack transmembrane domain. Instead, they are anchored on the

membrane b

typical SNAR

have two "Q"

Based

arbitrarily: v-S

membrane of

are on the ta

them is a S

specifically r

this comple

(Antonin et

membrane

least, it ha

membrane

stable. F

snaptobre

To disso

(NSF) a

form a

ATPase

Palland

compa

membrane by a post-translationally added lipid group (Oyler *et al.*, 1989). Unlike typical SNAREs that contain one coiled coil domain, SNARE 25 type SNAREs have two "Q" type coiled-coil domains.

Based on their locations, SNAREs can also be divided into two groups arbitrarily: v-SNAREs (a lot of them are also R SNAREs) are localized on the membrane of transport vesicles and t-SNAREs (Most of them are Q SNAREs) are on the target membranes. Typically, 3 t-SNAREs (or 2 t-SNAREs if one of them is a SNAP25 type SNARE) form a *cis*-SNARE complex. The v-SNARE specifically recognizes this *cis*-SNARE complex and align its coil-coil region with this complex to form a structure called 4-helices bundle or the SNAREpin (Antonin *et al.*, 2000). The formation of this structure brings the vesicle and target membrane together for fusion. In the case of syntaxin-SNAP 25 and VAMP2 at least, it has been shown 3 SNARE complexes are needed to fulfill the task of membrane fusion (Hua and Scheller, 2001). The SNARE complex is extremely stable. For instance, the SNAREpin formed by Snytaxin-1, SNAP25 and snaptobrevin does not unfold until heated up to 95°C (Fasshauer *et al.*, 1998b). To dissociate the SNAREpin, soluble factors, N-ethylamleimide sensitive factor (NSF) and soluble NSF attachment protein (α-SNAP) are recruited afterwards to form a 20S complex with the SNAREs. Energy is used by NSF, an AAA type ATPase, to dissociate the SNAREpin. (Whiteheart *et al.*, 1994; Tolar and Pallanck, 1998). The freed v-SNAREs are then recycled back to the original compartment.

The SN

see Hay and S

evidence ind

require other p

There a

iSanderfoot e

roles in develo

be involved in

SYR1, a SNA

K-channels r

AtVTI11 mig

Sato, et al.,

trafficking is

important fo

from its ma

proteins in

III. Vacuo

Pla

lysosome

vacuole

specializ

lysosom

recycle

The SNARE hypothesis is supported by large number of studies (review see Hay and Scheller, 1997; Chen and Scheller, 2001). However, a large body of evidence indicate that *in vivo*, the specificity of vesicle docking and fusion may require other protein and lipid factors besides SNAREs (review see Pfeffer 1999).

There are 55 genes identified as SNAREs in *Arabidopsis* genome so far (Sanderfoot *et al.*, 2000). Several SNAREs have been found to play important roles in development and physiology of plants. For example, KNOLLE is found to be involved in cell plate formation (Lukowitz *et al.,* 1996; Lauber *et al.*, 1997). SYR1, a SNARE in tobacco is identified by its involvement in plasma membrane K-channels regulation in guard cells (Leyman *et al.,* 1999). SYP21, SYP22 and AtVTI11 might be involved in vacuolar protein transport (Bassham *et al.*, 1995; Sato, *et al.*, 1997; Zheng *et al.*, 1999a). In plants, the basic machinery of vesicle trafficking is most likely to be conserved. However, those trafficking steps are important for the cell and the whole plant's development in unique ways different from its mammalian and yeast counterpart. This made functional study of SNARE proteins in plant more intriguing.

III. Vacuolar Protein Trafficking in Mammalian and Yeast Cells

Plant vacuoles are thought to be equivalent organelles to mammalian lysosomes and yeast vacuoles. In mammals and yeast, there is one kind of vacuole, although in mammals, differentiated cells sometimes develop specialized lysosomes like melanosomes and platelet dense granules. For most lysosomes and vacuoles, the basic function is to digest expired proteins and recycle cellular components or sequester toxic secondary metabolite. They are

normally ma

biosynthetic p

majority of the

The third one

In mam

(M-6-P) to N-g

lysosome (Gr

recognizes a

catalyzes the

membrane bo

sorts them a

M6PR46 and

dileucine mo

motif are effic

γ-ear-contain

recruits the c

to form clath

SNAREs th

compartmen

vacuoles of

the lysosom

1995).

normally maintained at low pH and contain mostly hydrolyases. For the biosynthetic pathway, there are three routes to the vacuole. One is taken by majority of the soluble protein. Another is mostly by vacuolar membrane proteins. The third one is a direct cytoplasm-to-vacuole (Cvt) transport pathway.

In mammalian cells, a post-translational addition of mannose-6-phosphate (M-6-P) to N-glycans acts as a signal to target the majority of hydrolyases to the lysosome (Griffiths *et al.,* 1988). The enzyme GlcNAc phosphotransferase recognizes a certain patch of the amino acid sequence in the protein and catalyzes the modification of N-linked oligosaccharide. At the *trans*-Golgi, a membrane bound M-6-P receptor recognizes the M6P group on the cargo and sorts them away from the bulk flow (Albert *et al.*, 1994). M-6-P receptors like M6PR46 and M6PR300 contain a signal comprised of an acidic stretch and a dileucine motif at their C-terminus which faces cytosol (Chen *et al.*, 1997). This motif are efficiently recognized by a cytosolic protein called GGA (Golgi-localized, γ-ear-containing, ARFs-binding proteins, Puertollano *et al.*, 2001). GGA then recruits the clathrin, a type of cytosolic coat protein, and other accessory factors to form clathrin-coated vesicles (CCV) at the TGN. These CCVs probably carry v-SNAREs that promote fusion with the late endosome, an intermediate compartment on the way to the lysosome (an equivalent compartment to vacuoles of yeast and plant cells). There is also a M-6-P independent pathway to the lysosome which is utilized by certain cells like pepatocytes (Lodish *et al.*, 1995).

Yeast

report indicat

the sorting of

of this protein

mechanisms

In *Sac*

most other sc

to the M-6-P

a sugar moie

terminus of t

the precurso

et al., 1994

loaded with

prevacuolar

targeting ste

Vti1p, a mul

(Becherer e

for CPY del

Mem

SNARE Va

bypasses

component

of GGA, th

Yeast vacuolar proteins are not modified with M-6-P. However, a recent report indicates that a yeast homologue of mammalian M6PR also plays role in the sorting of vacuolar hydrolases (Whyte and Munro, 2001). Although the ligand of this protein has not been identified, it is possible yeast also utilize some similar mechanisms to deliver a subset of vacuolar proteins.

In *Saccharomyces cerevisiae,* hydrolase caboxypeptidase Y (CPY) and most other soluble proteins are transported to the vacuole through a route similar to the M-6-P pathway. One difference, however, is that instead of decorated with a sugar moiety, the cargo protein carries a peptide targeting signal at the N-terminus of the protein (Johnson *et al.*, 1987). At the TGN, this sorting signal in the precursor CPY is recognized by a membrane receptor, Vps10p (Marcusson *et al.,* 1994). GGA recognizes Vps10p and leads to the formation of vesicles loaded with CPY and other vacuolar proteins, which are then targeted to the prevacuolar compartment (PVC)/late endosome (Black *et al.*, 2000). The targeting step of these vesicles to the PVC was recently found to be facilitated by Vti1p, a multifunctional Q-SNARE and Pep12p, a t-SNARE localized on the PVC (Becherer *et al.*, 1996; Fischer von Mollard *et al.,* 1997). The subsequent steps for CPY delivery from the PVC to the vacuole are not well characterized.

Membrane proteins like alkaline phosphatase (ALP) and the vacuolar t-SNARE Vam3p in yeast (Darsow *et al.*, 1998), use an alternative pathway that bypasses the PVC. Thus their transport is not affected by some mutations in components of the CPY pathway (Cowles *et al.,* 1997; Piper *et al.,* 1997). Instead of GGA, this pathway requires another adaptor called AP3 (Adaptor Protein 3;

Cowles *et al*

the TGN. In

proteins lamp

1998. DeWAr

mammalian

membrane pr

In yeas

α-mannosidas

vacuole via th

mechanism c

involved in t

with the sec

transport (Ab

routes for p

autophagy.

proteins, ins

vacuole.

IV. Vacuola

IV-a.

The

to study th

functions n

Cowles *et al.*, 1997; Stepp *et al.*, 1997; Darsow *et al.*, 1998) to form vesicles from the TGN. In mammalian cells, the proper delivery of lysosomal membrane proteins lamp-2, limp-2 and CD63 (DellAngelica *et al.*, 1999; Le Borgne *et al.*, 1998; DellAngelica *et al.*, 2000) has also been reported to require AP3. Thus, mammalian cells also need different pathways for transport soluble and membrane proteins.

In yeast, some vacuolar resident proteins like aminopeptidase 1 (AP1) or α-manosidase (Ams1p) are synthesized in the cytosol and transported to the vacuole via the Cvt pathway (Klionsky 1998; Hutchins *et al.*, 2001). The transport mechanism of Cvt pathway is just beginning to be unraveled. Membrane fusion is involved in this process, since SNAREs Tlg2p, Vam3p, Ypt7 and Vti1p, along with the sec1 homologue Vps45p that interacts with Tlg2p are required for AP1 transport (Abeliovich *et al.*, 1999). Besides biosynthetic pathways, there are other routes for protein delivery to the vacuole, such as through endocytosis and autophagy. However, proteins transported by those routes are not resident proteins, instead, most of them are delivered as substrates for digestion in the vacuole.

IV. Vacuolar Protein Transport in Plants

IV-a. Traffic Routes for Plant Vacuoles

The plant vacuolar system is much more complex and much more difficult to study than its yeast and mammalian counterpart. Vacuolar content and functions not only vary depending on the cell types and developmental stages,

but different

co-exist in th

et al. 2001)

proteins to th

plant vacuola

counterpart in

indicate their

sorting signal

signals (ssVS

signals (psVS

1999). In the

ssVSS are p

eventually c

1991; Matsu

conserved m

their functio

precursor of

active A cha

is cleaved a

proteins car

vacuoles by

Mannose-6-

but different vacuoles containing different soluble and membrane proteins may co-exist in the same cell (Paris *et al.*, 1996; Jauh *et al.*, 1999; Di Sansebastiano *et al.*, 2001). It is likely that distinct transport pathways are used to transport proteins to these different types of vacuoles. (Robinson and Hinz, 1997). The plant vacuolar protein transport systems are illustrated as Figure 1-1. Like their counterpart in mammals or yeast, plant vacuolar proteins carry specific signals to indicate their destination. For soluble cargo proteins, three types of vacuolar sorting signals (VSS) have been identified: sequence-specific vacuolar sorting signals (ssVSS), C-terminal sorting signals (ctVSS), and physical structure signals (psVSS) (review see Vitale and Raikhel, 1999; Matsuoka and Neuhaus, 1999). In the cases of prosporamin and the cysteine protease proaleurain, ssVSS are propeptides at the N-terminus of the protein, (NTPP) which are eventually cleaved to release the mature protein. (Matsuoka and Nakamura, 1991; Matsuoka *et al.*, 1995). The NTPPs from aleurain and sporamin contain a conserved motif (NPIR). The N-terminal location of the signal is not required for their function as shown for sporamin A (Koide *et al.*, 1997). For instance, the precursor of ricin carries an NPIR signal in a 12aa linker joining the catalytically active A chain and the sugar-binding B chain. On reaching the vacuole, this linker is cleaved and mature proteins are released (Frigerio *et al.*, 2001a). Many proteins carrying ssVSS are acidic hydrolyases. They are transported to the lytic vacuoles by a route reminiscent to the yeast CPY pathway and the mammalian Mannose-6-phosphate pathway. The VSS is recognized at the TGN by vacuolar

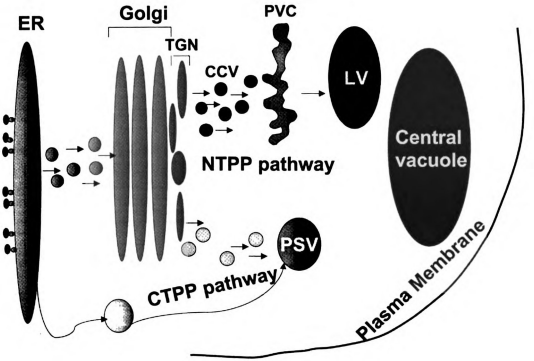

Figure 1-1. The routes for protein transport to the vacuole in plants. In plants, the lytic vacuole (LV) and the protein storage vacuole (PSV) may co-exist in the same cell. Proteins take different routes to these two vacuoles. Most vacuolar proteins are transported by endomembrane system. They all carry a N-terminal signal peptide that direct them to be co-translationally transported to the endoplasmic reticulum (ER). Proteins that belong to the lytic vacuole normally carry a vacuolar sorting signal at the N-terminus called N-treminal pro-peptide (NTPP). The route they travel is called NTPP pathway. From ER, these proteins are transported to the Golgi by vesicle transport. At the TGN, they are sorted away from other proteins by the NTPP signal and are transported from the TGN to the PVC via clathrin coated vesicles (CCV). The NTPP cargo eventually reach the lytic vacuole possibly are mediated by fusion of the PVC to the lytic vacuole. The proteins targeted to the PSV are transported either through the Golgi-apparatus or follow a Golgi-independent pathway, depending on whether they form aggregates at the ER or later. Some of these proteins carry the sorting signals at the C-terminal of the protein and the pathway they use is called the C-terminal propeptide (CTPP) pathway. In most mature cells, the lytic and the protein storage vacuoles may fuse to form the central vacuole.

sorting recep

unknown me

Putative sor

described in

indicate that

the pre-vacu

The lower pH

after dissocia

directly with t

Most s

propeptides

lack consen

that CTPP m

al., 1999). M

(PSV). Little

transport p

phaseolin, t

the involve

attempts to

cargo is not

protein fac

aggregates

vesicles fro

sorting receptors (VSRs) and sequestered to certain areas of the TGN by some unknown mechanism. The VSRs then recruit cytosolic factors to form CCVs. Putative sorting receptors have been identified by several groups and will be described in more detail below. Instead of directly to the lytic vacuole, most data indicate that CCV transports its cargo proteins to an intermediate compartment or the pre-vacuolar compartment (PVC, Paris *et al.*, 1997; Conceição *et al.*, 1997). The lower pH in the PVC lumen allows the VSRs to be recycled back to the TGN after dissociated with and the cargo. The PVC eventually fuse with each other or directly with the vacuole, delivering the cargo to its final destination.

Most storage proteins and certain hydrolyases carry ct-VSS, or C-terminal propeptides (CTPP) that is cleaved upon arrival to the vacuole. These signals lack consensus sequence, but the C-terminal location is critical. It is suggested that CTPP might share similar secondary structures (Matsuoka and Neuhaus *et al.*, 1999). Most CTPP- type cargoes are transported to protein storage vacuoles (PSV). Little is known about how these proteins are selected from the bulk of transport proteins and how they are transported. Although in the case of phaseolin, the transport has been shown to be a saturable process, suggesting the involvement of protein factors (Frigerio at al, 1998). However, numerous attempts to identify CTPP receptors have failed. It is conceivable that CTPP cargo is not selected by particular protein receptors. Rather, by the help of some protein factors, the hydrophobic CTPP signals promote the formation of aggregates that exit from ER as precursor accumulating vesicles or dense vesicles from Golgi (Hara-Nishimura *et al.*, 1998; Toyooka *et al.*, 2000 Frigerio *et*

al., 2001b).

the storage v

is cleaved o

different ma

concentratio

not affect the

Yet an

barley phyte

vacuolar so

proteins are

Schaewen a

or the route

The

independen

protein sto

(TIP). Thei

1999).

IV-2

Sev

have been

pathway. E

cotyledon

to NTPP s

al., 2001b). These vesicles either fuse with the existing PSV or are taken up by the storage vacuoles by autophagy at the vacuole (Levanony *et al.*, 1992). CTPP is cleaved once the protein arrives at the PSV. CTPP pathway apparently use different machinery from NTPP pathway since CTPP pathway is sensitive to a concentration of wortmannin (a phosphatidyl-inositol 3-Kinase inhibitor) that does not affect the NTPP protein transport (Matsuoka *et al.*, 1995).

Yet another group of cargo proteins such as bean phytohemagglutinin and barley phytepsin, use an internal sequence of the mature protein as their vacuolar sorting signal (Kervinen *et al.*, 1999). In most cases examined, these proteins are targeted to the PSV (Tague *et al.*, 1990; Saalbach *et al.*, 1991; von Schaewen and Chrispeels, 1993). However, little is known about either the signal or the route they pass.

The delivery of vacuolar membrane proteins has been shown to be independent of soluble proteins (Gomez and Chrispeels, 1993). Since lytic and protein storage vacuoles carry different isoforms of tonoplast intrinsic proteins (TIP). Their delivery routes might also be different (Jauh *et al.*, 1998; Jauh *et al.*, 1999).

IV-2. Components of the Plant Vacuolar Protein Delivery System

Several potential components of the vacuolar protein delivery machinery have been identified in plants. Most of them appear to be involved in the NTPP pathway. BP80 is a protein purified from CCV enriched fraction of pea developing cotyledon with apparent molecular weight of 80 kDa. Its ability to specifically bind to NTPP signals at an optimal pH of 6.0 and dissociate at pH5.5 (Kirsch *et al.*,

1994. Paris

AtELP, first i

homologue c

in CCV prepa

al., 1997; Sa

signals with

peptides (A

homologues

plants and

expression

suggesting

may also h

VSRs is u

identified i

1999). Ho

sequences

binding sit

SN

eukaryotic

plants. T

composition

and secon

genes in A

1994; Paris *et al.,* 1997) makes it a good candidate for NTPP cargo receptor. AtELP, first identified by its structural similarity to mammalian EGF receptor, is a homologue of BP80 in *Arabidopsis* (Ahmed *et al.,* 1997). AtELP is also enriched in CCV preparations and has been localized to the TGN and the PVC (Ahmed *et al.,* 1997; Sanderfoot *et al.,* 1998). Like BP80, it has the similar affinity to NTPP signals with a pH sensitive manner but fails to bind to CTPP or mutated NTPP peptides (Ahmed *et al.*, 2000). In the *Arabidopsis* genome, there are 6 homologues of AtELP, VSR1-6. Preliminary results from individual knock-out plants and RT-PCR show that these 6 genes might have different spatial expression patterns (Avila-Teeguarden E and Raikhel NV, unpublished data), suggesting that these proteins might function in different developing stages. They may also have different affinity to different NTPPs. The ligand specificity of these VSRs is under investigation. Homologues of AtELP or BP80 have also been identified in pumpkin (Shimada *et al.,* 1997) and *Nicotiana alata* (Miller *et al.*, 1999). However, in both cases, these VSRs recognize internal or C-terminal sequences that has no NPIR motif. BP80 may also has two separate ligand binding site that recognize different VSS (Cao *et al.*, 2000).

SNAREs are important components for vesicle transport machinery in all eukaryotic cells, so they are likely to play a role in vacuolar protein transport in plants. The completion of *Arabidopsis* genome allows us to examine the composition of SNARE genes at genome range. Based on sequence similarities and secondary structural analysis, Sanderfoot *et al.* (2000) reported 55 SNARE genes in *Arabidopsis*. The largest group is syntaxins. Syntaxins all share similar

secondary s

There are 2-

and named

extensively

trafficking. S

functionally c

complex of S

and an NSF

iBassham a

SYP21 is lo

previously c

structure m

and recycle

Sanderfoot

incoming A

SYP2 homo

One of the

CPY in yea

localized c

related to t

localized to

have found

(Sanderfoo

secondary structures. They are always found as a part of the t-SNARE complex. There are 24 syntaxins in *Arabidopsis*. They can be grouped to 10 subgroups and named SYP (syntaxin protein) 1 to 10. One group, SYP2, has been extensively studied due to its likelihood to be involved in vacuolar protein trafficking. SYP21, a homologue of yeast Pep12p, was found by its ability to functionally complement a yeast *pep12* mutant (Bassham *et al.*, 1995). A 20S complex of SYP21 has been partially characterized. It contains SYP21, α-SNAP and an NSF homologue. This complex readily dissociates when ATP is present (Bassham and Raikhel, 1999). Immuno-electron microscopy studies show that SYP21 is localized to an electron dense tubular structure that had not been previously characterized. Since AtELP is also found in this compartment, this structure might be the plant PVC where AtELP dissociates with the NTPP cargo and recycles back to the TGN. (Bassham *et al.,* 1995; Conceição *et al.,* 1997; Sanderfoot *et al.*, 1998). Thus, SYP21 may be a SNARE involved in receiving the incoming AtELP-containing CCV derived from the TGN. There are two other SYP2 homologues in *Arabidopsis*. They show around 65-70% identity to SYP21. One of them, SYP22 was first identified by its ability to restore the transport of CPY in yeast *vam3* mutant (Sato *et al.*, 1997). In yeast, Vam3p is the t-SNARE localized on the vacuole that is responsible for all membrane fusion events related to the vacuole (Darsow *et al.,* 1997). However, in *Arabidopsis*, SYP22 is localized to different places in different tissues by different labs. In root tips, we have found SYP21 and SYP22 are both localized on the same PVC membrane (Sanderfoot *et al.*, 1999). In shoot meristem, however, SYP22 has been

observed or

and SYP22

SYP21 or S

must each p

and probab

was first ide

SYP21 and

lacking a tra

(another eco

with a trans

1999b). Pre

domain can

explain why

effect on me

(Zheng *et al*

this mutatio

effects.

SYP4

Syntaxin 16

Golgi and t

functions. T

(Abeliovich

and 42 are

observed on the tonoplast of small vacuoles (Sato *et al.*, 1997). Although SYP21 and SYP22 interact with identical set of other SNAREs, knockouts of either SYP21 or SYP22 result in a pollen-lethal phenotype. SYP21 and SYP22 thus must each perform critical and nonredundant functions in pollen development and probably in later stages of development (Sanderfoot *et al.*, 2000b). SYP23 was first identified from *Arabidopsis* EST collections due to its high similarity with SYP21 and 22. Surprisingly, in Columbia ecotype, this gene encodes a protein lacking a transmembrane domain due to a frame shift. The same gene from RLD (another ecotype) background, on the other hand, encodes a full length SYP23 with a transmembrane domain similar to the other two SYP2s (Zheng *et al.*, 1999b). Previous reports show that some syntaxins lacking a transmembrane domain can be localized correctly by interacting with other SNAREs. That may explain why SYP23 without transmembrane domain has no dominant negative effect on membrane fusion. Alternatively, SYP23 are not abundantly expressed (Zheng *et al.*, 1999b) and may have redundant functions with other SYP2s. Thus this mutation in recent evolution is tolerated and preserved with no adverse effects.

SYP4 group of syntaxins are most closely related to Tlg2p in yeast and Syntaxin 16 in mammals. In yeast and mammals, this syntaxin is found on the Golgi and the TGN (Holthuis *et al.*, 1998; Simonsen *et al.*, 1998). Among other functions, Tlg2p is involved delivering vacuolar proteins via the Cvt pathway (Abeliovich *et al.*, 1999). In *Arabidopsis,* there are 3 genes in this group. SYP41 and 42 are both localized on the TGN but on separate domains (Bassham *et al.*,

2000). Like

SYP42 lead

roles in plan

The S

syntaxin Tlg

is only one S

membranes

both SYP41

other (Sande

NTPP cargo

Vti1p

associate w

proven an a

been show

trafficking. S

cause the r

suggesting

von Mollard

Vam3p and

docking and

SNAREs, i

that are re

interaction

2000). Like SYP2 group syntaxins, single knock-out mutation of *SYP41* and *SYP42* lead to pollen lethal phenotype, suggesting that they play non-redundant roles in plant development.

The SYP5 and SYP6 group of syntaxins share similarity with yeast syntaxin Tlg1p. The SYP5 gene family is composed of 2 members, where there is only one SYP6. Both SYP5 and 6 are localized on both the TGN and the PVC membranes. SYP5 proteins associate with SYP2 at the PVC, while SYP6 with both SYP41 and SYP42 on the TGN. SYP5 and SYP6 also interact with each other (Sanderfoot *et al.*, 2001). Figure 1-2 shows the likely players involved in the NTPP cargo transport between the TGN and the PVC.

Vti1p is a v-SNARE first identified in yeast because of its ability to associate with Vps10p, the cargo receptor for CPY. This interaction was later proven an artifact (Fischer von Mollard and Stevens, 1997). However, Vti1 has been shown to be an important SNARE with multiple functions in vesicle trafficking. Some temperature sensitive mutant alleles of this v-SNARE in yeast cause the mistargeting of CPY to the extracelluar space as a precursor form, suggesting that the CPY transport be blocked at the step after the TGN (Fischer von Mollard and Stevens 1997). More over, VTI1p forms a SNARE complex with Vam3p and Vam7p on the vacuolar membrane that is necessary for vesicle docking and fusion to the vacuole (Fischer von Mollard and Stevens 1997). Five SNAREs, including Vti1p, Vam3p, Vam7p, Ykt6p, Nyv1p form SNARE complex that are required for vacuolar homotypic fusion (Ungermann *et al.*, 1999). The interaction between Vam3p and Vti1p contributes to all membrane docking and

GOLG

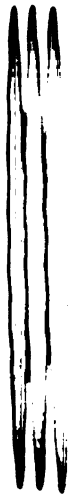

Figure 1-
TGN and
recognitio
formation
These v-S
PVC, and
dissociate
found on

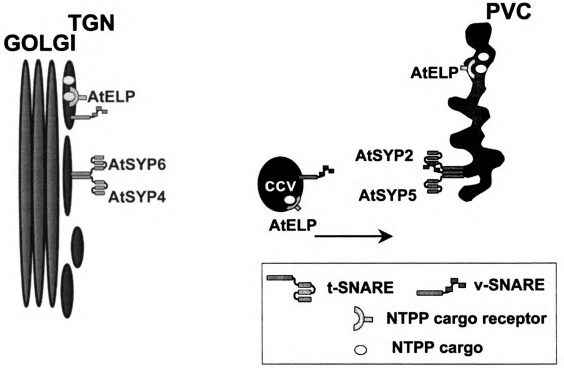

Figure 1-2. The likely players involved in the NTPP cargo transport between the TGN and the PVC. NTPP signals are recognized by AtELP at the TGN. This recognition leads to the sorting of NTPP cargo away from other proteins and the formation of CCV. On the CCV membrane, besides AtELP, there are v-SNAREs. These v-SNAREs interact with SYP2 and SYP5, the t-SNAREs localized on the PVC, and leads to membrane fusion. Because the pH is lower in the PVC, AtELP dissociates NTPP cargo and is recycled back. SYP4 and SYP6 are t-SNAREs found on the TGN membrane. The functions of these SNAREs are not clear.

fusion even

vacuole (Fis

routes to th

Vti1p also i

1997; Fisch

transport sys

and Tlg2, th

in multiple s

achieve spe

needed for s

Vti1p

1997, Fisch

two *Vti1* ge

between m

30% simil

organisms

tasks. In m

cell (Xu *et*

In A

sequence

peptide s

presence

and AtVT

fusion events with the vacuolar membrane and thus affect all traffic routes to the vacuole (Fischer von Mollard *et al.*, 1999). Thus, Vti1p plays important roles in all routes to the vacuole in yeast. Besides the roles in delivering vacuolar proteins, Vti1p also interacts with Sed5p, the t-SNARE on the *cis*-Golgi (Lupashin *et al.*, 1997; Fischer von Mollard *et al.*, 1997), probably as part of the retrograde transport system. Vti1p also interacts with Tlg1p, a syntaxin on early endosomes and Tlg2, the syntaxin on the TGN (Holthuis *et al.*, 1998). Vti1p is thus involved in multiple steps of the endomembrane transport system in yeast. The way to achieve specific targeting is not clear. It is possible that other SNAREs are needed for specific SNARE complex formation and membrane docking.

Vti1p homologues are also found in mouse and human (Lupashin *et al.*, 1997, Fischer von Mollard and Stevens 1998). Interestingly, in higher organisms, two *Vti1* genes are found although there is only one gene in yeast. The homology between mouse and human Vti1a is 98% while mouse Vti1a and Vti1b only share 30% similarity. The notion is that the endomembrane systems in higher organisms are more complex. Two *Vti1* genes thus evolved to share the multiple tasks. In mouse, Vti1a and Vti1b are localized on different membranes within the cell (Xu *et al.*, 1998). Presumably, they perform different functions.

In *Arabidopsis*, several EST cDNA clones were found to share significant sequence similarity with Vti1p of other organisms (about 25-34% identity at peptide sequence level). A search of the *Arabidopsis* genome reveals the presence of three VTI1 gene homologues. We named them AtVTI11, AtVTI12 and AtVTI13. The comparison of their deduced amino acid sequences show that

they are be
identical wi
proteins ha
long. They
sequence c
SNAREs be
AtVTI13 is c
at high leve
genes are
sequence.
AtVTI11 is a
to the PVC
transport of
protein) and
1999a). In A
the TGN are
SYP21 (Zhe
AtVTI12 is fo
(Sanderfoot
been shown
mutant has
protein extra
comparing to

they are between 65% (AtVTI11-12, AtVTI11-AtVTI13) to 75% (AtVTI12-AtVTI13) identical with each other. Like other Vti1 proteins, these three *Arabidopsis* VTI1 proteins have a C-terminal hydrophobic domain around 17 to 20 amino acids long. They also contain a coiled-coil region that shows highest amino acids sequence conservation. Like other Vti1 proteins, they are classified as "Q" SNAREs because of a conserved glutamate residue at the 0 layer of the helices. AtVTI13 is only expressed at very low level. AtVTI11 and AtVTI12 are expressed at high levels. Thus, we characterized AtVTI11 and AtVTI12 in more detail. Both genes are expressed in all tissues of the plant. Although very similar in sequence, AtVTI11 and AtVTI12 complement different *vti1* mutant in yeast. AtVTI11 is able to substitute for yeast Vti1p in the transport of CPY from the TGN to the PVC. AtVTI12, on the other hand, is more efficient at facilitating the transport of the vacuolar membrane protein alkaline phosphatase (the membrane protein) and aminopeptidase 1 (a marker of the Cvt pathway, Zheng *et al.*, 1999a). In *Arabidopsis* root tips, AtVTI11 is found to be located with AtELP on the TGN area and with SYP21 on the PVC where it physically interacts with SYP21 (Zheng *et al.*, 1999a) and SYP51 (Sanderfoot *et al.* 2001). In contrast, AtVTI12 is found in the complex with SYP4 (Bassham *et al.*, 2000) and SYP6 (Sanderfoot *et al.*, 2001). A T-DNA insertion mutant of AtVTI12 (*Atvti12*) has been shown to lack *AtVTI12* gene expression and the protein. However, this mutant has no apparent phenotypes. Immunoprecipitation of AtVTI11 from protein extract of this mutant co-precipitated much more SYP4 and SYP6 comparing to that from the wild type plant. Thus, it is likely that AtVTI11 takes

place of m

Recently, A

deletion mu

indicating a

function. T

between the

mutant of At

of AtVTI fam

Besid

characterize

sec1 homo

presumably

the interact

There is no

protein is

and SYP4

Moreover

Sanderfoo

functions

V. Conclu

Ou

been dra

tools ava

place of missing AtVTI12 to maintain the normal functioning of the plant. Recently, A shoot meristem gravitropic mutant *zig1 (sgr4)* is found to have a deletion mutation in *AtVTI11* gene (Morita *et al.*, 2001; Kato *et al.*, 2001), indicating at least some level of non-overlap between AtVTI11 and AtVTI12 function. This mutant might give us more information about the relationship between the endomembrane system and gravity sensing in plants. The double mutant of *Atvti12* and *zig-1* will also be helpful for us to understand the function of AtVTI family proteins.

Besides SNAREs, a homologue of the yeast Vps45 protein has been characterized in *Arabidopsis* (Bassham and Raikhel, 1998). Vps45 protein is a sec1 homologue that associates with Pep12p and Tlg2p. This association presumably helps the syntaxin to adopt a functional conformation or to facilitate the interactions between syntaxins and other proteins (Bryant and James, 2001). There is no transmembrane domain on AtVPS45. However, in *Arabidopsis*, this protein is associated peripherally with membrane and co-localizes with AtELP and SYP4 in subcellular fractionation studies and immuno-electron microscopy. Moreover, AtVPS45 physically interacts with SYP4 (Bassham *et al.*, 2000; Sanderfoot *et al.*, 2001). Thus, AtVPS45 might be involved in regulating the functions of SYP4.

V. Conclusion

Our understanding about how protein is transported to the vacuole has been dramatically advanced by the knowledge of the *Arabidopsis* genome and by tools available such as reverse genetics in *Arabidopsis*. Our approach of

characteriz

between the

trafficking s

the basic m

transport ha

other syste

involved in r

The

phenomena

isoforms of

redundancy

have differe

secretory pa

cope with

challenges

machinery.

of the plant

Alon

of the SNA

included t

used. To

are appea

characterizing the molecular components of vesicle trafficking machinery between the TGN and the PVC has already offered a lot of information of this trafficking step and the vacuolar protein transport. We have shown that although the basic machinery is conserved in all eukaryotic cells, plant vacuolar protein transport has unique features that can not be inferred from studies conducted in other systems. In particular, mutant studies have shown that vesicle trafficking is involved in many specific aspects of plant development and physiology.

The presence of small families of related proteins are common phenomena for secretory machinery components in plants. These multiple similar isoforms of secretory machinery components probably indicate some functional redundancy. However, the few cases studied thus far, indicate these proteins have different duties to meet the unique and complex requirement for plant secretory pathway. Alternatively, they could be required in different tissues or to cope with different environment conditions. These gene families are great challenges in addressing functional questions of the various components of the machinery, but they also provide us opportunities to examine the unique features of the plant cell machinery in the context of the whole organism

Along the rapid advance in our knowledge about plant genome, the names of the SNAREs have been changed during past several years. This dissertation included two chapters that are published papers where historical names were used. To clarify the confusion, Table 1-1 indicates all the names changed that are appeared in this dissertation.

Table 1-1. T

current nam
AtVTI11
AtVTI12
SYP21
SYP22
SYP23
SYP41
SYP42

Table 1-1. The name changes for SNARE proteins used in this dissertation.

current name	old name
AtVTI11	AtVTI1a
AtVTI12	AtVTI1b
SYP21	AtPEP12p, atPEP12p
SYP22	AtVAM3p. atVAM3
SYP23	AtPLP
SYP41	AtTLG2a
SYP42	AtTLG2b

VI. Thesis S

When

been identi

PEP12 and

plants that

identified a

database.

Columbia a

surprisingl

transmemb

gone throu

sequence

To

partners

identified

revealed

system i

speculat

Since A

ATVTI1

localize

AtVTI1

VI. Thesis Scheme

When I joined the lab, SYP21 (AtPEP12p) and SYP22 (AtVAM3p) had just been identified by their ability to complement the yeast mutation in genes of *PEP12* and *VAM3* respectively. These were the first cases of syntaxins found in plants that might be involved in vacuolar protein transport. Subsequently, I identified a partial cDNA for AtPLP or SYP23, from an *Arabidopsis* EST database. I cloned full-length cDNAs from *Arabidopsis thaliana* ecotypes Columbia and RLD. The RLD cDNA sequence encodes a full length protein but surprisingly, the cDNA from Columbia encoded a protein that lacked the transmembarne domain. Careful examination revealed that this gene has also gone through evolutionary changes in its DNA sequence recently that caused the sequence difference among different ecotypes.

To further characterize the SYP2 gene family, I searched the potential partners of this group syntaxins. At the time, the yeast Vti1p had just been identified and shown that it interacts with yeast Pep12p. A database search revealed three *Vti1* type genes in *Arabidopsis*. Since plant endomembrane system is more complicated and advanced than that of yeast, it is reasonable to speculate that these three *Arabidopsis* proteins might have functional difference. Since AtVTI13 is only expressed in very low level, I extensively studied the ATVTI11 (AtVTI1a) and AtVTI12 (AtVTI1b). I was able to show that AtVTI11 is localized on the TGN and the PVC. It also interacts with SYP21 (Chapter III). AtVTI12, although very similar to AtVTI11, may have different functions. The first

evidence to

of yeast *vti1*

III). In p

immunopre

AtVTI12 inte

In an *AtVT*

SYP4 and S

different fun

will take ove

evidence to support this notion is that these two proteins rescue different alleles of yeast *vti1* mutant that block different trafficking routes to the vacuole (Chapter III). In plants, their functional difference has been indicated in immunoprecipitation assays. AtVTI11 interacts with SYP2 and 5, whereas AtVTI12 interacts preferentially with SYP4 and SYP6 groups syntaxins. However, In an *AtVTI12* knock-out mutant (*Atvti12*), AtVTI11 is found to associate with SYP4 and SYP6 (Chapter IV). This indicates that, although AtVTI11 and 12 have different functions, in the absence of one family member, the remaining member will take over its function.

Reference

Abeliovich
of aminopep
Vps45p. EM

Ahmed SU.
location of a
protein-sort.

Ahmed SU,
K, and Raik
in the trans
Arabidopsis

Albert B, B
biology of th

Allan BB,
compartme

Antonin W
(2000). A
conserved

Bar-Pele
eukaryoti

Basshar
syntaxin
mutant.

Bassha
implicat

Bassha
forms a
603.

Bassh
AtVPS
2265.

Beche
homo
lysoso

References

Abeliovich H, Darsow T, and Emr SD (1999) Cytoplasm to vacuole trafficking of aminopeptidase I requires a t-SNARE-Sec1p complex composed of Tlg2p and Vps45p. *EMBO* **18:** 6005-6016.

Ahmed SU, Bar-Peled M, and Raikhel NV (1997). Cloning and subcellular location of an *Arabidopsis* receptor-like protein that shares common features with protein-sorting receptors of eukaryotic cells. *Plant Physiol.* **114:** 325-336.

Ahmed SU, Rojo E, Kovaleva V, Venkatarmam S, Dumbrowski JE, Matsuoka K, and Raikhel NV (2000) The plant vacuolar sorting receptor AtELP is involved in the transport of NH2-terminal propeptides-containing vacuolar proteins in *Arabidopsis thaliana. J. Cell Biol.* **149:** 1335-1344.

Albert B, Bray D, Lewis J, Raff M, Roers K, and Watson J (1994). Molecular biology of the cell. 3rd ed. Pp613-618.

Allan BB, and Balch WE (1999). Protein sorting by directed maturation of Golgi compartments. *Science* **265:** 63-66.

Antonin W, Holroyd C, Fasshauer D, Pabst SV, Mollard, GF, and Jahn R (2000). A SNARE complex mediating fusion of late endosomes defines conserved properties of SNARE structure and function. *EMBO J.* **19:** 6453-6464.

Bar-Peled M, Bassham DC, and Raikhel NV (1996). Transport of proteins in eukaryotic cells: More questions ahead. *Plant Mol. Biol.* **32:** 223-249.

Bassham DC, Gal S, Conceição AS, and Raikhel NV (1995). An *Arabidopsis* syntaxin homologue isolated by functional complementation of a yeast pep12 mutant. *Proc. Natl. Acad. Sci. USA* **92:** 7262-7266.

Bassham DC, and Raikhel NV (1998) An *Arabidopsis* VPS45p homolog implicated in protein transport to the vacuole. *Plant Physiol.* **117:** 407-415

Bassham DC, and Raikhel NV (1999). The pre-vacuolar t-SNARE AtPEP12p forms a 20S complex that dissociates in the presence of ATP. *Plant J.* **19:** 509-603.

Bassham DC, Sanderfoot AA, Kovaleva V, Zheng H, and Raikhel NV (2000). AtVPS45 complex formation at the *trans*-Golgi network. *Mol. Biol. Cell* **11:** 2251-2265.

Becherer KA, Rieder SE, Emr SD and Jones EW (1996). Novel syntaxin homologue, Pep12p, required for the sorting of lumenal hydrolases to the lysosome-like vacuole in yeast. *Mol. Biol. Cell* **7:** 579-594.

Black M, a
endosomes

Bryant NJ.
Tlg2p and
3388.

Cao X, Ro
requiremen
Plant Cell 1

Chen YA,
Rev. Mol. C

Chen H, Y
cation-inde
cytoplasmic
function in

Conceição
Raikhel N
Golgi comp

Cowles C
complex is
109-118.

Darsow
homologu
the vacuo

Darsow T
3 depend
vacuolar

Dell'Ang
(1999) A
due to m

Dell'An
Bonifac
Hemans

Di San
Regene

Black M, and Pelham H (2000). A selective transport route from Golgi to late endosomes that requires the yeast GGA proteins. *J Cell Biol.* **151:** 587-600.

Bryant NJ, and James DE (2001). Vps45p stabilizes the syntaxin homologue Tlg2p and positively regulates SNARE complex formation. *EMBO J.* **20:** 3380-3388.

Cao X, Rogers SW, Bulter J, Beevers L, and Rogers JC (2000). Structural requirements for ligand binding by a probable plant vacuolar sorting receptor. *Plant Cell* **12:** 493-506.

Chen YA, and Scheller RH (2001). SNARE-mediated membrane fusion. *Nat. Rev. Mol. Cell Biol.* **2:** 98-106.

Chen H, Yuan K, and Lobel P (1997). Systematic mutational analysis of the cation-independent mannose 6-phosphate/insulin-like growth factor II receptor cytoplasmic domain. An acidic cluster containing a key aspartate is important for function in lysosomal enzyme sorting. *J. Biol. Chem.* **14:** 7003-7012.

Conceição AS, Marty-Mazars D, Bassham DC, Sanderfoot AA, Marty F, and Raikhel NV (1997). The syntaxin homologue AtPEP12p resides on a late post-Golgi compartment in plant. *Plant Cell* **9:** 571-582.

Cowles CR, Snyder WB, Burd CG and Emr SD (1997). The AP-3 adaptor complex is essential for cargo-selective transport to the yeast vacuole. *Cell* **91:** 109-118.

Darsow T, Rieder SE, and Emr SD (1997). A multispecificity syntaxin homologue, Vam3p, essential for autophagic and biosynthetic protein transport to the vacuole. *J. Cell Biol.* **138:** 517-529.

Darsow T, Burd CG and Emr SD (1998). Acidic dileucine motif essential for AP-3 dependent sorting and restriction of the functional specificity of the Vam3p vacuolar t-SNARE. *J Cell Biol.* **142:** 913-922.

Dell'Angelica EC, Shotelersuk V, Aguilar RC, Gahl WA, and Bonifacino JS (1999) Altered trafficking of lysosomal proteins in Hermansky-Pudlak syndrome due to mutations in the β3A subunit of the AP-3 adaptor. *Mol Cell* **3:** 11-21.

Dell'Angelica EC, Aguilar RC, Wolins N, Haxelwood S, Gahl WA, and Bonifacino JS (2000). Molecular characterization of the protein encoded by the Hemansky-Pudlak syndrome type 1 gene. *J. Biochem.* **275:** 1300-1306.

Di Sansebastiano GP, Paris N, Marc-Martin S, and Neuhaus JM (2001) Regeneration of a lytic central vacuole and of neutral peripheral vacuoles can be

visualized b
Physiol. 126

Fasshauer
structural fe
as Q- and R

Fasshauer
minimal core
and disasse

Fischer von
SNARE Vti1
the t-SNARE

Fisher von
replace the
273: 2624-2

Fisher von
v-SNARE V
vacuole. *Mo*

Frigerio L
phaseolin
Plant Cell 1

Frigerio L,
Ceriotti A
precursor
Physiol. 12

Frigerio L
fate of trim
route to va

Gomez L
are targete

Griffiths
manose-6

Hara--Nis
(1998). T
large prec

visualized by green fluorescent proteins targeted to either type of vacuoles. *Plant Physiol.* **126:** 78-86.

Fasshauer D, Sutton RB, Brunger AT, and Jahn R (1998a). Conserved structural features of the synaptic fusion complex: SNARE proteins reclassified as Q- and R-SNAREs. *Proc. Natl. Acad. Sci. U S A.* **95:** 15781-15786.

Fasshauer D, Eliason W, Brunger AT, and Jahn R (1998b). Identification of a minimal core of the synaptic SNARE complex sufficient for reversible assembly and disassembly. *Biochemistry* **37:** 10354-10362.

Fischer von Mollard G, Northwehr SF, and Stevens TH (1997). The yeast v-SNARE Vti1p mediates two vesicle transport pathways through interactions with the t-SNAREs Sed5p and Pep12p. *J. Cell Biol.* **137:** 1511-1524.

Fisher von Mollard and Stevens TH (1998). A human homolog can functionally replace the yeast v-SNARE Vti1p in two vesicle transport pathways *J. Biol Chem.* **273:** 2624-2630.

Fisher von Mollard G, and Stevens, TH (1999). The *Sacchromyces cerevisiae* v-SNARE Vti1p is required for multiple membrane transport pathways to the vacuole. *Mol. Biol. Cell* **10:** 1719-1732.

Frigerio L, de Virgilio M, Prada A, Faoro F, Vitale A (1998) Sorting of phaseolin to the vacuole is saturable and requires a short C-terminal peptide. Plant Cell **10:** 1031-1042.

Frigerio L, Jolliffe NA, Di Cola A, Felipe DH, Paris N, Neuhaus JM, Lord JM, Ceriotti A, and Roberts LM (2001). The internal propeptide of the ricin precursor carries a sequence-specific determinant for vacuolar sorting. *Plant Physiol.* **126:** 167-175.

Frigerio L, Pastres A, Prada A, and Vitale A (2001). Influence of KDEL on the fate of trimeric or assembly-defective phaseolin: selective use of an alternative route to vacuoles. *Plant Cell* **13:** 1109-1126.

Gomez L and Chrispeels MJ (1993). Tonoplast and soluble vacuolar proteins are targeted by different mechanisms. *Plant Cell* **5:** 1113-1124.

Griffiths G, Holflack B, Simons K, Mellman I, and Kornfeld S (1988). The manose-6-phospate receptor and the biogenesis of lysosomes. *Cell* **52:** 329-341.

Hara--Nishimura I, Shimada I, Hatono Y, Takeuchi Y, and Nishimura M (1998). Transport of storage proteins to protein storage vacuoles is mediated by large precursor accumulating vesicles. *Plant Cell* **10:** 825-836.

Hay JC an
fusion. *Cur*

Holthuis J
syntaxin hc
126.

Hua Y, and
membrane

Hutchins M
mannosidas
pathway co
23498.

Jauh GY,
tonoplast i
Acad. Sci.

Jauh GY,
isoforms as

Johnson
determinar
protease.

Kato T, M
(2001). S
involved i

Kervinen
(1999). C
and vacuo

Klionsky
Chem. **27**

Kirsch T
and initia
Nat. Acad

Koide Y
propeptid
at the C-
870.

Hay JC and Scheller RH (1997). SNAREs and NSF in targeted membrane fusion. *Curr. Opin. Cell Biol.* **9:** 505-512.

Holthuis JCM, Nichols BJ, Dhruvakumar S, and Pelham HRB (1998). Two syntaxin homologues in the TGN/endosomal system of yeast. *EMBO J.* **17:** 113-126.

Hua Y, and Scheller RH (2001). Three SNARE complexes cooperate to mediate membrane fusion. *Proc. Nat. Acad. Sci. USA* **98:** 8065-8070.

Hutchins MU, and Klionsky DJ (2001). Vacuolar localization of oligomeric α-mannosidase requires the cytoplasm to vacuole targeting and autophagy pathway components in *Saccharomyces cerevisiae. J. Biol. Chem.* **276:** 20491-20498.

Jauh GY, Fischer AM, Frimes HD, Ryan CA, and Rogers JC (1998). δ-tonoplast intrinsic protein defines unique plant vacuole functions. *Proc. Natl. Acad. Sci. USA* **95:** 12995-12999.

Jauh GY, Philips TE, and Rogers JC (1999). Tonoplast intrinsic protein isoforms as markers of vacuolar functions. *Plant Cell* **11:** 1867-1882.

Johnson LM, Bankaitis VA and Emr SD (1987). Distinct sequence determinants direct intracellular soting and modification of a yeast vacuolar protease. *Cell* **48:** 875-885.

Kato T, Morita MI, Fukaki H, Yoshiro Y, Uehara M, Nihama M, and Tasaka M (2001). SGR2, a phospholipase-like protein, and ZIG/SGR4, a SNARE, are involved in the shoot gravitropism of *Arabidopsis* (Submitted).

Kervinen J, Tobin GJ, Costa J, Waugh DS, Wlodaver A, and Zdanov A (1999). Crystal structure of plant aspartic proteinase prophytepsin: inactivation and vacuolar targeting. *EMBO J.* **18:** 3947-3955.

Klionsky DK (1998). Nonclassical protein shorting to the yeast vacuole. *J. Biol. Chem.* **273:** 10807-10810.

Kirsch T, Paris N, Butler JM, Beevers L, and Rogers JC (1994). Purification and initial characterization of a potential plant vacuolar targeting receptor. *Proc. Nat. Acad. Sci. USA* **91:** 3403-3407.

Koide Y, Hirano H, Matsuoka K and Nakamura K (1997). The N-terminal propeptide of the precursor to sporamin acts as a vacuole-targeting signal even at the C-terminus of the mature part in tobacco cells. *Plant Physiol.* **114:** 863-870.

Lauber MH
Lukowitz V
cytokinesis-

Le Borgne
3 adaptor
membrane

Levanony
route of wh

Leyman B.
with a role

Lodish H,
(1995). Mo
711.

Lupashin
Characteriz
traffic. *Mol.*

Lukowitz W
embryo invo

Marcusson
SD (1994)
encoded by

Matsuoka
vacuolar pu
834-838.

Matsuoka
sensitivity
distinct so

Matsuoka
plant vacu

Miller E
character
Plant Cel

Lauber MH, Waizenegger I, Steinmann T, Schwarz H, Mayer U, Hwang I, Lukowitz W, and Jürgens G (1997). The *Arabidopsis* KNOLLE protein is a cytokinesis-specific syntaxin. *J. Cell Biol.* **139:** 1485-1493.

Le Borgne R, Alconda A, Bauer U, and Hoflack B (1998). The mammalian AP-3 adaptor-like complex mediates the intracellular transport of lysosomal membrane glycoproteins. *J. Biol. Chem.* **273:** 29451-29461.

Levanony HR, Rubin Y, Altschuler Y and Galili G (1992). Evidence for a novel route of wheat storage proteins to vacuoles. *J. Cell Biol.* **119:** 1117-1128.

Leyman B, Geelen D, Quintero FJ, and Blatt MR (1999). A tobacco syntaxin with a role in hormonal control of guard cell ion channels. *Science* **283:** 537-540.

Lodish H, Baltimore D, Berk A, Zipursky L, Matsudaira P, and Darnell J (1995). Molecular Cell Biology 3rd ed. Scientific American Books, Inc., pp709-711.

Lupashin VV, Pokrovskaya ID, McNew JA, and Waters MG (1997) Characterization of a novel yeast SNARE protein implicated in Golgi retrograde traffic. *Mol. Biol. Cell* **8:**1379-1388.

Lukowitz W, Mayer U, and Jürgens G (1996). Cytokinesis in the *Arabidopsis* embryo involves the syntaxin-related KNOLLE gene product. *Cell* **84:** 61-71.

Marcusson EG, Horazdovsky BF, Ceregjino JL, Gharakhanian E and Emr SD (1994). The sorting receptor for yeast vacuolar carboxypeptidase Y is encoded by the VPS10 gene. *Cell* **77:** 579-586.

Matsuoka K, and Nakamura K (1991). Propeptide of a precursor to a plant vacuolar protein required for vacuolar targeting. *Proc. Natl. Acad. Sci USA* **88:** 834-838.

Matsuoka K, Bassham DC, Raikhel NV, Nakamura K (1995). Different sensitivity to wortmannin of two vacuolar sorting signals indicates the presence of distinct sorting machineries in tobacco cells. *J. Cell Bio.* **130:** 1307-1318.

Matsuoka K, and Neuhaus JM (1999). *Cis*-elements of protein transport to the plant vacuoles. *J. Exp Bot.* **50:** 165-174.

Miller EA, Lee MCS, and Anderson MA (1999). Identification and characterization of a prevacuolar compartment in stigmas of *Nicotiana alata*. *Plant Cell* **11:** 1499-1508.

Morita MT,
(2001). Inv
gravitropism

Oyler GA,
Wilson M
protein. SN
Bio. **109:** 3

Paris N, St
functionally

Paris N, R
(1997). Mo
vacuolar so

Pfeffer SR
Cell Biol. **1:**

Pelham HR
49.

Puertollan
Sorting of
1712-1716

Rapoport
Biochem.

Rayner JC
of proteins

Rothman
55-63.

Robinson
the plant
lysosome

Saalbach
Different
695-708.

Sanderf
Marty F,

Morita MT, Kato T, Nagafusa K, Saito C, Ueda T, Nakano A and Tasaka M (2001). Involvement of the vacuoles of the endodermis in early process of shoot gravitropism in *Arabidopsis* (Submitted).

Oyler GA, Higgins GA, Hart RA, Battenberg E, Billingsley M, Bloom FE, and Wilson MC (1989). The identification of a novel synaptosomal-associated protein, SNAP-25, differentially expressed by neuronal subpopulations. *J. Cell Bio.* **109:** 3039-3052.

Paris N, Stanley CM, Jones, RL, and Rogers JC (1996). Plant cells contain two functionally distinct vacuolar compartments. *Cell* **85:** 563-572.

Paris N, Rogers SW, Jiang L, Kirsch T, Beevers L, Philips TE, Rogers JC (1997). Molecular cloning and further characterization of a probable plant vacuolar sorting receptor. *Plant Physiol.* **115:** 29-39

Pfeffer SR (1999). Transport-vesicle targeting: tethers before SNAREs. *Nature Cell Biol.* **1:** E17-E22.

Pelham HR (1998). Getting through the Golgi complex. *Trends Cell Biol.* **8:** 45-49.

Puertollano R, Aguilar R, Gorshkova I, Crouch R, and Bonifacino J (2001). Sorting of mannose 6-phosphate receptors mediated by the GGAs. *Science* **292:** 1712-1716.

Rapoport TA (1990). Protein transport across the ER membrane. *Trends. Biochem. Sci.* **15:**355-358.

Rayner JC, and Pelham HR (1997). Transmembrane domain-dependent sorting of proteins to the ER and plasma membarne in yeast. *EMBO J.* **16:** 1832-1841.

Rothman JE (1994). Mechanisms of intracellular protein transport. *Nature* **372:** 55-63.

Robinson DG, and Hinz G (1997). Vacuole biogenesis and proteins transport to the plant vacuole: a comparison with the yeast vacuole and the mammalian lysosome. *Protoplasma* **197:** 1-25.

Saalbach G, Jung R, Kunzy G, Saalbach I, Adler K, and Muntz K (1991). Different legumin protein domains act as vacuolar targeting signals. *Plant Cell* **3:** 695-708.

Sanderfoot AA, Ahmed SU, Marty Mazars D, Rapopot I, Kirchhausen I, Marty F, and Raikhel NV (1998). A putative vacuolar cargo receptor partially

colocalizes
Proc. Natl.

Sanderfoo
AtVAM3p r
Plant Phys

Sanderfoo
An abund
receptors.

Sanderfoo
between s
Golgi/preva

Sato MH,
Nishimura
molecule i
Chem. **272**

Shimada
pumpkin
characteris

Simonser
Syntaxin-

Sönller
(1993). A
sequentia
418.

Stepp J
complex.
the altern

Sutton F
a SNAR
395: 347

Tague B
plant va
Plant Ce

colocalizes with AtPEP12p on a prevacuolar compartment in *Arabidopsis* Roots. *Proc. Natl. Acad. Sci. USA* **95:** 9920-9925.

Sanderfoot AA, Kovaleva V, Zheng H, and Raikhel NV (1999). The t-SNARE AtVAM3p resides on the prevacuolar compartment in *Arabidopsis* root cells. *Plant Physiol.* **121:** 929-938.

Sanderfoot AA, Assaad, FF, and Raikhel NV (2000), The *Arabidopsis* genome. An abundance of soluble N-ethylmaleimide-sensitive factor adaptor protein receptors. *Plant Physiol.* **124:** 1558-1569.

Sanderfoot AA, Kovaleva V, Bassham DC, Raikhel NV (2001). Interactions between syntaxins identify at least five SNARE complexes within the Golgi/prevacuolar system of the *Arabidopsis*. Mol. Biol. Cell (submitted)

Sato MH, Nakamura N, Ohsumi Y, Kouchi H, Kondo M, Hara-Nishimura I, Nishimura K, and Wada Y (1997). The atVAM3 encodes a syntaxin-related molecule implicated in the vacuolar assembly in *Arabidopsis thaliana*. *J Biol. Chem.* **272:** 24530-24535.

Shimada T, Kuroyanagi M, Nishimura M, and Hara-Nishimura I (1997). A pumpkin 72 kDa membrane protein of precursor-accumulating vesicles has characteristics of a vacuolar sorting receptor. *Plant Cell Physiol.* **38:** 1414-1420.

Simonsen A, Bremnes B, Ronning E, Aasland and Stenmark H (1998). Syntaxin-16, a putative Golgi t-SNARE. *Eur. J. Cell Biol.* **75:** 223-231.

Sönller T, Bennett MK, Whiteheart SW, Scheller RH, and Rothman JE (1993). A protein assembly-disassembly pathway *in vitro* that may correspond to sequential steps of synaptic vesicle docking, activation and fusion. *Cell* **75:** 409-418.

Stepp JD, Huang K, and Lemmon SK (1997). The yeast adaptor protein complex, AP-3, is essential for the efficient delivery of alkaline phosphatase by the alternate pathway to the vacuole. *J. Cell Biol.* **139:** 1761-1764.

Sutton RB, Fasshauer D, Jahn R, and Brunger AT (1998). Crystal sturcture of a SNARE complex involved in synaptic excocytosis at 2.4 Å resolution. *Nature* **395:** 347-353.

Tague BW, Dickinson CD, and Chrispeels, MJ (1990). A short domain of the plant vacuolar protein phytohemagglutinin targets invertase to the yeast vacuole. *Plant Cell* **2:** 533-546.

Tolar LA
involves i
vesicle doc

Toyooka K
of a KDEL
endoplasm
germinatin

Vitale A a
vacuoles?

Ungerman
Wickner W
pentameri
homotypic

Von Scha
informatio
44: 339-3

Watson R
intracellul
Physiol. C

Whitehea
Rothman
ATPase
126: 945-

Whyte J
6-phosp
Biol. **11**:

Xu Y, W
29-kiloda
receptor
Biol. Che

Zheng H
The pla
from the
2251-22

Tolar LA and Pallanck L (1998). NSF functions in neurotransmitter release involves in rearrangement of the SNARE complex downstream of synaptic vesicle docking. *J. Neuronsic.* **18:** 10250-10256.

Toyooka K, Okamoto I, and Minamikawa T (2000). Mass transport of pro-form of a KDEL tailed cysteine protease (SH-EP) to protein storage vacuoles by endoplasmic reticulum-derived vesicles is involved in protein mobilization in germinating seeds. *J. Cell Biol.* **148:** 453-463.

Vitale A and Raikhel NV (1999). What do proteins need to reach different vacuoles? *Trends Plant Sci.* **4:** 149-155.

Ungermann C, von Mollard GF, Jensen ON, Margolis N, Stevens TH, Wickner W (1999). Three v-SNAREs and two t-SNAREs, present in a pentameric *cis*-SNARE complex on isolated vacuoles, are essential for homotypic fusion. *J. Cell Biol.* **145:** 1435-1442.

Von Schaewen A, and Chrispeels MJ (1993). Identification of vacuolar sorting information in phytohemagglutinin, an unprocessed vacuolar protein. *J. Exp. Bot.* **44:** 339-342.

Watson RT, and Pessin JE (2001). Transmembarne domain length determines intracellular membarne compartment localization of syntaxins 3, 4, and 5. *Am. J. Physiol. Cell Physiol.* **28:** C215-C223.

Whiteheart SW, Rossnagel K., Buhrow SA, Brunner M, Jaenicke R, and Rothman JE (1994). *N*-ethylmaleimide-sensitive fusion protein: a trimeric ATPase whose hydrolysis of ATP is required for membrane fusion. *J. Cell Biol.* **126:** 945–954.

Whyte JRC, and Munro S (2001). A yeast homolog of the mammalian mannose 6-phosphate receptors contributes to the sorting of vacuolar hydrolases. *Cur. Biol.* **11:** 1074-1078.

Xu Y, Wong SH, Tang BL, Subramaniam VN, Xhang T, and Hong W (1998). A 29-kilodalton Golgi soluble N-ethylmaeimide-sensitive factor attachment protein receptor (Vti1-rp2) implicated in protein trafficking in the secretory pathway. *J. Biol. Chem.* **273:** 21783-21789.

Zheng H, von Mollard GF, Kovaleva V, Stevens TH, and Raikhel NV (1999a). The plant vesicle associated SNARE AtVTI1a likely mediates vesicle transport from the *trans*-Golgi network to the prevacuolar compartment. *Mol. Biol. Cell* **10:** 2251-2264.

Zheng H.
family of
polymorp

Zheng H, Bassham DC, Conceição AS, and Raikhel NV (1999). The syntaxin family of proteins in *Arabidopsis*: a new syntaxin homologue shows a polymorphism between two ecotypes. *J. Exp Bot.* **50:** 915-924.

This

Harya

V. Ra

Z.H.

Chapter II

The Syntaxin Family of Proteins in *Arabidopsis*: a New Syntaxin Homologue Shows Polymorphism Between Two Ecotypes

This chapter was published in:

Haiyan Zheng, Diane C. Bassham, Alexandre de Silva Conceição and Natasha V. Raikhel (1999) Journal of Experimental botany 50: 915-924.

Z.H. contributed to all the figures.

A

fu

pl

of

ıd

Pr

he

At

tra

Ar

la

du

pr

va

in

Abstract

The syntaxin family of proteins are involved in vesicle sorting, docking and fusion in the secretory pathway. The discovery of several syntaxin homologues in plants (AtPEP12p, KNOLLE, AtVAM3p) suggested that the general mechanisms of protein trafficking through the secretory pathway also apply to plant cells. The identification of another syntaxin homologues, the *AtPLP* (AtPEP12p-Like Protein) gene, in *Arabidopsis thaliana*, which is not present in yeast, is reported here. The putative amino acid sequence of AtPLP shows high similarity to AtPEP12p and AtVAM3p, and AtPEP12p antibodies cross-react with *in vitro* translated AtPLP. The *AtPLP* gene shows polymorphism between two *Arabidopsis* ecotypes: In ecotype Columbia, it encodes a syntaxin homologue lacking the C-terminal transmembrane domain (TMD), whereas in ecotype RLD, due to a frame shift in the genomic sequence, it results in a typical syntaxin like protein with a C-terminal TMD. The distribution pattern of *AtPLP* mRNA among various tissues is different from that of *AtPEP12*, *AtVAM3* and *KNOLLE* mRNA, indicating that the protein may play a novel role in vesicle trafficking in plant cells.

Introduction

The plant secretory system is a series of organelles including the endoplasmic reticulum (ER), Golgi apparatus, plasma membrane, and vacuole. Soluble proteins containing an N-terminal signal sequence are co-translationally inserted into the ER lumen and from here are transported through the secretory system in transport vesicles which bud from one compartment and fuse with the next. From the ER, proteins are transported through the Golgi, cisternae to the *trans*-Golgi network, where a major sorting event occurs. Proteins are either secreted to the outside of the cell (the default pathway) or they are targeted to the vacuole via a prevacuolar compartment (PVC), a route that is believed to be receptor-mediated.

Protein Sorting to the Vacuole

For a soluble protein to reach the vacuole, it must contain a specific vacuolar sorting signal. Three types of vacuolar sorting signal have been identified. Some proteins contain a propeptide which comprises the sorting signal and which is removed from the protein upon deposition in the vacuole. Several proteins are known to contain a propeptide at their N-terminus, including sweet potato sporamin (Matsuoka and Nakamura, 1991) and barley aleurain (Holwerda *et al.*, 1992). Deletion and mutagenesis studies have shown that the N-terminal propeptide is required for transport to the vacuole, and have defined a conserved motif within the propeptides which is essential for proper sorting and thus is thought to be recognized by the sorting machinery (Holwerda *et al.*, 1992; Nakamura *et al.*, 1993).

The second type of propeptide signal is found at the C-terminus of several vacuolar proteins, including barley lectin (Bednarek *et al.*, 1990) and tobacco chitinase (Neuhaus *et al.*, 1991). No common motif can be identified between these sortig signals, and while the propeptides have been shown to be both necessary and sufficient for vacuolar transport, extensive mutagenesis studies have determined that there is no sequence motif that is required for their function (Dombrowski *et al.*, 1993; Neuhaus *et al.*, 1994). It is still not known whether a receptor protein is present at the *trans*-Golgi network that recognizes this type of signal.

Finally, a region of the mature protein can also serve as a sorting signal. Bean phytohaemagglutinin contains this type of signal (von Schaewen and Chrispeels, 1993), although the nature of the signal means that it is very difficult to identify precisely the residues responsible for targeting information. Legumin also appears to contain vacuolar sorting information within the mature protein, and the entire legumin α chain is required for efficient sorting (Saalbach *et al.*, 1991). The mechanism of which these signals work is not known.

Studies using the fungal metabolite wortmannin, an inhibitor of phospholipid metabolism in tobacco cells, have shown that proteins containing an N-terminal signal are transported to the vacuole by a different mechanism to proteins containing a C-terminal propeptide signal (Matsuoka *et al.*, 1995). In the presence of wortmanin, proteins containing the barley lectin C-terminal propeptide were secreted, whereas those containing the sporamin N-terminal signal were correctly sorted to the vacuole. In addition, membrane proteins are

transported by a different pathway compared to soluble proteins (Gomez ad Chrispeels, 1993). Therefore, it appears that multiple pathways to the vacuole exist within a single plant cell. In fact, some specialized cell types have been shown to contain two distinct types of vacuoles, which have their won discrete complement of proteins (Paris *et al.*, 1996; Di Samsebastiano *et al.*, 1998). In mature vegetative cells, these vacuoles are thought to fuse to form a single large central vacuole upon which all the vacuolar targeting pathways converge (Schroeder *et al.*, 1993).

By affinity chromatography using the aleurain N-terminal propeptides, a protein was isolated from pea clathrin coated vesicles which is thought to represent a sorting receptor for this signal (Kirsch *et al.*, 1994). This protein (BP-80) is an integral membrane protein which can also bind to other N-terminal signals, but not to the barley lectin C-terminal propeptide (Kirsch *et al.*, 1996). An *Arabidopsis* homologue of BP-80 (named AtELP) was identified by searching the DNA sequence database using motifs common to sorting receptors from various eukaryotic species (Ahmed *et al.*, 1997). Both the pea and *Arabidopsis* versions have been localized by electron microscopy to the Golgi apparatus (Paris *et al.*, 1997; Sanderfoot *et al.*, 1998) and in addition, AtELP was found at the prevacuolar compartment (Sanderfoot *et al.*, 1998). These receptor-like proteins are proposed to bind to the cargos (Proteins containing an N-terminal vacuolar sorting signal). At the *trans*-Golgi network and package them into clathrin coated vesicles for transport to the prevavuolar compartment.

Mechanis

Aft

trans-Gol

that orga

which ar

vesicle v

fusion a

stages c

probabl

systems

membr

al., 19

memb

SNAP

assoc

assoc

to fu

hypo

mem

syna

to th

mech

Mechanisms of Vesicle Docking and Fusion

After the formation of vesicles containing vacuolar cargo proteins from the *trans*-Golgi network, the vesicles have to be directed to the PVC, and fuse with that organelle. A number of proteins have been identified from various organisms which are required for the correct targeting, docking and fusion of a transport vesicle with its target membrane. As some components for vesicle targeting and fusion appear to be similar between many different organisms and different stages of the secretory pathway, the basic mechanisms for these processes are probably conserved. Information from the better studied yeast and mammalian systems can therefore, be very useful in the study of vesicle trafficking in plants.

Syntaxin 1 was originally isolated as a protein on the synaptic plasma membrane of neurons, where it is involved in neurotransmitter release (Bennet *et al.*, 1992). It has been shown to form a complex with several soluble and membrane-bound proteins such as NSF (N-ethylmaleimide-sensitive factor), α-SNAP (soluble NSF attachment protein), SNAP-25 (25 kDa synaptosomal associated protein), and synaptorbrevin (also known as VAMP, vesicle-associated membrane protein; Söllner *et al.*, 1993). These proteins are believed to function in vesicle trafficking according to the SNARE (SNAP-receptor) hypothesis (Bennett, 1995). Syntaxin 1 and SNAP-25 (t-SNAREs) on the target membrane (the pre-synaptic plasma membrane) are able to interact with synaptobrevin (a v-SNARE on the synaptic vesicle). α-SNAP and NSF can bind to this complex, and fusion of the vesicle with the target membrane occurs by a mechanism which is yet unclear. A number of syntaxin homologues have now

been id

Schelter

predicte

similar

differen

secreto

the pro

about

part is

where

memb

the C

cells

Jaga

hon

inv

co

m

fr

to

m

ef

been identified in non-nerve cells and in various organisms (Bennett and Scheller, 1993; Ferro-Novick and Jahn 1994). They have similar sequences and predicted secondary structures to syntaxin 1 and therefore, may function in a similar way in a variety of vesicle fusion events. It has been hypothesized that a different syntaxin isoform may be required for each transport step of the secretory pathway (Rothman, 1996).

Typical syntaxin homologues are type II transmembrane proteins. Most of the protein is hydrophilic and faces the cytosol, except for a hydrophobic domain about 10-30 amino acids long at the C-terminus of the protein. They hydrophilic part is thought to interact with other factors involved in vesicle trafficking, whereas the hydrophobic domain is responsible for anchoring the protein in the membrane (Aalto *et al.*, 1993; Jäntti *et al.*, 1994). Interestingly, syntaxins without the C-terminal transmembrane domain have also been found in mammalian cells, although their functions remain unknown (Hirai, 1993; Ibaraki *et al.*, 1995; Jagadish *et al.*, 1997; Simonsen *et al.*, 1998; Tang *et al.*, 1998). Several syntaxin homologues have now been identified in plants which presumably also are involved in transport through the secertory pathway. By functional complementation of the yeast (*Saccharomyces cerevisiae*) secretory pathway mutant *pep12*, Bassham *et al.* (1995) have isolated a cDNA clone (AtPEP12) from *Arabidopsis thaliana* ecotype Columbia that encodes a protein homologous to yeast Pep12p and other members of the syntaxin family. The yeast pep12 mutant is defective in transport of some soluble proteins to the vacuole (Becherer *et al.*, 1996) and is thought to function in transport between the *trans*-Golgi

network a

in transpo

microscop

Golgi net

syntaxin-

to the va

Arabidop

has been

et al., 1

KNOLLE

embryo

1997). S

them m

differe

Prote

AtVA

ecot

whe

that

fram

and

the A

network and the prevacuolar compartment. AtPEP12p may therefore play a role in transport to the vacuole in plants. AtPEP12p has been localized by electron microscopy to a PVC in *Arabidopsis* roots, and may act as a receptor for *trans*-Golgi network derived transport vesicles en route to the vacuole. A second syntaxin-like protein, Vam3p, is thought to be involved in transport from the PVC to the vacuole in yeast (Darsow *et al.*, 1997; Wada *et al.*, 1997). AtVAM3p is an *Arabidopsis* Vam3p homologue that can complement the yeast vam3 mutant and has been localized to the tonoplast in *Arabidopsis* shoot apical meristems (Sato *et al.*, 1997). By genetic analysis, another *Arabidopsis* syntaxin homologue, KNOLLE (Lukowitz *et al.*, 1996), is presumably involved in cytokinesis in the embryo, and is located at the forming cell plate during cell division (Lauber *et al.*, 1997). Several syntaxin homologues therefore exist in *Arabidopsis* and each of them may be involved in separated steps of the secretory system or function at different developmental stages, or in different tissues.

Another syntaxin homologue in *Arabidopsis*, AtPLP (AtPEP12-Like Protein), which encodes a protein showing high similarity to AtPEP12p and AtVAM3p, is reported here. The original cDNA clone isolated from the Columbia ecotype encodes a protein that has no transmembrane domain. Interestingly, when the AtPLP sequence of another ecotype, RLD, was examined. It was found that a typical syntaxin syntaxin transmembrane domain was regenerated by a frame shift at the 3' end of this gene. Although the protein sequences of AtPLP and AtPEP12p are very similar, and AtPEP12p antibody cross-react with AtPLP, the *AtPLP* mRNA has a distinct distribution pattern from that of *AtPEP12*. This

indicates that they may have different functions. The function of AtPLP in plants remains to be determined. But due to its high similarity to other proteins thought to be involved in vacuolar protein transport, it may also function in this process.

Materials and Methods

DNA and RNA Preparation

One gram of *Arabidopsis* rosette leaves was used for genomic DNA preparation according to Murry and Thompson (1980). Total RNA extraction from plant tissues was performed based on Bar-Peled *et al.*, (1995), except that the RNA was further purified by phenol:chloroform: sioamyl alcohol (25: 24: 1, by vol.) and chlorofrom sioamyl alcohol (24:1 v/v) extraction followed by ethanol precipitation. The pellets were resuspended in 200 μl DEPC-treated water. The concentrations of DNA or RNA in the extracts were determined by the OD_{260} value.

Reverse Transcription of mRNA and PCR

Reverse transcription reactions ere performed using AMV (avian myeloblastosis virus) reverse transcriptase (Boehringer Mannheim) following the manufacturer's protocol. 0.5-2 μg of total *Arabidopsis* RNA were added as template and 10 pmol of oligonucleotide (Primer 2: AAC ATA TAC TCA TTG ATG CTT) as the antisense primer. The reaction was incubated at 42°C for 1 hour.

For PCR reactions, 10 μl of reverse transcribed product or 0.1 μg of genomic DNA were amplified by using Taq polymerase (Gibco BRL) with primers

designed for *AtPLP* (Primer 1: CTT CCC TCA AGC CTA CAC ATC CAG and primer 2 as shown above) under the general conditions offered by Gibco BRL.

To construct a cDNA encoding AtPLP containing the transmembrane domain, reverse transcrition of RNA from roots of ecotype RLD was performed using oligo d(T) as a primer. Primer 1 (see above) and oligo d(T) were used to further amplify a DNA fragment from the reverse transcription product. This fragment was cloned into the *EcoRV* site of Bluescript SK (-) (Stratagene). The full length cDNA was reconstructed from this PCR fragment and the *AtPLP* EST cDNA (from Columbia) using *a BglII* site located within the PCR-amplified region.

DNA sequence analysis

The *AtPLP* cDNA was isolated as an Expressed Sequence Tag (EST clone F3C11T7, GeneBank accession number N95926) and inserted at the *EcoRI* site of Bluescript SK(-). The complete sequence was determined by the DNA sequencing facility at the WM Keck Foundation of Yale University and deposited in the GenBank database (Accession number U85036). For PCR and RT-PCR products, blunt ends were generated using Klenow fragment and inserted into the *EcoRV* site of Bluescript KS (-). Sequencing was performed by using a Sequenase 2.0 kit (United States Biochemical). Three independent clones of each product were analyzed to determine a final sequence.

Blotting Procedure

For northern analysis, 20 μg of *Arabidopsis* RNA were applied to each lane of a formaldehyde denaturing agarose gel which was run as described by Sambrook *et al.* (1989). For Southern analysis, 5 μg of genomic DNA were sued

for each restriction endonulcease reaction and digested DNA fragments were separated on a 0.7% agarose gel. Separated RNA or DNA samples were transferred to Hybound-N (Amersham) nylon membrane. Alternatively, various amounts of *in vitro*-transcribed mRNA were applied to a membrane for dot blot analysis. Blots were hybridized with either RNA or DNA probes. Antisense RNA probes were labeled using ^{32}P α-UTP by *in vitro* transcription of linearized plasmid. DNA probes were generated by random priming using ^{32}P α-dATP.

In vitro translation followed by immunoprecipitation

In vitro transcription, translation and immunoprecipitation were performed as described by Conceição *et al.* (1997). Antiserum used for immunoprecipitation was generated against AtPEP12p (Conceição, *et al.*, 1997).

***In vitro* Membrane Association Assay**

Two µl of canine pancreas microsomes (Promega) were added to 25 µl of *in vitro* translation product described above. The reaction was incubated at room temperature for 30 min. One ml of buffer A (50 mM trimethanolamine, pH 7.5, 0.4 M sucrose) was added to the reaction at the end of the incubation. Microsomes were pelleted by ultracentrifugation at 140, 00*0 g* for 10 min at 4°C. The pellets were washed with 1 ml of buffer A and resuspended in 25 µl of SNS sample buffer. Pellets and supernatant were separated on a SDS-PAGE gel and analyzed by autoradiography.

Results

AtPLP* Encodes a Putative Syntaxin Homologue in *Arabidopsis

Pep12p is a yeast syntaxin homologue required for the sorting of certain lumenal proteins to the lysosome-like vacuole (Becherer, *et al.*, 1996). An *Arabidopsis* homologue of PEP12 (AtPEP12) was isolated by complementation of the yeast pep12 mutant (Bassham *et al.*, 1995) and may be involved in protein transport to the vacuole in *Arabidopsis* (Bassham *et al.*, 1995; Conceição *et al.*, 1997). In order to identify other proteins potentially involved in transport to the plant vacuole, the *AtPEP12* nucleotide sequence was used to search the *Arabidopsis* EST database using the BLAST algorithm (Altschul *et al.*, 1990). A sequence was identified that showed similarity with AtPEP12. This 1263bp cDNA (From the PRL2 cDNA library, Newman *et al.*, 1994) was named *AtPLP* (*Arabidopsis thaliana* PEP12p-Like Protein) and sequence analysis indicated that it contains an open reading frame of 256 amino acids. This putative protein is 55% identical to AtPEP12p (Figure 2-1) and 74% identical to another syntaxin homologue found recently in *Arabidopsis*, AtVAM3p (Sato *et al.*, 1997). It displays a much lower sequence similarity to yeast Pep12p (Becherer *et al.*, 1996; 20% identity) and a mammalian Pep12p homologue synatxin 7 (Wang *et al.*, 1997; 26% identity), and no equivalent gene to *AtPLP* can be identified in the yeast genome. However, the AtPLP sequence lacks one feature contained within most members of the syntaxin family, including AtPEP12p and AtVAM3p: a C-terminal transmembrane domain (TMD), important for anchoring the protein in the target membrane and therefore for its function as a t-SNARE.

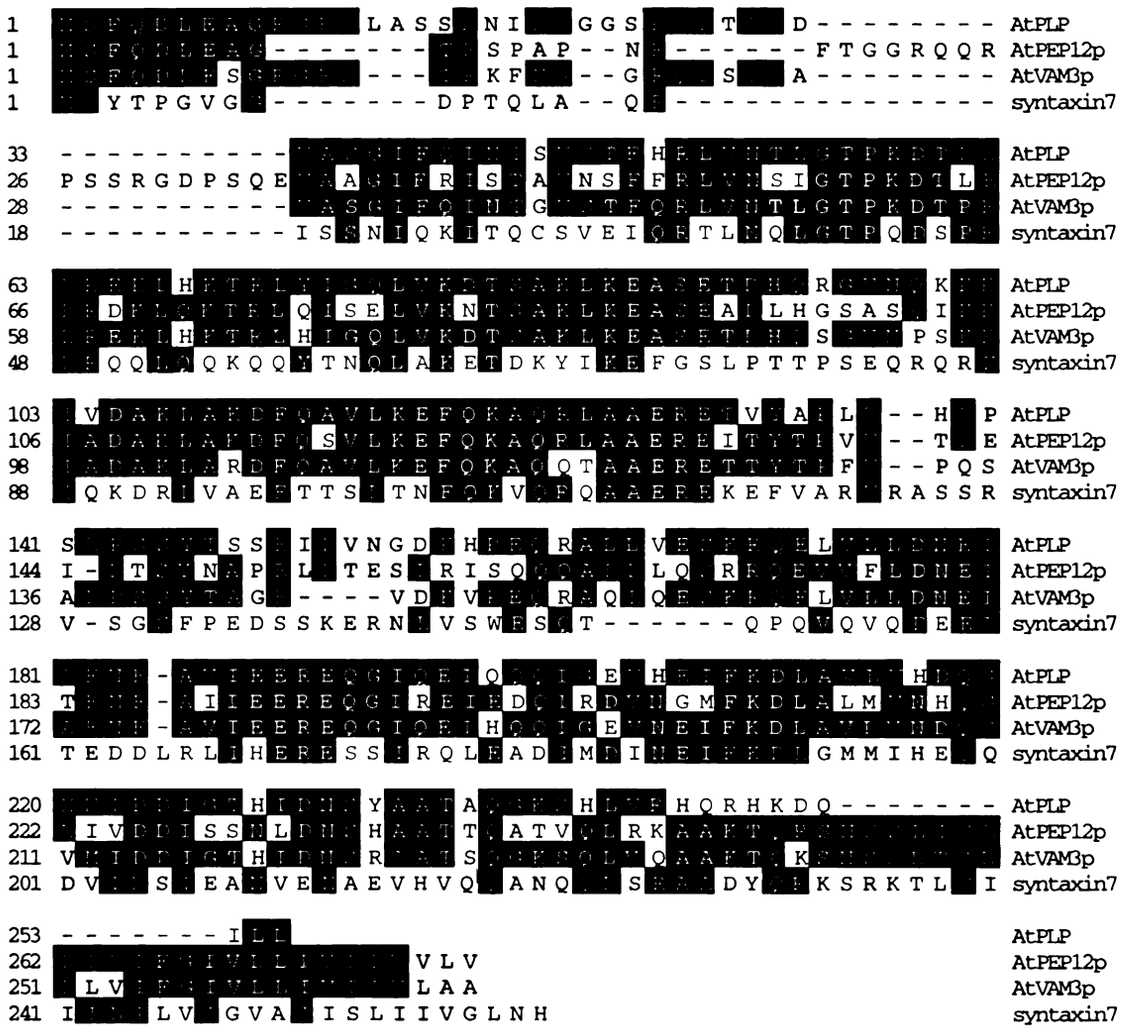

Figure 2-1. Amino acid sequence alignment of AtPLP and other plant, yeast and mammalian syntaxins. The sequence alignment was generated using the MegAlign program (DNASTAR Inc., Madison, WI, USA). The AtPLP sequence is based on *Arabidopsis* ecotype Columbia. Consensus amino acid residues are shaded.

Figure 2-2. The AtPLP amino acid sequence differs between *Arabidopsis* ecotypes. **A)** Nucleotide and amino acid sequences of the AtPLP cDNA from *Arabidopsis thaliana* ecotype Columbia. The sequence difference from ecotype RLD is shown in bold. Primers used for RT-PCR and PCR are marked here as primer 1 (sense) and primer 2 (antisense). **B)** Partial nucleotide sequence and derived amino acid sequences of AtPLP cDNA from *Arabidopsis* ecotype RLD based on RT-PCR products. The sequence difference from Columbia is shown in bold.

A

```
   1   A TTC GCG GCC GCG AGA GAG AGA AAC TCA CCG GGG AAT CTT GAA ATC ACC ATC ACA TCC TCT CTT CCC TCG ATC TCC

  79  GTT ATC GAC TGT AAA TCG AAT TTT GTT GTT GCT TTG TTT TCT TGG GCG AAT AAA AGA GGA TAA TTT AGT GGC GGG GTT

                                   M   S   F   Q   D   L   E   A   G   R   G   R   S   L   A   S   S   R   N
 157  TTC GAG AAA GAG AGA GAA AGA ATG AGT TTT CAA GAT TTA GAG GCG GGA AGA GGA AGA TCA TTA GCT TCT TCA AGG AAC

       I   N   G   G   G   S   R   Q   D   T   T   Q   D   V   A   S   G   I   F   Q   I   N   T   S   V   S
 235  ATC AAT GGT GGT GGT AGT AGA CAA GAC ACG ACT CAA GAT GTT GCT TCT GGT ATA TTT CAG ATC AAT ACA AGT GTT TCC

       T   F   H   R   L   V   N   T   L   G   T   P   K   D   T   P   E   L   R   E   K   L   H   K   T   R
 313  ACT TTC CAT CGT CTT GTC AAT ACT CTT GGT ACT CCT AAA GAT ACG CCT GAG CTC AGA GAG AAG CTG CAT AAG ACA AGA

       L   Y   I   G   Q   L   V   K   D   T   S   A   K   L   K   E   A   S   E   T   D   H   Q   R   G   V
 391  TTA TAT ATT GGA CAG TTA GTG AAA GAT ACA TCA GCT AAA CTT AAA GAA GCT AGT GAA ACT GAT CAT CAA AGA GGT GTA

       N   Q   K   K   K   I   V   D   A   K   L   A   K   D   F   Q   A   V   L   K   E   F   Q   K   A   Q
 469  AAT CAA AAG AAG AAG ATT GTG GAT GCT AAG CTT GCA AAG GAC TTT CAA GCT GTG TTG AAA GAG TTT CAA AAG GCT CAG

       R   L   A   A   E   R   E   T   V   Y   A   P   L   V   H   K   P   S   L   P   S   S   Y   T   S   S
 547  CGT CTT GCT GCT GAA AGA GAA ACC GTA TAT GCT CCT CTT GTC CAC AAG CCA TCT CTT CCC TCA AGC TAC ACA TCC AGT
                                                                                 primer1

       E   I   D   V   N   G   D   K   H   P   E   Q   R   A   L   L   V   E   S   K   R   Q   E   L   V   L
 625  GAG ATA GAT GTG AAT GGA GAT AAG CAT CCA GAG CAG CGT GCC CTT CTT GTG GAA TCA AAA AGA CAA GAA CTT GTA CTG

       L   D   N   E   I   A   F   N   E   A   V   I   E   E   R   E   Q   G   I   Q   E   I   Q   Q   Q   I
 703  TTG GAC AAT GAG ATT GCG TTC AAT GAG GCT GTT ATT GAG GAA AGA GAG CAA GGG ATA CAA GAA ATT CAG CAG CAA ATT

       G   E   V   H   E   I   F   K   D   L   A   V   L   V   H   D   Q   G   N   M   I   D   D   I   G   T
 781  GGC GAG GTG CAC GAG ATC TTC AAA GAC TTG GCA GTG TTG GTG CAC GAT CAA GGA AAC ATG ATA GAT GAT ATT GGT ACT

       H   I   D   N   S   Y   A   A   T   A   Q   G   K   S   H   L   V   R   H   Q   R   H   K   D   Q   I
 859  CAC ATC GAT AAC TCT TAC GCT GCA ACT GCC CAA GGA AAA TCC CAT CTC GTA AGG CAT CAA AGA CAC AAA GAT CAA ATT

       L   L   *
 937  CTT CTC TGA CGT GCT TGC TCT TGG TGA TTT TTG GTA TCG TGC TCA TGA TTG TTA TTA TAG TGC TCG CAG TTT GAT TTC

1015  CCC AAG CTC ATA AAA GCA TGG ACA AGT GCT TCA TCA TCA ATC AAG AAG CAT CAA TGA GTA TAT GTT TGT CAC GAC TCT
                                                                 primer2

1093  CTT TGT TCC TAC AAT TTA GTC TGT TGG ACT ATT GGT CTC TTG TTT CTT GTT ATC GAG TAT ATA GAG TAG TTC ACT TTG

1171  GTT TGA TTT GGC TTG TGT TTG CTG AGT CTT GGT TCT GAA GGA GAG AGT GTT ACT GCT TTG TCT CTG TAA TAT AAC TTG

1249  GTT CTG AAG CGG CCG CG
```

B

```
       R   L   A   A   E   R   E   T   V   Y   A   P   L   V   H   K   P   S   L   P   S   S   Y   T   S   S
 547  CGT CTT GCT GCT GAA AGA GAA ACC GTA TAT GCT CCT CTT GTC CAC AAG CCA TCT CTT CCC TCA AGC TAC ACA TCC AGT

       E   I   D   V   N   G   D   K   H   P   E   Q   R   A   L   L   V   E   S   K   R   Q   E   L   V   L
 625  GAG ATA GAT GTG AAT GGA GAT AAG CAT CCA GAG CAG CGT GCC CTT CTT GTG GAA TCA AAA AGA CAA GAA CTT GTA CTG

       L   D   N   E   I   A   F   N   E   A   V   I   E   E   R   E   Q   G   I   Q   E   I   Q   Q   Q   I
 703  TTG GAC AAT GAG ATT GCG TTC AAT GAG GCT GTT ATT GAG GAA AGA GAG CAA GGG ATA CAA GAA ATT CAG CAG CAA ATT

       G   E   V   H   E   I   F   K   D   L   A   V   L   V   H   D   Q   G   N   M   I   D   D   I   G   T
 781  GGC GAG GTG CAC GAG ATC TTC AAA GAC TTG GCA GTG TTG GTG CAC GAT CAA GGA AAC ATG ATA GAT GAT ATT GGT ACT

       H   I   D   N   S   Y   A   A   T   A   Q   G   K   S   H   L   V   K   A   S   K   T   Q   R   S   N
 859  CAC ATC GAT AAC TCT TAC GCT GCA ACT GCC CAA GGA AAA TCC CAT CTC GTA AAA GCA TCA AAG ACA CAA AGA TCA AAT

       S   S   L   T   C   L   L   L   V   I   F   G   I   V   L   M   I   V   I   I   V   L   A   V   *   F
 937  TCT TCT CTG ACG TGC TTG CTC TTG gTG ATT TTT GGT ATC GTG CTC ATG ATT GTT ATT ATA GTG CTC GCA GTT TGA TTT
```

The *AtPLP* Gene Displays an Ecotype Difference Between RLD and Columbia

From sequence analysis of the cDNA, AtPLP appeared to be a syntaxin homologue that lacked a transmembrane domain. However, the C-terminal transmemberane domain is thought to be critical for the membrane targeting of t-SNAREs (Jäntti *et al.*, 1994; Banfield *et al.*, 1994). In addition, membrane association is thought to be important for the function of syntaxin homologues in vesicle docking and fusion steps. To establish that this truncation was not due to an artifact during the PRL2 cDNA library generation, RT-PCR was performed using a pair of primers that would amplify the 3' end of the *AtPLP* mRNA. The same set of primers was also used for PCR from genomic DNA. Two ecotypes of *Arabidopsis* were used: Columbia, the ecotype from which the cDNA library was derived, and RLD, the ecotype used for most of the work on *AtPEP12* gene in this laboratory. The sequences derived from RT-PCR and genomic DNA PCR generated from *Arabidopsis* ecotype Columbia confirmed the cDNA sequence and therefore, that the protein truncation was genuine. However, the PCR sequences from RLD, unlike those from Columbia, turned out not to be in agreement with the original EST clone (Figure 2-2). Compared to the EST clone or Columbia sequence, the sequence from RT-PCR of RLD (and the genomic sequence at the corresponding region) had an additional adenosine that generated a frame shift as well as an a G-to-A transition (905-TCT CGT **AAA** **A**GC-916 instead of 905-TCT CGT **AAG** **G**C-915). Such a changed sequence

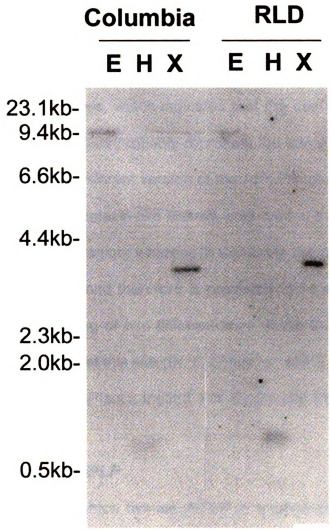

Figure 2-3. DNA gel blot analysis of the *AtPLP* gene. 5 μg of Arabidopsis DNA digested with *EcoRI* (E), *HindIII* (H) or *XbaI* (X) was hybridized with a ^{32}P-labeled *AtPLP* probe generated by random priming from the complete cDNA and visualized by autoradiography. Molecular size markers in kilobases (kb) are shown on the left.

results in a longer open reading frame with an extended C-terminus that shows a higher similarity to the C-terminal transmembrane domain of AtPEP12p and AtVAM3p.

Southern blot analysis (Figure 2-3) suggested that this gene is a single copy gene in both ecotypes, which indicates that the sequences from RT-PCR products of the two ecotypes probably represent the same gene. Each ecotype may therefore contain a different version of the AtPLP protein. AtPLP in ecotype RLD would be a typical syntaxin-like protein, anchored in the membrane by a C-terminal transmembrane region, whereas in Columbia the protein would lack the transmembrane domain, and therefore is predicted to be soluble. Interestingly, direct genomic sequencing of two different lines of the Columbia ecotype also revealed a polymorphism at this site (Dr. C Schueller, MIPS *Arabidopsis* genomic sequencing project, Max-Planck-Institut Für Biochemie Martinsried, Germany, personal communication).

Expression Pattern of *AtPLP*

To determine in which tissues *AtPLP* is expressed, RNA bybridization analysis was performed. Total RNA of flowers, leaves, roots and stems was extracted from *Arabidopsis* ecotypes Columbia and RLD. Equal amounts of RNA from the different tissues were separated on an agarose/formaldehyde gel and probed using a 3' gene-specific RNA probe of *AtPLP* including the 3' part of the translated region and the whole untranslated region. This probe specifically recognizes *AtPLP* (Figure 2-4A), but not *AtPEP12*. Figure 2-4B shows that *AtPLP* is expressed in both ecotypes and the expression patterns are similar to

Figure 2-4. *AtPLP* mRNA distribution pattern among tissues of *Arabidopsis* ecotype Columbia and RLD. **A)** Dot blot to demonstrate the specificity of the *AtPLP* probe. *In vitro*-transcribed mRNA of *AtPLP* and *AtPEP12* (1 ng or 0.1 ng) were applied to the membrane and hybridized with an *in vitro* transcribed $\alpha^{32}P$ UTP-labeled RNA probe. **B)** RNA gel blot analysis of *AtPLP* expression in different tissues of *Arabidopsis*. 20 μg of total RNA extracted from flowers (F), leafs (L), roots (R) and stems (S) at the comparable stages of ecotypes Columbia and RLD were separated by gel eletrophoresis, transferred to nylon membrane and hybridized with the *AtPLP*-specific probe described in **A**. **C)** RNA gel blot analysis of *AtPEP12* expression in different tissues of *Arabidopsis*. Identical to **B** except hybridized with a ^{32}P-labled AtPEP12 probe derived by random priming of the whole cDNA.

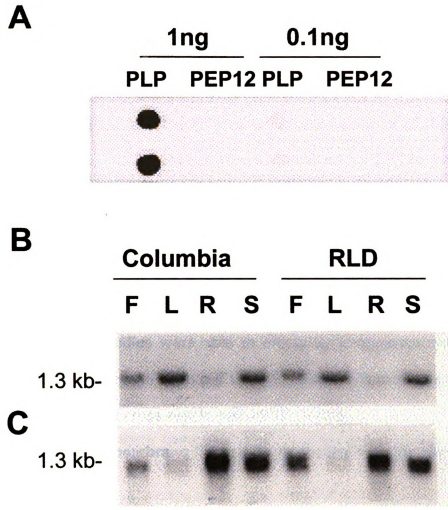
A
1ng
0.1ng
PLP
PEP12
PLP
PEP12
B
Columbia
RLD
F
L
R
S
F
L
R
S
1.3 kb-
C
1.3 kb-

each other. Unlike *AtPEP12*, which is highly expressed in roots but low in leaves (Figure 2-4C), *AtPLP* was expressed at higher levels in leaves, flowers, and stems than in roots.

AtPEP12p Antibodies Cross-react with AtPLP

The molecular weight of the *in vitro*-synthesized product of the *AtPLP* cDNA is about 33 kDa, smaller than *in vitro* synthesized AtPEP12p (about 35 kDa, Figure 2-5). This is consistent with AtPLP from the Columbia ecotype lacking the 17 amino acids at the carboxy-terminus that are present on AtPEP12p. Antiserum generated against AtPEP12p (Conceição *et al.*, 1997) was used to immunoprecipitate *in vitro* translation products of the *AtPEP12* and *AtPLP* cDNAs. The antibodies were able to efficiently immunoprecipitate the AtPLP product in addition to AtPEP12p (Figure 5). This result indicates that the antibody against AtPEP12p cross-reacts with AtPLP *in vitro*.

AtPLP Requires a Transmembrane Domain to Associate with Membranes *in vitro*

The transmembrane domain is important for the function of syntaxin homologues. There are two versions of AtPLP in different ecotypes of *Arabidopsis*. One has a TMD and the other one does not. To determine whether the TMD is essential for anchoring AtPLP to the membrane, an *in vitro* membrane association assay was performed. AtPLP was synthesized *in vitro* with or without the TMD and mixed post-translationally with canine pancreatic microsomes to allow membrane insertion. Figure 2-6 shows that AtPLP + TMD was associated with the microsomal fraction, but AtPLP-TMD was not. Thus, the

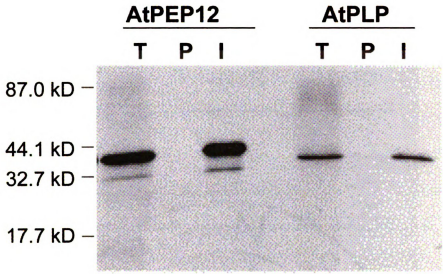

Figure 2-5. Immunoprecipitation of *in vitro* translation products of AtPEP12 and AtPLP using antiserum against AtPEP12p. T: 1/25 of total in vitro translation products. P: 1/10 of immunoprecipitated pellets using pre-immune serum. I: 1/10 of immunoprecipitated pellets using AtPEP12p antiserum. Molecular mass markers in kilodaltons (kDa) are given on the left.

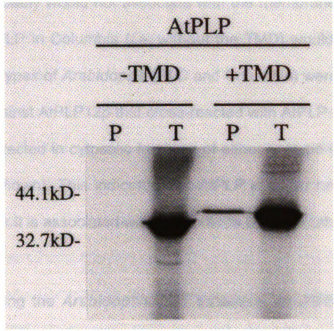

Figure2-6. *In vitro* membrane association assay for AtPLP ± TMD. The mRNA encoding AtPLP-TMD or AtPLP+TMD was translated *in vitro* and incubated with canine pancreatic microsomes. Microsomes were pelleted and equal amounts of the total reaction (T) or pellet (P) were separated by SDS-PAGE and visualized by fluorography. Molecular weight markers in kilodaltons (KDa) are given on the left.

C-terminal hydrophobic domain is likely to be critical for membrane association of syntaxin homologues. AtPLP lacking this domain, unlike other syntaxin homologues, probably would not associate with the membrane. If this were the case *in vivo*, AtPLP in Columbia (*i.e.* without the TMD) would be cytosolic. To test this, two ecotypes of *Arabidopsis* (RLD and Columbia) were examined using the antiserum against AtPLP12p that cross-reacted with AtPLP *in vitro*. However, no signal was detected in cytosolic fractions of either ecotype (Conceição *et al.*, 1997, data not shown). This indicates that *AtPLP* is either not expressed at a detectable level or it is associated with membranes by some other means.

Discussion

By searching the *Arabidopsis* EST database, an *AtPEP12* homologue, *AtPLP* was identified. The RNA distribution pattern of *AtPLP* was distinct from any of the know *Arabidopsis* syntaxin homologues, including *AtPEP12* (Bassham *et al.*, 1995), *AtVAM3* (Sato *et al.*, 1997) and *KNOLLE* (Lukowitz *et al.*, 1996). *KNOLLE* mRNA accumulates chiefly in flowers and siliques, and the protein is probably involved in cell cytokinesis (Lukowitz *et al.*, 1996), The *AtPEP12* and *AtVAM3* mRNA level is high in roots but very low in leaves. In contrast, *AtPLP* mRNA accumulated more in leaves than in roots. If similar mechanisms of vesicle sorting, docking and fusion found in mammalian cells and yeast operate in plant cells, there are likely to be several different syntaxin homologues located on the surface of different syntaxin homologues located on the surface of different organelles. *AtPLP* may encode a syntaxin homologue responsible for a step in the secretory pathway different from AtPLP12p or AtVAM3p, or it may

perform its function in a separated developmental stage or tissue. For example, there are known to be several pathways for the transport of soluble and membrane proteins to the vacuole in plants (Gomez and Chrispeels, 1993, Matsuoka *et al.*, 1995, Hohl *et al.*, 1996). It is possible that AtPEP12p functions in one pathway and the APLP in another.

Each syntaxin homologue is thought to be associated with a specific membrane by its C-terminal hydrophobic domain. The cytosolic part of the protein interacts with other factors of the secretory pathway. The lack of the transmembrane domain in the Columbia from of AtPLP is of great interest. There are some examples of syntaxin-like proteins without the transmembrane domain in mammalian cells (Bennett *et al.*, 1993; Hirai 1993; Ibaraki *et al.*, 1995; Jagadish *et al.*, 1997; Simonsen *et al.*, 1998; Tang *et al.*, 1998). Possibly the result of alternative splicing. In our case, however, a frame shift probably transforms this protein from an integral membrane protein to a soluble protein. Based on *in vitro* experiments done here and with yeast Sso2p (Jäntti *et al.*, 1994), syntaxin homologues without the C-terminal hydrophobic domain cannot insert into the membrane. It is possible that they are localized in the cytosol and function by binding to other factors, such as synaptobrevin, NSF etc. that normally interact with membrane-associated syntaxin homologues. These soluble forms of syntaxin homologues apparently occur in both mammalian cells and plant. Thus, they may play some specialized role. These proteins may regulate vesicle sorting, docking and fusion by binding to factors interacting with membrane-bound syntaxins.

In *Arabidopsis* ecotype Columbia, AtPLP without the transmembrane domain is expressed at least at the mRNA level, and antiserum raised against AtPEP12p cross-reacts with the *in vitro* translation product of AtPLP. Using this antiserum, it would be expected that AtPEP12p and AtPLP are localized both to the membrane (AtPEP12p) and cytosolic (AtPLP) fractions of plant protein extracts. However, no signal has ever been detected in the soluble fraction (data not shown) using these antibodies. The AtPLP protein level may not be high enough to be detected by the antibody. It is also possible that this protein still associates with the membrane by a post-translational modification or through protein-protein interactions. In that case, AtPLP could perform a normal function as a syntaxin homologue in plants. The authors had some difficulty in generating a specific antibody against this protein that dos not cross-react with AtPEP12p. Therefore, in order to determine the subcelluar location of this protein, transgenic plants containing epitope-tagged AtPLP are being generated. Introducing the untagged *AtPLP* gene (Without the TMD) into plant will also be useful to investigate possible dominant negative or regulatory effects of this syntaxin homologue in plants.

Even before the genomic sequencing of *Arabidopsis* has been completed, genes encoding putative syntaxin-like proteins have been identified which do not exist in yeast. This is not surprising, given the complexity of different tissues and developmental stages in plants. It is expected that the complete sequence of the *Arabidopsis* genome will reveal that the total number of syntaxin-like proteins in plants is greater than that in yeast. The challenge for the future will be to discern

the function of all of these homologues and their role in vesicle trafficking between different organelles of the secretory pathway and in different cell types.

References

Aalto MK, Ronne H, and Keränen S (1993). Yeast syntaxins Sso1p and Sso2p belong to a family of related membrane proteins that function in vesicular tranport. *EMBO J.* **12:** 4095-4104

Ahmed SU, Bar-Peled M, and Raikhel NV (1997). Cloning and subcellular localization of an *Arabidopsis* receptor-like protein that shares common features with protein-sorting receptors of eukaryotic cells. Plant Phys. 114: 325-336.

Altschul SF, Gish V, Miller W, Myers EW, and Lipman DJ (1990). Basic local alignment search tool. *J. Mol. Biol.* **215:** 403-410.

Banfield DK, Lewis MJ, Rabouille C, Warren G, and Pelham HRB (1994). Localization of Sed5, a putative vesicle targeting molecule to the *cis*-Golgi network, involves both its transmembrane and cytoplasmic domains. *J. Cell Biol* **127:** 357-371.

Bar-Peled M, Conceição AS, Frigerio L, and Raikhel NV (1995). Expression and regulation of aERD2, a gene encoding the KDEL receptor homologue in plants, and other genes encoding proteins involved in ER-Golgi vesicular trafficking. *Plant Cell* **7:** 667-676.

Bassham DC, Gal S, Conceição AS, and Raikhel NV (1995). An *Arabidopsis* syntaxin homologue isolated by functional complementation of a yeast pep12 mutant. *Pro. Nat. Acad. Sci. USA* **92:** 7262-7266.

Becherer KA, Rieder SE, Emr SD, and Jones EW (1996). Novel syntaxin homologue, Pep12p, required for the sorting of lumenal hydrolases to the lysosome-like vacuole in yeast. *Mol. Biol. Cell* **7:** 579-594.

Bednarek SY, Wiklins TA, Dombrowski JE, and Raikhel NV (1990). A carboxy-terminal propeptide is necessary for proper sorting of barley lectin to vacuoles of tobacco. *Plant Cell* **2:** 1145-1155.

Bennett MK (1995). SNAREs and the specificity of transport vesicle targeting *Curr. Opin. Cell Biol.* **7:** 581-586.

Bennett MK, Calakos N, and Scheller RH (1992). Syntaxin: a synaptic protein implicated in docking of synaptic vesicles at presynaptic active zones. *Science* **257:** 255-259.

Bennett MK, Garcia-Arraras JE, Elferink LA, Peterson K, Fleming AM, Hazuka CD, and Scheller RH (1993). The syntaxin family of vesiclar transport receptors. *Cell* **74:** 863-873.

Conceição AS, Marty-Mazars D, Bassham DC, Sanderfoot AA, and Marty F, Raikhel NV (1997). The syntaxin homologue AtPEP12p resides on a late post-Golgi compartment in plants. *Plant cell* **9:** 571-582.

Darsow T, Rieder SE, and Emr SD (1997). A multispecificity syntaxin homologue, Vam3p, essential for autophagic and biosynthetic protein transport to the vacuole. *J. Cell Biol.* **138:** 517-529.

Di Sansebastiano GP, Paris N, Marc-Martin S, and Neuhaus JM (1998). Specific accumulation of GFP in a non-acidic vacuolar compartment via a C-terminal propeptide-mediated sorting pathway. *Plant J.* **15:** 449-457.

Dombrowski JE, Schroeder MR, Bednarek SY, and Raikhel NV (1993). Determination of the functional elements within the vacuolar targeting signal of barley lectin. *Plant Cell* **5:** 1113-1124.

Ferro-Novick S, and Jahn R (1994). Vesicle fusion from yeast to man *Nature* **370:** 191-193.

Gomez L, and Chrispeel MJ (1993). Tonoplast and soluble vacuolar proteins are targeted by different mechanisms *Plant Cell* **5:** 1113-1124.

Hirai Y (1993). Molecular cloning of human epimorphin. *Biochem. Biophys. Res. Commun.* **191:** 1332-1337.

Hohl I, Robinson DG, Chrispeels MJ, and Hinz G (1996). Transport of storage proteins to the vacuole is mediated by vesicles without a clathrin coat. *J. Cell Sci.* **109:** 2539-2550.

Holwerda BC, Padgett HS, and Rogers JC (1992). Proaleurain vacuolar targeting is mediated by short contiguous peptide interactions. *Plant Cell* **4:** 307-318.

Ibaraki K, Horikawa HP, Morita T, Mori H, Sakimura K, Mishina M, Saisu J, and Abe T (1995). Identification of four different forms of syntaxin 3. *Biochemi. Biophys. Res. Commun.* **211:** 997-1005.

Jagadish MN, Tellam JT, Macaulay SL, Gough KH, James DE, and wsard CW (1997) Novel isoform of syntaxin 1 is expressed in mammalian cells. *Biochem. J.* **321:** 151-156.

Jäntti J, Keränen S, Toikkanen J, Kuismanen E, Ehnholm C, Söderlumd J, and Olkkonen VM (1994) Membrane insertion and intracellular transport of yeast syntaxin Sso2p in mammalian cells. *J. Cell Sci.* **107:** 3623-3633.

Kirsch T, Paris N, Bulter JM, Beevers L, and Rogers JC (1994). Purification and initial characterization of a potential plant vacuolar targeting receptor. *Proc. Natl. Acad. Sci. USA* **91:** 3403-3407.

Krisch I, Sallbach G, raikhel NV, and Beevers L (1996). Interaction of a potential vacuolar targeting receptor with amino- and carboxy-terminal targeting determinants. *Plant Physiol.* **111:** 469-474.

Lauber MH, Waizenegger I, Steinmann T, Schwarz H, Mayer U, Hwang I, Lukowitz W, and Jürgens G (1997). The *Arabidopsis* KNOLLE protein is a cytokinesis-specific syntaxin. *J. Cell Biol.* **139:** 1485-1493.

Lukowitz W, Mayer U, and Jürgens G (1996) Cytokinesis in the *Arabidopsis* embryo involves the syntaxin-related KNOLLE gene product. *Cell* **84:** 61-71.

Matsuoka K, Bassham DC, Raikhel NV, and Nakamura K (1995). Different sensitivity to wortmannin of two vacuolar sorting signals indicates the presence of distinct sorting machineries in tobacco cells. *J. Cell Biol.* **130:** 1307-1318.

Matsuoka K, and Nakamura K (1991). Propeptides of a precursor to a plant vacuolar protein required for vacuolar targeting. *Proc. Natl. Acad. Sci. USA* **88:** 834-838.

Murray MG, and Thompson WF (1980). Rapid isolation f high molecular weight plant DNA. *Nucleic Acids Res.* **8:** 4321-4325.

Makamura K, Matsuoka K, Mikumoto F, and Watanabe N (1993). Processing and transport to the vacuole of a precursor to sweet potato sporamin in transformed tobacco cell like BY-2. *J. Experi. Bot.* **44 (Supplement):** 331-338.

Neuhaus JM, Pietrzak M, and Boller T (1994). Mutation analysis of the C-terminal vacuolar targeting peptide of tobacco transition between intracellular retension and secretion into the extracellular space. *Plant J.* **5:** 45-54.

Neuhus JM Sticher KL, Meins F, and Boller T (1991). A short C-terminal sequence is necessary and sufficient for the targeting of chitinases to the plant vacuole. *Proc. Natl. Acad. Sci. USA* **88:** 10362-10366.

Newman T, de Bruiin FJ, Green P, Keegstra K, Kende H, McIntosh L, Ohirogge K, Raikhel N, Sommerville S, Thomashow M, Retzel E, and Somerville C (1994). Genes galore: a summary of methods for accessing results from large -scale partial sequencing of anonymous *Arabidopsis* cDNA clones. *Plant Phys.* **106:** 1241-1255.

Paris N, Stanley CM, Jones RJ, and Rogers JC (1996). Plant cells contain two functionally distinct vacuolar compartments. *Cell* **85:** 563-572.

Rothman JE (1996). The protein machinery of vesicle budding and fusion *Protein Sci* **5:** 185-194.

Saalbach G, Jung R, Kunze G, Saalbach I, Adler K, and Müntz K (1991). Different legumin protein domains act as vacuolar targeting signals. *Plant Cell* **3:** 695-708.

Sambrook K, Frisch EF, and Maniatis T (1989). Molecular Cloning, a laboratory manual 2nd ed. NY: Cold Spring Harbor Laboratory Press.

Sanderfoot AA, Ahmed SU, Marty-Mazars D, Rapoport I, Kirshhausen T, Marty F, and Raikhel NV (1998). A putative vacuolar cargo receptor partially colocalizes with AtPEP12p on a prevacuolar compartment in *Arabidopsis* roots. *Proc. Natl. Acad. Sci. USA* **95:** 9920-9925.

Sato MH, Nakamura N, Ohsumi Y, Kouchi H, Kondo M, Hara-Nishimura I, Mishimura M, and Wada Y (1997). The *AtVAM3* encodes a syntaxin-related mulecule implicated in the vacuolar assembly in *Arabidopsis thaliana*. *J. Bio. Chem.* **272:** 24530-24535.

Schroeder MR. Borkhsenious ON, Matsuoka K, Nakamura K, and Raikhel NV (1993). Colocalization of barley lectin and sporamin in vacuoles of trangenic tobacco plants. *Plant Physol* **101:** 451-458.

Simonsen A, Bremners B, Ronning E, Aasland R, and Stenmark H (1998). Syntaxin -16, a putative Golgi t-SNARE. *Eur. J. Cell Biol.* **75:** 223-231.

Söllner I, Whiteheart SW, Brunner M, Erdjument-Bromage H, Geromanos S, Tempst P, and Rothman JE (1993). SNAP receptors implicated in vesicle trageting and fusion. *Nature* **362:** 318-324.

Tang BL, Low DYH, and Hong WJ (1998). Syntaxin 11: a member of the syntaxin family without a carboxyl terminal transmembrane domain. *Biochem. Biophys. Res. Commun.* **245:** 627-632.

Von Schaewen A, and Chrispeels MJ (1993). Identification of vacuolar sorting information in phytohemagglutinin, an unprocessed vacuolar protein. *J. Experi. Bot.* **44 (Supplement)**: 339-342.

Wada Y, Nakamura N, Obsumi Y, and Hirata A (1997). Vam3p, a new member of syntaxin-related proteins, is required for vacuolar assembly in the yeast *Saccharomyces cerevisiae*. *J. Cell Sci.* **110:** 1299-1306.

Wang H, Frelin L, and Pevsner J (1997). Human syntaxin 7: a Pep12p/Vps6p homologue implicated in vesicle trafficking to lysosomes. *Gene* **199:** 39-48.

Chapter III

The Plant V-SNARE AtVTI1a Likely Mediates Vesicle Transport from the TGN to the PVC

This chapter was published in :

Haiyan Zheng, Gabriele Fischer von Mollard, Valentina Kovaleva, Tom H. Stevens, and Natasha V. Raikhel (1999) The plant vesicle associated SNARE AtVTI1a likely mediates vesicle transport from the *trans*-Golgi network to the prevacuolar compartment. Molecular Biology Of the Cell 10: 2251-2264.

Z.H. and G.F.M. contributed equally to this work. H.Z. has major contributions to all the figures except yeast complementation experiments were done in collaboration with G.F.M, and the immunocytochemical work was done in collaboration with V.K.

Abstract

Membrane traffic in eukaryotic cells relies on recognition between v-SNAREs on transport vesicles and t-SNAREs on target membranes. Here we report the identification of AtVTI1a and AtVTI1b, two *Arabidopsis* homologues of the yeast v-SNARE Vti1p, which is required for multiple transport steps in yeast. AtVTI1a and AtVTI1b share 60% amino acid identity with one another and are 32 and 30% identical to the yeast protein, respectively. By suppressing defects found in specific strains of yeast *vti1* temperature sensitive mutants, we show that AtVTI1a can substitute for Vti1p in Golgi-to-PVC transport, whereas AtVTI1b substitutes in two alternative pathways: the vacuolar import of alkaline phosphatase and the so-called cytosol-to-vacuole pathway utilized by aminopeptidase I. Both AtVTI1a and AtVTI1b are expressed in all major organs of *Arabidopsis*. Using subcellular fractionation and immuno-electron microscopy, we show that AtVTI1a co-localizes with the putative vacuolar cargo receptor AtELP on the *trans*-Golgi network (TGN) and the prevacuolar compartment (PVC). AtVTI1a also co-localizes with the t-SNARE AtPEP12p to the PVC. In addition, AtVTI1a and AtPEP12p can be co-immunoprecipitated from plant cell extracts. We propose that AtVTI1a functions as a v-SNARE responsible for targeting AtELP-containing vesicles from the TGN to the PVC, and that AtVTI1b is involved in a different membrane transport process.

Introdcution

In the secretory and endocytic pathways, the movement of proteins and membranes from one location to another relies mostly on vesicular transport. One fundamental question is how the vesicles recognize the correct target membrane. The SNARE hypothesis offers a widely accepted explanation of the mechanism of specificity in vesicle targeting (Söllner *et al.*, 1993). SNAREs (SNAP receptors) are membrane proteins found on both transport vesicles (v-SNARE) and target organelles (t-SNARE). The specific interactions between t- and v-SNAREs ensure that vesicles are targeted to the correct compartment and lead to membrane fusion. The best-characterized SNARE complex consists of syntaxin, SNAP25 (t-SNAREs on the presynaptic membrane), and VAMP-1/synaptobrevin (v-SNARE on synaptic vesicles); it is involved in synaptic vesicle exocytosis (Hanson *et al.,* 1997; Sutton *et al.*, 1998). Homologues of these SNAREs are found to be involved in intracellular vesicle transport processes in yeast and mammalian systems, further supporting this hypothesis (for review see Hay and Scheller, 1997). Several t-SNAREs have been found in plant cells recently (Bassham *et al.*, 1995; Lukowitz *et al.*, 1996; Sato *et al.,* 1997; Zheng *et al.,* 1999), suggesting that the SNARE hypothesis also applies to plant cells.

Much of our knowledge about vesicular transport to the vacuole has been gained from yeast studies. Several pathways to the yeast vacuole have been described. The best characterized pathway for delivery of soluble proteins to the vacuole is the carboxypeptidase Y (CPY) pathway. At the *trans*-Golgi or *trans*-Golgi network (TGN), CPY is bound by its receptor (Pep1p/Vps10p) and

packaged into transport vesicles. These vesicles then fuse with the prevacuolar compartment (PVC)/late endosome. The PVC t-SNARE Pep12p is required for correct sorting of CPY (Jones, 1977; Becherer *et al.*, 1996). The v-SNARE Vti1p interacts both genetically and biochemically with Pep12p (Fischer von Mollard *et al.*, 1997). It was thus proposed that Vti1p and Pep12p form a SNARE complex that is involved in docking and fusion of TGN-derived transport vesicles with the PVC. It has recently been reported that a subset of proteins, including alkaline phosphatase (ALP), is transported to the vacuole by an alternative route, independent of the CPY pathway, that bypasses the PVC (Cowles *et al.,* 1997a; Piper *et al.,* 1997). This transport pathway requires the AP-3 adaptor complex (Cowles *et al.,* 1997b; Stepp *et al.,* 1997) and Vam3p, the vacuolar t-SNARE (Darsow *et al.*, 1997; Piper *et al.*, 1997; Wada *et al.,* 1997; Srivastava and Jones, 1998). Vti1p has very recently been implicated as the v-SNARE that interacts with Vam3p in the ALP pathway to the yeast vacuole (Fischer von Mollard and Stevens, 1999). Another route to the vacuole, directly from the cytoplasm, has recently been analyzed using the hydrolase aminopeptidase I (API) (Klionsky, 1998). This cytosol-to-vacuole transport (Cvt) pathway is blocked in *vam3* mutant cells (Darsow *et al.*, 1997; Srivastava and Jones, 1998) as well as in *vti1* mutant cells (Fischer von Mollard and Stevens, 1999). Thus, in yeast, multiple pathways are used for delivering vacuolar proteins, all of which require Vti1p. In addition to a role in transport pathways to the vacuole, Vti1p also functions in retrograde transport within the Golgi complex by interacting with the *cis*-Golgi t-SNARE Sed5p (Lupashin *et al.*, 1997; Fischer von Mollard *et al.*, 1997). Furthermore,

Holth

additi

these

transp

identi

the f

prote

the r

term

Alth

prot

tha

con

Ara

con

loc

al.

str

19

to

(Ar

pro

Holthuis *et al.* (1998) reported the biochemical interaction of Vti1p with two additional yeast Golgi/endosomal t-SNAREs, Tlg1p and Tlg2p. Taken together, these data suggest that Vti1p is a v-SNARE involved in multiple membrane transport pathways in yeast.

In plants, three types of vacuolar sorting signals (VSSs) have been identified (for review see Bassham and Raikhel, 1997). These VSSs can occur in the form of a propeptide (either N-terminal or C-terminal) that is removed proteolytically during or after transport to the vacuole, or they can form a part of the mature protein. Interestingly, plant vacuolar proteins with N-terminal and C-terminal VSSs appear to use independent pathways (Matsuoka *et al.*, 1995). Although very little information is available on the targeting signals of tonoplast proteins in plants, it is known that they are transported by a different mechanism than that of soluble vacuolar proteins (Gomez and Chrispeels, 1993). Several components of the plant secretory machinery have been isolated as well. In *Arabidopsis*, a Pep12p homologue, AtPEP12p, is found by its ability to complement a yeast *pep12* mutant (Bassham *et al.*, 1995). AtPEP12p is localized to a novel compartment by EM and biochemical analysis (Conceição *et al.*, 1997; Sanderfoot *et al.*, 1998). AtELP was identified in *Arabidopsis* by its structural similarity to the EGF receptor and other cargo receptors (Ahmed *et al.*, 1997). AtELP is enriched in clathrin-coated vesicles (CCVs), it has been localized to the TGN, and colocalized with AtPEP12p on the PVC by electron microscopy (Ahmed *et al.*, 1997; Sanderfoot *et al.*, 1998). AtELP is homologous to BP-80, a protein from pea CCVs that has been shown to bind a broad range of plant

VSSs
anoth
sequ
data
some
AtPE
mam
TGN
the r

enc
gen
yea
colo
PVC
AtP
prop
carg

Mat

Plas

leu2-

(*MAT*

VSSs, but not to the C-terminal VSSs (Kirsch *et al.*, 1994, 1996). Recently, another AtELP-homologue from pumpkin has been found to recognize certain sequence patches in some cargo proteins (Shimada *et al.*, 1997). All of these data support the notion that AtELP is a cargo receptor involved in transport of some but not all vacuolar proteins. It is postulated that the compartment where AtPEP12p resides is the equivalent of the PVC in yeast or the late endosome in mammalian cells. This compartment accepts the transport vesicles formed at the TGN as CCVs. Those vesicles contain at least a subset of vacuolar proteins and the receptors (such as AtELP) involved in packaging them at the TGN.

We have identified two *Arabidopsis* genes (*AtVTI1a* and *AtVTI1b*) encoding proteins homologous to yeast Vti1p. Although each *Arabidopsis VTI1* gene can function in yeast, they function in different sorting pathways to the yeast vacuole. By studying T7-epitope-tagged AtVTI1a, we found that AtVTI1a colocalized with the putative vacuolar cargo receptor AtELP on the TGN and the PVC, and with AtPEP12p on the PVC. Co-immunoprecipitation of AtVTI1a with AtPEP12p suggested that these two proteins associate in the cell. Thus, we propose that AtVTI1a is a plant v-SNARE involved in the transport of vacuolar cargo from the Golgi to the PVC.

Materials and Methods

Plasmids, Yeast Strains and Growth Media

Mutant strains of *vti1* were derived from the yeast strains SEY6210 (*MAT_ leu2-3,112 ura3-52 his3-Δ200 trp1-Δ901 lys2-801 suc2-Δ9 mel-*) and SEY6211 (*MATα leu2-3,112 ura3-52 his3-Δ200 trp1-Δ901 ade2-101 suc2-Δ9 mel-*

(Robin

(FvMY

been d

Steven

GAL1-

mutatio

introdu

codons

vector

AtVTI1

open r

the sa

fusion

subclo

expres

fragm

Inc., F

the A

cytop

fragm

coli B

(Robinson *et al.*, 1988). The strains *vti1Δ* (FvMY6), *vti1-1* (FvMY7), *vti1-2* (FvMY24), and *vti1-11* (FvMY21) and the *GAL1-VTI1* plasmid (pFvM16) have been described earlier (Fischer von Mollard *et al.*, 1997; Fischer von Mollard and Stevens, 1998). The *vti1Δ* yeast strain (FvMY6) was propagated carrying the *GAL1-VTI1* plasmid (pFvM16) in the presence of galactose, because the *vti1Δ* mutation is lethal to yeast cells.

To express AtVTI1a and AtVTI1b in yeast, *BamHI* and *PstI* sites were introduced by PCR into *AtVTI1a* and *AtVTI1b* cDNAs flanking the start and stop codons. The *BamHI/PstI* fragments were inserted into the yeast expression vector pVT102U (Vernet *et al.*, 1987). To construct N-terminal T7-tagged AtVTI1a, *BamHI* and *SalI* sites were generated by PCR flanking the *AtVTI1a* open reading frame. The *BamHI/SalI* fragment of *AtVTI1a* was then inserted into the same sites of pET21a (Novagen, Madison, WI) to create a T7-N-terminal fusion of AtVTI1a (pETT7-AtVTI1a). The *T7-AtVTI1a* fragment was then subcloned into the *XbaI* and *XhoI* sites of the pVT102U vector for yeast expression. To construct pBI-T7-AtVTI1a for plant transformation, the *XbaI/SacI* fragment of pETT7-AtVTI1a was subcloned into pBI121 (Clontech Laboratories, Inc., Palo Alto, CA). For *E. coli* overexpression of 6xHis-AtVTI1a, the *NdeI* site at the ATG start codon and the *BamHI* site immediately downstream of the cytoplasmic domain were introduced by PCR amplification. The *NdeI/BamHI* fragment of *AtVTI1a* was then subcloned into pET14b and transformed into *E. coli* BL21(DE3) cells for overexpression.

Yeast strains were grown in rich medium (1% yeast extract, 1% peptone, 2% dextrose, YEPD) or standard minimal medium (SD) with appropriate supplements (Fischer von Mollard *et al.*, 1997). To induce expression from the *GAL1* promoter, dextrose was replaced by 2% raffinose and 2% galactose.

Immunoprecipitation of ^{35}S-labeled yeast proteins

CPY, ALP, and API were immunoprecipitated as described earlier (Klionsky *et al.*, 1992; Vater *et al.*, 1992; Nothwehr *et al.*, 1993). SEY6211 wild-type cells and *vti1* mutant cells were grown at 24°C and preincubated for 15 min at 36°C before labeling at 36°C.

For CPY immunoprecipitations, log-phase growing yeast cells were labeled for 10 min with ^{35}S-Express label (10 µl/0.5 OD of cells) followed by a 30-min chase with cysteine and methionine. The medium was separated and the cell pellet spheroplasted and lysed. CPY was immunoprecipitated from the medium and cellular extracts. For ALP immunoprecipitations, yeast cells were labeled for 7 min and chased for 30 min. The cell pellet was spheroplasted. The spheroplast pellet was extracted with 50 µl 1% SDS, 8M urea at 95°C, and diluted with 950 µl 90 mM Tris-HCl pH 8.0, 0.1% Triton X-100, 2 mM EDTA; the supernatant was used for immunoprecipitations. To investigate API traffic, 0.25 OD of yeast cells in 500 µl medium were labeled with 10 µl ^{35}S-Express label for each time point. After a 10 min pulse, cells were chased for 120 min. The cell pellet was spheroplasted. Extracts for immunoprecipitations were prepared from spheroplast pellets by boiling in 50 µl 50 mM sodium phospate, pH 7.0, 1% SDS, 3 M urea and diluted with 950 µl 50 mM Tris-HCl, pH 7.5, 0.5% Triton X-100, 150

mM M

Immu

(IgGs

radio

RNA

Bar-

phen

alcoh

from

conc

5' R

Gai

use

TA

An

Pri

Co

th

ne

S

(

mM NaCl, 0.1 mM EDTA. The API antiserum was kindly provided by D. Klionsky. Immuno complexes were precipitated using fixed cells of *Staphylococcus aureus* (IgGsorb). Immunoprecipitates were analyzed by SDS-PAGE and auto-radiography.

RNA Preparation from *Arabidopsis*

Total RNA extraction from different plant organs was performed based on Bar-Peled and Raikhel (1997), except that the RNA was further purified by phenol:chloroform:isoamyl alcohol (25:24:1 by vol.) and chloroform:isoamyl alcohol (24:1, v/v) extraction followed by ethanol precipitation. Purified total RNA from one gram of tissue was resuspended in 200 μl DEPC-treated water. The concentration of the RNA was determined by the OD_{260} value.

5' RACE (Rapid Amplification of cDNA 5' Ends)

5' RACE was performed according to the manufacturer's (Gibco BRL, Gaithersburg, MD) instruction. Total RNA (0.5 μg) from *Arabidopsis* roots was used as a template and the required amount of Primer 1 (5'-GTG AGT TTG AAG TAC AA-3') was used for the first-strand cDNA synthesis. 5' RACE Abridged Anchor Primer (AAP) supplied by the manufacturer was used as a sense primer. Primer 2 (5'- TGC GAT GAT GAT GGC TCC AA -3') and Primer 3 (5'- GTT CAT CCT CCT CGT CAT -3') were used as antisense primers for the first round and the following nested PCR reactions, respectively. DNA fragments produced from nested PCR were end-blunted, cloned into Bluescript SK(-) (Stratagene Cloning Systems, La Jolla, CA) and manually sequenced using Sequenase Version 2.0 (United States Biochemical, Cleveland, OH).

RNA

each

by Sa

(Ame

blot a

Hybo

Antib

tagge

Mad

antib

desc

seru

gift

desc

Sub

cen

(21

KO

PM

disc

RNA Blot Analysis

For northern analysis, 20 μg of *Arabidopsis* total RNA were applied to each lane of a formaldehyde denaturing agarose gel and separated as described by Sambrook *et al.* (1989). Separated RNA was then transferred to a Hybond-N (Amersham Life Science, Buckinghamshire, England) nylon membrane. For dot blot analysis, various amounts of *in vitro* transcribed mRNA were applied to a Hybond-N membrane. Blots were hybridized with ^{32}P-UTP labeled RNA probes.

Antibody Production

6XHis-tagged AtVTI1a was overexpressed by IPTG induction. The His-tagged protein was purified by passing through a Ni-NTA column (Novagen, Madison, WI). The purified protein was then injected into a guinea pig for antibody production. AtPEP12p rabbit antiserum and pre-immune serum were described in Conceição *et al.* (1997). AtELP rabbit antiserum and pre-immune serum were described in Ahmed *et al.* (1997). H^+-pyrophosphatase antibody is a gift from Dr. S. Yoshida (Hokkaido University, Sapporo, Japan) and was described in Maeshima and Yoshida (1989).

Subcellular Fractionation

To fractionate subcellular compartments based on their mass, differential centrifugation was performed as follows: 0.5 grams of *Arabidopsis* root cultures (21 days old) were homogenized in one milliliter extraction buffer (50 mM Hepes-KOH, pH 7.5, 10 mM KOAc, 1 mM EDTA, 0.4 M sucrose, 1 mM DTT and 0.1 mM PMSF). The lysate was centrifuged at 4°C, 1,000 *g,* for 10 min. The pellet was discarded and the supernatant (S1) was then centrifuged at 4°C, 8,000 *g,* for 20

mi

Th

(P

(S

us

su

A

by

us

se

in

(N

E

fi

s

r

t

(

min. The pellet (P8) was resuspended in 200 μl of 2x Laemmli loading buffer. This supernatant was ultracentrifuged at 4°C, 100,000 *g,* for 2 hrs. The pellet (P100) was resuspended in 200 μl of 2x Laemmli loading buffer. The supernatant (S100), P8, and P100 were analyzed by SDS-PAGE, followed by immunoblotting using different antibodies.

Based on density differences, the microsomes were separated on a step sucrose gradient as described in Sanderfoot *et al.* (1998).

***Arabidopsis* Transformation**

pBI-T7-AtVTI1a was introduced into *Agrobacterium tumefaciens* LBA4404 by $CaCl_2$-based transformation. *Arabidopsis* Columbia plants were transformed using vacuum infiltration as described in Bent *et al.* (1994). Transformants were selected by kanamycin, and the presence of T7-AtVTI1a was detected in several independent lines by protein gel blot analysis using T7-monoclonal antibody (Novagen, Madison, WI) and guinea pig polyclonal antiserum against AtVTI1a.

EM Procedure

The root tips of *Arabidopsis* plants transformed with T7-AtVTI1a were fixed in a buffer containing 1.5% formaldehyde, 0.5% glutaraldehyde, and 0.05 M sodium phosphate, pH 7.4, for 2.5 hrs at room temperature. The specimens were rinsed in the same buffer and post-fixed in 0.5% OsO_4 for 1 hr at room temperature. Dehydrated specimens were embedded in London Resin White (Polysciences, Warrington, PA). Ultrathin sections were made with an Ultracut S microtome (Reichert-Jung, Vienna, Austria) by a diamond knife and collected on nickel grids precoated with 0.25% Formvar.

wa
ep
1
str
gri
us
PE
las
ar
ar
pa
ar
w
m
w
w
co
d

A
in
S

For immunolabeling, the protocol according to Sanderfoot *et al.* (1998) was used with modification. Primary mouse monoclonal antibody against T7 epitope tag (Novagen, Madison, WI) were detected by rabbit-anti-mouse IgG for 1 hr, followed by biotinylated goat anti-rabbit IgG for 1 hr, and then by streptavidin conjugated to 10 nm colloidal gold particles. For double labeling, the grids were first treated as above for T7 tag antibody, then a second fixation step using 0.1% glutaraldehyde, followed by a second blocking step with 2% BSA in PBST (PBS+0.1% Tween20) to prevent cross-reactivity of the T7 tag-antibody in later steps (Slot *et al.*, 1991). The grids were then incubated with specific rabbit antiserum for AtELP for 4 hrs, followed by a 1-hr incubation with biotinylated goat anti-rabbit IgG and then by streptavidin conjugated to 5 nm colloidal gold particles. The control sections were treated with 2% BSA in PBST instead of antibody against the T7-tag and with the AtELP preimmune serum. The grids were washed in distilled water and stained with 2% uranyl acetate in H_2O for 30 min and lead citrate for 10 min (Reynold's Solution). The sections were examined with a Philips CM 10 transmission electron microscope. All labeling experiments were conducted several times each on independent sections. Fifty Golgi complexes were analyzed for AtVTI1a distribution and forty complexes for double-immunolabeling of AtVTI1a and AtELP.

Cryosections of *Arabidopsis* roots were utilized for investigation of AtVTI1a and AtPEP12p co-localization. The sectioning procedure was described in Sanderfoot *et al.* (1998). Immunolabeling was also performed as described in Sanderfoot *et al.* (1998) with some modifications. T7-AtVTI1a localization was

dete

with

and

was

acc

Imm

extr

mM

(10

was

the

This

(No

cen

buff

elut

flov

imm

Re

The

(Alt

detected as described above when LR White sections were used and visualized with 10 nm colloidal gold. AtPEP12p was detected using AtPEP12p antiserum and visualized with 5 nm colloidal gold. For final embedding, the grids were washed and stained by a mixture of polyvinyl alcohol and uranyl acetate according to Tokuyasu (1989).

Immunopurification of T7-AtVTI1a From Plant Extract

Three grams of 21-day-old plants were homogenized on ice in 6 ml of extraction buffer (50 mM HEPES-KOH, pH 6.5, 10 mM potassium acetate, 100 mM sodium chloride, 5 mM EDTA, 0.4 M sucrose) with protease inhibitor cocktail (100 μM PMSF, 1 μM pepstatin, 0.3 μM aprotinin, 20 μM leupeptin). The debris was pelleted by centrifugation at 1,000 *g* for 10 min. Triton X-100 was added to the supernatant to final concentration of 1% to solubilize membrane proteins. This solubilized protein extract was incubated with 50 μl T7-tag antibody agarose (Novagen, Madison, WI) at 4°C for 5 hrs. The agarose was then collected by centrifugation at 4°C, 500 *g,* for one minute and washed 5 times in extraction buffer + 1% Triton X-100. Protein purified by T7-tag antibody agarose was then eluted in 50 μl 2x Laemmli buffer. Equal volume of total protein extract, flowthrough or eluate were separated on a SDS-PAGE followed by immunoblotting using different antibodies.

Results

There Are Two Highly Similar *AVTI1* Genes Found in *Arabidopsis*

A search of the *Arabidopsis* EST database using the Blast program (Altschul *et al.*, 1990) resulted in a partial sequence that showed similarity to

yeas
cDN
sea
no.
AtV
22
sir
ar
(K
p
w
u
p
s

yeast Vti1p. 5' RACE was performed to obtain the upstream sequence of this cDNA. With this 5' RACE sequence, the *Arabidopsis* EST database was searched again and two sets of EST clones were found. The clone (accession no. T14238) containing an open reading frame of 221 amino acids was termed *AtVTI1a*. The clone (accession no. T75644) containing an open reading frame of 224 amino acids was termed *AtVTI1b* (Figure 3-1). These two genes share similarity at the nucleotide sequence level (58.4% identity) and the deduced amino acid sequence level (59.5% identity; see Table 3-1). Hydropathy analysis (Kyte and Doolittle, 1982) predicted similar structures for AtVTI1a and AtVTI1b proteins (our umpublished results). The sequences predicted hydrophilic proteins with a short hydrophobic region at their extreme C-termini (Figure 3-1, underlined), possibly serving as a membrane anchor. The region immediately preceding the probable membrane-spanning domain contains two heptad repeat structures that would potentially form amphiphilic alpha helices. Predicted amino acid sequences of these two AtVTI1 and Vti1 proteins found in other organisms were compared using the J. Hein method in the MegAlign program (DNAStar software package) (Figure 3-1 and Table 3-1). The alignment showed that Vti1 proteins exhibit significant similarities between yeast, mammals and plants (yVti1p and AtVTI1a: 32.4% identical, yVti1p and AtVTI1b: 30.8% identical, yVti1p and hVti1p: 23.9% identical, yVti1p and mVti1a: 33.8% identical, yVti1p and mVti1b: 23.5% identical). All Vti1 proteins have a short hydrophobic region at the C-terminus. The most conserved amino acid residues among Vti1 proteins are concentrated in the heptad repeat region next to the transmembrane

Figure 3-1. Sequence comparison of AtVTI1a and AtVTI1b with other members of the family including yVti1p (*Saccharomyces cerevisiae*, accession no. 2497184), hVti1p (*Homo sapiens,* accession no. 268740), mVti1a (*Mus musculus,* accession no. 3213227), mVti1b (*Mus musculus*, accession no. 3213229). The sequence comparison was generated using the J. Hein method in MegAlign (DNASTAR© program). Amino acids identical with yVti1p are shaded in black. The C-terminal hydrophobic domain is underlined.

```
1   DA------FDG RQYCELSAS SKKCSSAISD-DG-- AtVTI1a
1   DV------FEG RQYCELSTN SRKCHSASVSNG-- AtVTI1b
1   L-------LIS SD---KTT---QAKASEA-P yVti1
1   ASSAASSEHFEKLHEI---RGLH---NLQGVPERLLG hVti1
1   D-------FEG QD---AVLTA---EITSKIRV-P mVti1a
1   AASAASSEHFEKLHEI---RGL---DLQGVPERLLG mVti1b

32  ----EQKKQKLSEIKSGLENAEVIRKLARTL--PPN AtVTI1a
33  ----EEKKGKIAQIKSGIEEADVIRKLARSL--QP AtVTI1b
28  SQPLSQRNTTLKHEQQDELFDLDQMVVNNSIGDA yVti1
35  TAGTEEKKKLIRDFDEKQEANETLAEEEEELRYA--PL hVti1
28  RLPPDEKKQMVANEKQLEEAREEEQMLVREI--PPQ mVti1a
35  TAGTEEKKKLVRDFDENQEANETLAEEEELRYA--PLT mVti1b

66  LKSSLLVLRFSDLNNFKTEVITSGQLNAAADE- AtVTI1a
67  AKAVCLSKLREYSDLNQLKKEFVSSADAKPSSEE- AtVTI1b
68  ETTKAKLREW---KTIQSDIPLQSLVSGDDR- yVti1
73  FNPMMSHLRNYRKDLAKLHREVRSTPLTATP-GGGDMK hVti1
66  SGMSNRMSYQEMGKLETDFSRIAYS-EVNE- mVti1a
73  FNPMMSHLRNYRKDLAKLHREVRSTPLTAAP-GGGDK mVti1b

105 -----LEAGMADTKTAS-AIIARMMSTERGRTTDVK AtVTI1a
106 -----MESGMADLHAVS-AIIRGRLAMSVERDQSEIR AtVTI1b
104 -----FGE--LNANID-DDDRQQLLSNHAIQKGELK yVti1
112 YGIYAVEN--EHMN--RLQSDRAMLLQGTESNRATQSIE hVti1
104 -----LGE--AGN--S-ENEAHLLDNTERERSRELE mVti1a
112 YGTYTLEN--EHLN--RLQSEALLQGTESNRATQSIE mVti1b

139 SRETMMEEEEIVSILQLLHGEQSILRAHETHGVDN AtVTI1a
140 ESRELMLETEEVIISIVQLLSQEQTILHAHNKHGVDA AtVTI1b
136 ASKIANETEGIGSQIMMLLRSEETIENRQTFQASY yVti1
148 RSHEIATETDQIGSEIIEELGEERDQIERTKSRVNTSEN hVti1
134 AGYQIAVETEQIQEMLENLSHDEEKIQRRDRRDAIAN mVti1a
148 RSHEIATEDQIETEIIEELGEERDQIERTKSRVNTNEN mVti1b

179 IGEKPIITDETEEMNKE--WTIGAAIIA-IAAFFII AtVTI1a
180 IDEKKVITAESEEMTRE--WIITSVIVA-VLAIIIII AtVTI1b
176 VDKSIKTITKTETREILVAE--FISYAAIAV-ILIILLVE yVti1
188 LSESRKIIRSESEKVTTE--LLLSIIILLEAIILGGIVY hVti1
174 LGESSRIITGELEEIIQERILLVILGIIVV-IAIITAIAF mVti1a
188 LSERRIIRSESEKVITE--LLLSVIILLEAIIVGIVY mVti1b

216 YF--ELTK AtVTI1a
217 SY--ELSH AtVTI1b
213 FS--EF-K yVti1
226 YKFFRS-H hVti1
213 FV--EG-H mVti1a
226 YKFFRH-H mVti1b
```

Table 3-1. Relative sequence identity between Vti1 protein homologues

	AtVTI1a	AtVTI1b	yVti1	hVti1	mVti1	mVti1
AtVTI1a	100%	59.9	32.4	26.7	33.3	28.1
AtVTI1b		100%	30.8	27.5	31.8	28
yVti1			100%	23.9	33.8	23.5
hVti1				100%	30.1	91.9
mVti1					100%	31.5
mVti1						100%

Amino acid sequence similarity shown as identical sequence percentage. AtVTI1a, and yVti1p, *Saccharomyces cerevisiae* (accetion number 2497184); HVti1p, Homo sapiens (accession number 268740); mVti1a, *Mus musculus* (accession number 3213227); mVTI1b, *Mus musculus* (accession number 3213229). The optimal alignments were produced using the J. Hern method in the DNAstar program.

dom

(Ca

199

At

fu

ye

in

V

e

t

t

c

P

t

l

domain, a region thought to be involved in interaction between t-and v-SNAREs (Calakos *et al.*, 1994; Hayashi *et al.*, 1994; Fischer von Mollard and Stevens, 1998).

AtVTI1a and AtVTI1b Function in Different Trafficking Steps in Yeast

Next, we investigated whether either AtVTI1a or AtVTI1b could functionally replace the yeast Vti1p in various membrane trafficking steps in yeast. For this purpose the coding sequences of *AtVTI1a* or *AtVTI1b* were cloned into a multicopy yeast expression vector behind the *ADH1* promoter. In yeast the *VTI1* gene is essential for cell growth. Therefore, we determined whether expression of the *Arabidopsis* Vti1 homologues would allow yeast cells to grow in the absence of the yeast Vti1p. The expression of yeast *VTI1* was placed under the control of the *GAL1* promoter. These cells (FvMY6/pFvM16) were able to divide on galactose plates (Figure 3-2A, Gal), but not on glucose plates (Glc). Expression of either AtVTI1a or AtVTI1b allowed for growth on glucose medium. Cells expressing AtVTI1b grew more slowly than cells expressing AtVTI1a. *vti1Δ* cells (FvMY6) expressing AtVTI1a divided with a doubling time of 3.5 hrs and *vti1Δ* cells expressing AtVTI1b had a doubling time of about 8 hrs, compared to 2.5 hrs for wild-type cells (our unpublished results). These data indicate that either AtVTI1a or AtVTI1b could replace yeast Vti1p in its essential function, although to different extents.

Various membrane trafficking steps in yeast can be analyzed by following the fate of newly synthesized proteins in experiments involving pulse-chase labeling with ^{35}S followed by immunoprecipitation. The soluble vacuolar

hy
p1
ap
the
the
the
vo
in
ac
no
CP
eff
fou
se
ter
Go
et
se
(F
ac
lar
wa
inc

hydrolase carboxypeptidase Y (CPY) is glycosylated in the ER to produce the p1CPY precursor (Stevens *et al.*, 1982). Further modification in the Golgi apparatus gives rise to p2CPY. CPY is sorted in the TGN and transported from there through the prevacuolar/endosomal compartment (PVC) to the vacuole and then cleaved to the mature mCPY (Bryant and Stevens, 1998). Transport from the Golgi to the PVC is blocked in the temperature-sensitive *vti1-1* cells (Fischer von Mollard *et al.,* 1997) . Compared to wild-type yeast where CPY was retained in the vacuole as mature form (Figure 3-2B, lane 1), the *vti1-1* cells (FvMY7) accumulated p2CPY within the cell (lane 3) and secreted p2CPY (lane 4) at the non-permissive temperature. As indicated by the prevalence of mCPY (lane 5), CPY was transported to the vacuole in *vti1-1* cells expressing AtVTI1a as effectively as in wild-type cells. By contrast, only low amounts of mCPY were found in *vti1-1* cells expressing AtVTI1b (lane 7), and most of the CPY was secreted (lane 8). *vti1-11* cells (FvMY21) accumulated p1CPY at the restrictive temperature (Figure 3-2C, lane 1) due to a defect in retrograde traffic to the *cis*-Golgi as well as a defect in traffic from the TGN to the PVC (Fischer von Mollard *et al.*, 1997). *vti1-11* cells, but not *vti1-1* cells, display a severe temperature-sensitive growth defect, indicating that retrograde traffic to the Golgi is essential (Fischer von Mollard *et al.*, 1997). Expression of AtVTI1a suppressed the accumulation of p1CPY and resulted in the appearance of mCPY (Figure 3-2C, lane 3). Expression of AtVTI1b also reduced the amount of p1CPY (lane 5); CPY was not directed to the vacuole, but was secreted instead (lane 6). These results indicate that AtVTI1a can replace yeast Vti1p both in transport from the TGN to

Figure 3-2. Expression of either AtVTI1a or AtVTI1b allows yeast cells to grow in the absence of Vti1p, but only AtVTI1a functions in TGN-to-PVC traffic.

A) Growth of the *vti1Δ GAL1-VTI1* strain (FvMY6/pFvM16) alone or expressing AtVTI1a or AtVTI1b on plates containing galactose (Gal) or glucose (Glc). The *vti1Δ GAL1-VTI1* strain could not grow on glucose after the expression of *VTI1* was shut off, but expression of either AtVTI1a or AtVTI1b supported growth.

B) CPY traffic in wild-type, *vti1-1* (FvMY7, and C) *vti1-11* cells (FvMY21) alone (-) or expressing AtVTI1a or AtVTI1b. Cells were grown at 24°C, preincubated at 36°C for 15 min, pulse labeled for 10 min, and chased for 30 min at 36°C. CPY was immunoprecipitated from cellular extracts (I) and extracellular fractions (E) and analyzed by SDS-PAGE and autoradiography. The TGN to PVC traffic block in *vti1-1* cells (FvMY7) was suppressed by AtVTI1a expression, as indicated by the presence of vacuolar mCPY, but not by AtVTI1b expression.

C) *vti1-11* cells (FvMY21) accumulated p1CPY due to a block in retrograde traffic to the *cis*-Golgi. Expression of either AtVTI1a or AtVTI1b reduced the amount of p1CPY that accumulated.

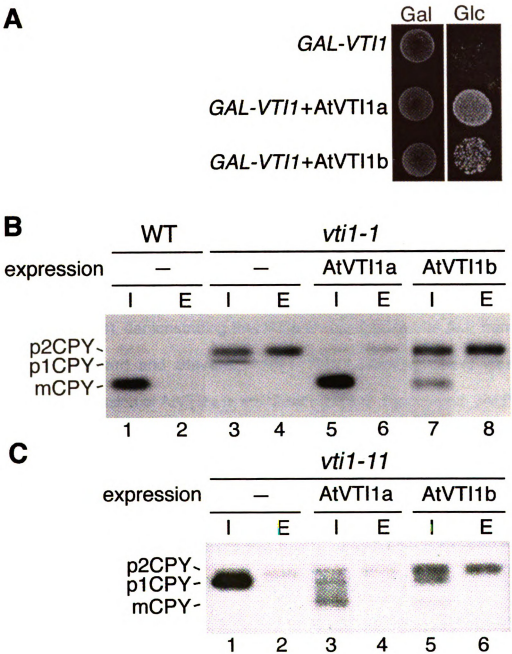
A
Gal
Glc
GAL-VTI1
GAL-VTI1+AtVTI1a
GAL-VTI1+AtVTI1b
B
WT
vti1-1
expression
–
–
AtVTI1a
AtVTI1b
I
E
I
E
I
E
I
E
p2CPY
p1CPY
mCPY
1
2
3
4
5
6
7
8
C
vti1-11
expression
–
AtVTI1a
AtVTI1b
I
E
I
E
I
E
p2CPY
p1CPY
mCPY
1
2
3
4
5
6

the

cis

ret

dif

thr

In

pr

AL

ty

te

(F

co

tra

At

AL

(A

do

(K

pA

th

vt

the PVC (interaction with the t-SNARE Pep12p) and in retrograde traffic to the *cis*-Golgi (interaction with the t-SNARE Sed5p). By contrast, AtVTI1b functions in retrograde traffic to the *cis*-Golgi but not in traffic from the TGN to the PVC.

The vacuolar membrane protein alkaline phosphatase (ALP) utilizes a different transport pathway from the TGN to the vacuole and does not travel through the PVC as does CPY (Bryant and Stevens, 1998; Odorizzi *et al.*, 1998). In pulse-chase labeling experiments, arrival at the vacuole is indicated by processing of pALP to mALP (Figure 3-3A, Line 2) (Klionsky and Emr, 1989). ALP traffic to the vacuole occurs with a half time of about five minutes in wild-type cells. *vti1-2* cells (FvMY24) accumulated pALP at the non-permissive temperature (lane 4), demonstrating that Vti1p is also required for ALP transport (Fischer von Mollard and Stevens, 1999). This trafficking defect was not corrected by expression of AtVTI1a in *vti1-2* cells (lane 6). By contrast, pALP was transported to the vacuole and processed to mALP in *vti1-2* cells expressing AtVTI1b after a 30-min chase period (lane 8), indicating that AtVTI1b functions in ALP traffic to the vacuole.

A third biosynthetic pathway to the vacuole is taken by aminopeptidase I (API). API is synthesized as a cytoplasmic precursor, pAPI, and engulfed by a double membrane that forms cytoplasm-to-vacuole transport (CVT) vesicles (Klionsky, 1998). These CVT vesicles fuse with the vacuolar membrane and pAPI is cleaved to vacuolar mAPI (Figure 3-3B, lane 2). Transport of API along this pathway has a half time of about 45 min. Transport of API was blocked in *vti1-11* cells (FvMY21) at the restrictive temperature (Fischer von Mollard and

Figure 3-3. AtVTI1b but not AtVTI1a could replace yeast Vti1p in ALP and API traffic to the vacuole, which are transported to the vacuole via two different biosynthetic pathways.

A) Wild-type and *vti1-2* cells (FvMY24) alone (-) or expressing either AtVTI1a or AtVTI1b were grown at 24°C, preincubated at 36°C for 15 min, pulse labeled for 7 min, and chased for 0 min or 30 min at 36°C. ALP was immunoprecipitated from cellular extracts and separated by SDS-PAGE. The accumulation of pALP in *vti1-2* cells was suppressed by expression of AtVTI1b but not by AtVTI1a.

B) Wild-type and *vti1-11* cells (FvMY21) alone (-) or expressing AtVTI1a or AtVTI1b were grown at 24°C, preincubated at 36°C for 15 min, labeled for 10 min, and chased for 0 min or 120 min at 36°C. API was immunoprecipitated from cellular extracts and analyzed by SDS-PAGE. Vacuolar mAPI was found only in *vti1-11* cells expressing AtVTI1b, not in *vti1-11* cells expressing AtVTI1a.

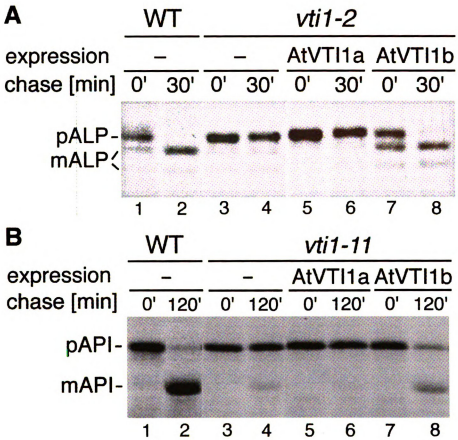
A
WT
vti1-2
expression
–
–
AtVTI1a
AtVTI1b
chase [min]
0'
30'
0'
30'
0'
30'
0'
30'
pALP-
mALP
1
2
3
4
5
6
7
8
B
WT
vti1-11
expression
–
–
AtVTI1a
AtVTI1b
chase [min]
0'
120'
0'
120'
0'
120'
0'
120'
pAPI-
mAPI-
1
2
3
4
5
6
7
8

Stevens, 1999), as indicated by the absence of mAPI after a 120-min chase period (lane 4). Expression of AtVTI1a in *vti1-11* cells did not suppress the API traffic defect (lane 6). As indicated by the presence of mAPI in *vti1-11* cells expressing AtVTI1b (lane 8), AtVTI1b can partially fulfill the function of Vti1p in API traffic along the Cvt pathway.

Taken together, these data indicate that whereas AtVTI1a can function in traffic from the TGN to the PVC, AtVTI1a cannot replace Vti1p in traffic along either the ALP or Cvt pathway to the vacuole. By contrast, AtVTI1b functions in membrane traffic along the ALP and Cvt pathways to the vacuole but not in transport from the TGN to the PVC.

Both *AtVTI1a and AtVTI1b* Transcripts Are Expressed in All Organs in *Arabidopsis*

Finding that AtVTI1a and AtVTI1b function in different vacuolar transport pathways in yeast prompted us to analyze their specific distribution in *Arabidopsis* plants. To detect the expression pattern of these *AtVTI1* genes, we performed northern analysis of various *Arabidopsis* plant organs. Because of the high similarity of *AtVTI1a* and *AtVTI1b*, an untranslated region of each clone was used to prepare gene-specific RNA probes. The specificity of these two probes was first checked by dot blot of *in vitro* translated *AtVTI1a* and *AtVTI1b* mRNA, as revealed in Figure 3-4 A. The dot blot of *in vitro* transcribed *AtVTI1a* hybridized with the *AtVTI1a* antisense RNA probe. Similarly, *in vitro* transcribed *AtVTI1b* hybridized only with the *AtVTI1b* antisense RNA probe. These results demonstrate that the probes are specific under stringent hybridization and

Figure 3-4. Northern blot analyses of *AtVTI1a* and *AtVTI1b*.

A) Dot blot for testing the specificity of the *AtVTI1a* and *AtVTI1b* probes. One microliter of *in vitro* transcribed mRNAs of *AtVTI1a* and *AtVTI1b* in serial 10X dilutions were applied to the Hybond N membrane and hybridized with *in vitro* transcribed α-^{32}P UTP-labeled RNA probes at high stringency (65°C for 16 hrs). The blot was washed under highly stringent consitions (2xSSC + 1% SDS for 30 min at 65°C, 0.2xSSC + 1% SDS 10 min for three times at room temperature). The signal was then detected by autoradiography.

B) RNA gel blot analysis of *AtVTI1* expression in several *Arabidopsis* organs. Twenty micrograms of total RNA extracted from roots (R), stems (S), flowers (F), and leaves (L) were separated on denaturing gel and transferred to Hybond N. The membrane was then hybridized with probes described in **A** following the same procedure.

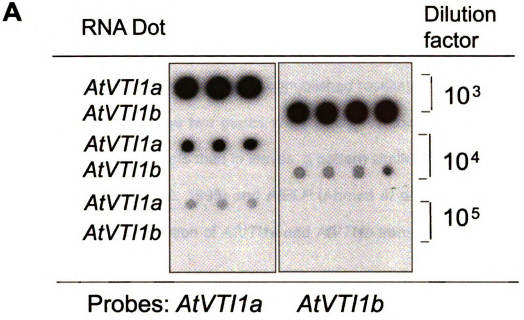
A
RNA Dot
Dilution factor
AtVTI1a
AtVTI1b
AtVTI1a
AtVTI1b
AtVTI1a
AtVTI1b
10³
10⁴
10⁵
Probes: AtVTI1a AtVTI1b

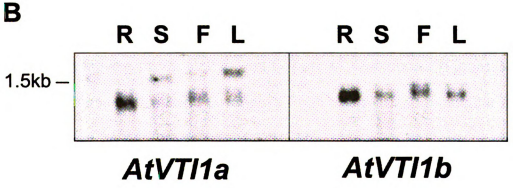
B
R S F L
R S F L
1.5kb
AtVTI1a
AtVTI1b

washing conditions. These two gene-specific probes were used to hybridize RNA blots of total RNAs from roots, stems, leaves, and flowers. As shown in Figure 3-4B, *AtVTI1a* and *AtVTI1b* were expressed in all organs investigated. The *AtVTI1a* probe also recognized a band that migrated at about 1.6 kb, however, this band was found to be irrelevant to the *AtVTI1a* gene since another probe toward *AtVTI1a* failed to recognize it (our unpublished results). The mRNA organ distribution patterns of these two genes were similar to each other; however, there was more mRNA in roots than in leaves, a pattern similar to the distribution of *AtPEP12* (Bassham *et al.*, 1995) and *AtELP* (Ahmed *et al.*, 1997). Thus, we found no variation in distribution of *AtVTI1a* and *AtVTI1b* transcripts among plant organs.

AtVTI1a Is an Integral Membrane Protein

To study the behavior of AtVTI1a, we raised antibodies towards the cytosolic part of this protein in guinea pig. The antisera specifically recognized a 28 kDa band in leaves, roots, stems, and flowers of *Arabidopsis* (Figure 3-5A). The molecular mass of this band agreed well with the deduced molecular mass of AtVTI1a based on sequence information. The sequence analysis predicted that AtVTI1a, like most other v-SNAREs, has a C-terminal hydrophobic domain as a membrane anchor. Therefore, differential centrifugation experiments were conducted to investigate whether AtVTI1a was associated with membranes. The majority of the AtVTI1a protein was precipitated at 8,000 *g* and no AtVTI1a remained in the supernatant after centrifugation at 100,000 *g* (Figure 3-5B). To confirm that AtVTI1a is an integral membrane protein, various treatments that

Figure3-5. AtVTI1a is an integral membrane protein.

A) Distribution of AtVTI1a in *Arabidopsis* organs. Equal amounts of total protein from leaves (L), flowers (F), stems (S) or roots (R) were separated by SDS-PAGE and immunoblotted with guinea pig antiserum against AtVTI1a. Molecular weight is indicated on the left.

B) AtVTI1a fractionates with heavy membranes during differential centrifugation. A post-nuclear supernatant from 0.5 g cultured roots was centrifuged at 8,000 *g* for 20 min. The pellet (P8) was solubilized in 200 µl 2xLaemmli-loading buffer. The supernatant (S8) was further ultracentrifuged at 100,000 *g* for 2 hrs. The pellet (P100) was solubilized in 200 µl of 2xLaemmli buffer. Equal amounts of the supernatant (S100), P100, and P8 were separated by SDS-PAGE and immunoblotted with anti-AtVTI1a antiserum. Molecular weight is indicated on the left.

C) AtVTI1a is an integral membrane protein. Equal amounts of total membranes from *Arabidopsis* cultured cells were treated with 2 M urea, 0.1% or 1% Triton X-100, 0.1% or 1% SDS, 1 M NaCl, 0.1 M Na_2CO_3 (pH 11), or extraction buffer alone. All treatments were performed at room temperature for 30 min. An aliquot of each treatment was saved as total. Membranes were pelleted by centrifugation at 100,000 *g* for one hr after the treatments. Equal volumes of supernatant or total were separated by SDS-PAGE and immunoblotted with anti-AtVTI1a antiserum. S: supernatant, T: total.

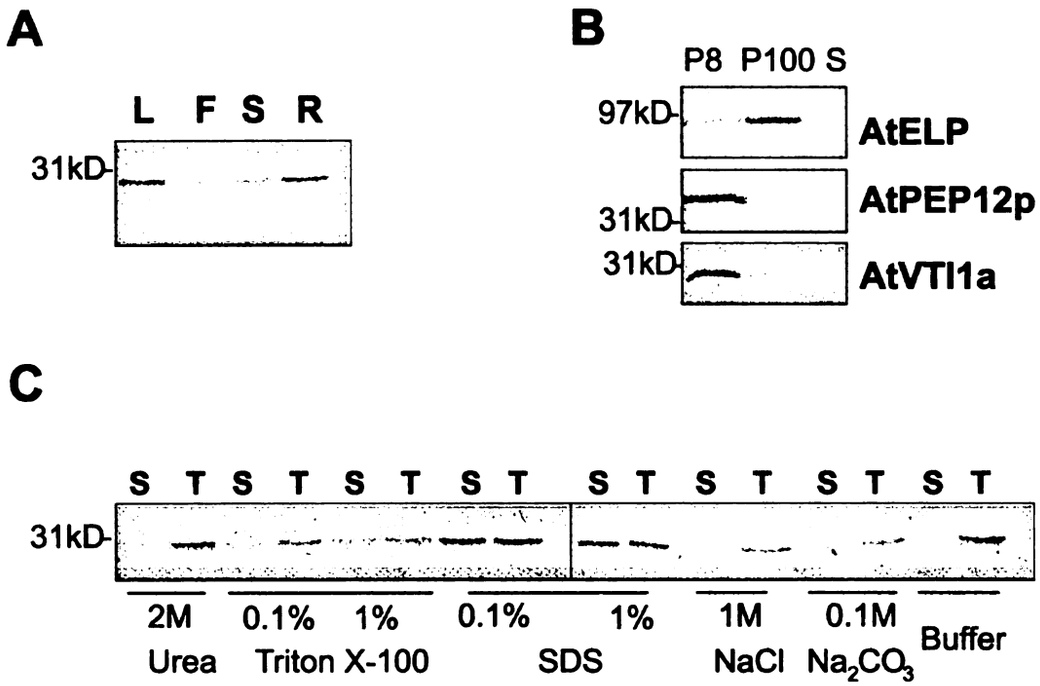
A
L F S R
31kD
B
P8 P100 S
97kD
AtELP
31kD
AtPEP12p
31kD
AtVTI1a
C
S T S T S T S T S T S T S T S T
31kD
2M
Urea
0.1%
1%
Triton X-100
0.1%
1%
SDS
1M
NaCl
0.1M
Na_2CO_3
Buffer

affect the membrane association of peripheral proteins were applied to total membranes from *Arabidopsis* suspension cells. The membranes were pelleted afterwards and the amounts of AtVTI1a in the supernatants were compared with those in the starting material. AtVTI1a was not stripped from the membrane by 2 M urea, 1 M NaCl, or 0.1 M Na_2CO_3, conditions that dissociate peripheral proteins from membranes (Figure 3-5C). AtVTI1a was solubilized by detergents, indicating that it is an integral membrane protein.

Cofractionation of AtVTI1a and Other Markers in Sucrose Density Gradients

To determine the subcellular localization of AtVTI1a, we performed a sucrose density step gradient analysis. Post-nuclear supernatant from 3-week-old *Arabidopsis* cultured roots was loaded on top of a step sucrose gradient (15%, 24%, 33%, 40%, and 54% from top to bottom). The gradient was equilibrated by ultracentrifugation at 100,000 *g* for 3 hrs at 4°C and fractions of 0.5 ml were collected from the top to the bottom. The sucrose density distribution was close to linear after the centrifugation step (Figure 3-6B). Fractions were then analyzed by immunoblotting. The fractionation of AtVTI1a was compared with three other subcellular marker proteins, as shown in Figure 3-6A. AtVTI1a co-fractionated with AtPEP12p, which peaked at 36.5% and 54.4%; AtELP mostly co-fractionated with AtVTI1a, with peaks at densities of 36.5% and 54.4%. A separate peak of AtELP was also observed at a sucrose concentration of 32.2%. The vacuolar tonoplast marker H^+-pyrophosphatase (H^+PPase; Maeshima *et al.*, 1994) fractionated at the top of the gradient, separated from AtVTI1a and other marker proteins. These data suggest that AtVTI1a does not

Figure 3-6. Subcellular fractionation of AtVTI1a by step sucrose gradient. Post-nuclear membranes of *Arabidopsis* roots were loaded on a step sucrose gradient. After equilibrium by ultracentrifugation at 100,000 *g* for 3 hrs, 0.5 ml fractions were collected from top (1) to bottom of the gradient (25). Equal volumes of odd-numbered fractions were loaded on SDS-PAGE gel and immunoblotted with anti-AtVTI1a, anti-AtELP, anti-AtPEP12p, and anti-H^+pyrophosphatase (H^+PPase) antibodies. Blots were analyzed by densitometry and the percentage of the total marker protein detected in each fraction for AtVTI1a, AtPEP12p, AtELP, and H^+PPase was plotted in **A.** The sucrose concentration of each fraction was determined by refractometry and plotted in **B**.

A

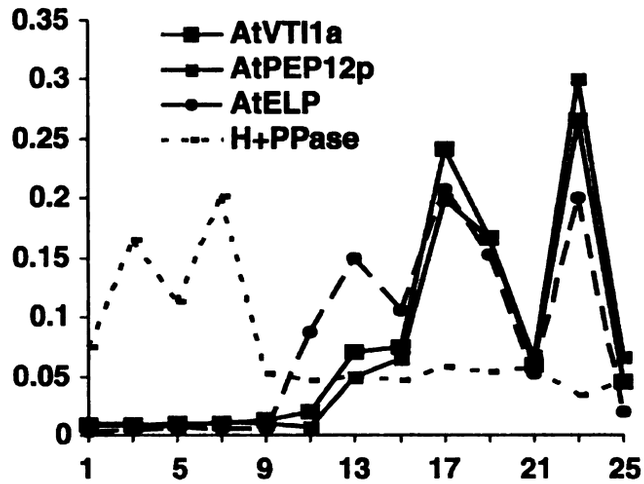
0.35
0.3
0.25
0.2
0.15
0.1
0.05
0
1
5
9
13
17
21
25
AtVTI1a
AtPEP12p
AtELP
H+PPase

B

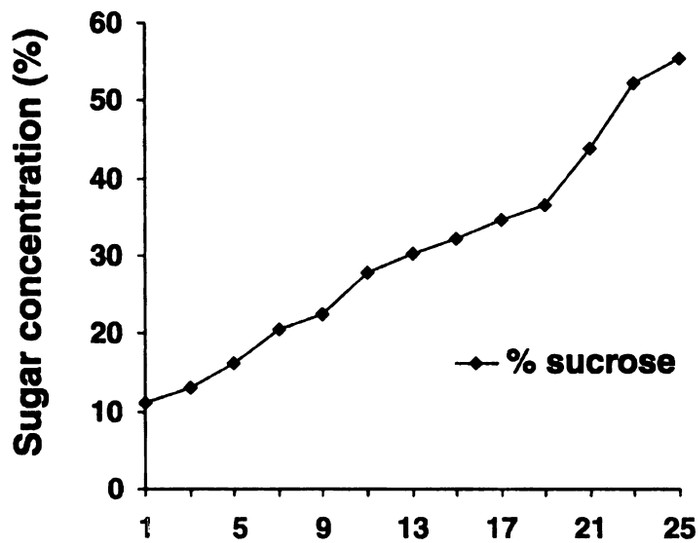
Sugar concentration (%)
60
50
40
30
20
10
0
1
5
9
13
17
21
25
% sucrose

reside on the tonoplast membrane, but rather co-fractionates with AtPEP12 on the PVC or with AtELP on the TGN and the PVC.

T7-tagged AtVTI1a Behaves Similarly to Endogenous AtVTI1a in Yeast and in Plants

To further differentiate the two AtVTI1 proteins and investigate AtVTI1a specifically, an 11-amino-acid T7 tag (Novagen, Madison, WI) was fused at the N-terminus of AtVTI1a. The behavior of this tagged version of AtVTI1a was first compared with wild-type AtVTI1a in yeast and plants. T7-AtVTI1a was expressed in yeast to determine whether the epitope-tagged protein retained function. The growth behavior of *vti1Δ* cells (FvMY6) expressing either AtVTI1a or T7-AtVTI1a was compared by measuring the optical density of cultures growing in logarithmic phase (Figure 3-7A). These two strains grew at similar rates and had doubling times of approximately 3.5 hrs. These data indicated that the T7-tagged AtVTI1a was functional in yeast.

The T7-tagged *AtVTI1a* was transformed into *Arabidopsis* ecotype Columbia. One of the transgenic lines expressing medium amounts of T7-AtVTI1a was chosen for further study. On a western blot, in addition to endogenous AtVTI1a migrating at 28 KDa, AtVTI1a antibodies also detected a protein band migrating at about 29 KDa, which was also recognized by monoclonal T7-antibody (Figure 3-7B). Thus this 29-kDa protein band was determined to be T7-tagged AtVTI1a. T7-antibody did not recognize any other protein bands in extracts from either the transgenic or wild-type line (Figure 3-7B), suggesting that these antibodies were specific in *Arabidopsis*. Since we

Figure 3-7. T7-tag does not affect AtVTI1a function and is expressed in transgenic plants.

A) Growth curves of *vti1Δ* cells expressing AtVTI1a or T7-AtVTI1a. *vti1Δ* cells (FvMY6) expressing either AtVTI1a or epitope-tagged T7-AtVTI1a grew at similar rates, indicating that T7-AtVTI1a was functional. Cells were grown in a rich medium at 30°C at logarithmic phase. The cell density was determined by measuring the optical density at 600 nm.

B) T7-antibodies specifically recognized T7-AtVTI1a in transgenic plants. Equal amounts of post-nuclear supernatant of *Arabidopsis* (T7-AtVTI1a transgenic plants or wild type) were separated on SDS-PAGE gel and immunoblotted with monoclonal T7 antibody or polyclonal antiserum against AtVTI1a raised in guinea pig.

s expressed

l1a. vti1Δ cells

grew at similar

rown in a rich

determined by

plants. Equal

1a transgenic

noblotted with

sed in guinea

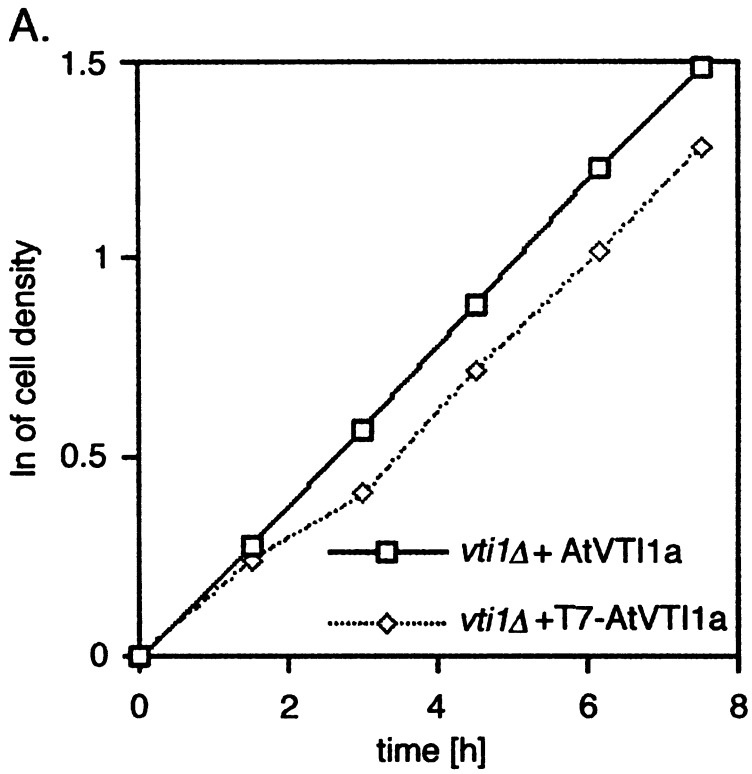

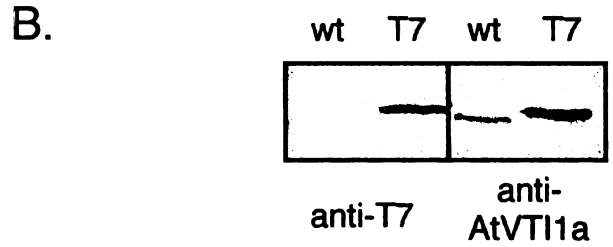

lacked any functional assay for AtVTI1a in plants, the fractionation patterns of tagged and endogenous AtVTI1a on sucrose density gradients were compared. No differences in fractionation patterns were observed between tagged and endogenous AtVTI1a in transgenic plants, or between the fractionation pattern of tagged AtVTI1a in transgenic plants and endogenous AtVTI1a in wild-type plants (our unpublished results). There were also no observable phenotypic differences between the transgenic plants and wild-type plants (our unpublished results). These data indicate that T7-AtVTI1a expressed in plants behaves indistinguishably from endogenous AtVTI1a and the expression of tagged protein does not affect the physiology of the plant.

Cytochemical Analysis of T7-tagged AtVTI1a in Transgenic Plants

We have shown above that AtVTI1a co-fractionated with AtPEP12p and AtELP on a sucrose step density gradient. Therefore, we attempted to further investigate the subcellular localization of AtVTI1a and the relationship between AtVTI1a and AtPEP12p or AtELP by immunocytochemistry. We found that AtVTI1a antiserum was unsuitable for these studies, probably because of low amounts of endogenous protein and loss of antigenicity during fixation. However, the T7-tagged AtVTI1a transgenic plants allowed us to study the localization of AtVTI1a in the cell, and to perform colocalization experiments with other membrane markers. The majority of the T7-AtVTI1a-associated labeling was found on the TGN (Figure 3-8A) and on electron-dense, uncoated vesicular structures that were often found near the Golgi of the root cells (Figure 3-8B). We performed statistical analysis of many independent micrographs showing T7-

AtVTI1a localization. This analysis indicated that the distribution of T7-VTI1a was evenly split between TGN (51%) and dense vesicles (49%). The orientation of the Golgi was determined based upon appearance and the more electron-dense staining pattern of the *trans*-Golgi and the TGN. Almost no T7-AtVTI1a was found on the cytoplasm, ER, nuclei or plasma membrane (our unpublished results), and control sections showed almost no background (Figure 3-8C).

Our fractionation experiments indicated that AtVTI1a partially cofractionated with AtELP, suggesting at least partial colocalization. To analyze this possibility directly, we performed double-labeling experiments on T7-AtVTI1a plants. AtVTI1a was first labeled with specific monoclonal antibody against T7, and detected with 10 nm gold. A second fixation and blocking step was then performed prior to incubating the sections with antiserum specific to AtELP, followed by detection with 5 nm gold. It was observed that both T7 monoclonal antibody and AtELP antiserum specifically labeled the TGN compartment (Figure 3-8D) and electron-dense structures (Figure 3-8E). In control experiments we substituted pre-immune serum for one of the primary antibodies. An example of one of these experiments is shown in Figure 3-8F. In this case, sections were labeled with T7 antibody, followed by pre-immune serum instead of AtELP antibody. No labeling of any structures with 5 nm gold was seen; however, T7-AtVTI1a labeling was present on the TGN. The converse experiments were also done omitting the T7 antibody. Again, no labeling with 10nm gold was seen (our unpublished results). Also, no labeling of the TGN and dense structures was

Figure 3-8. *In situ* localization of T7-AtVTI1a and AtELP on ultrathin sections of *Arabidopsis* roots from T7-AtVTI1a transgenic plants. T7-AtVTI1a and AtELP are localized on the TGN and on dense vesicles.

A and B) Ultrathin sections were incubated with T7 monoclonal antibody followed by rabbit anti-mouse IgG and biotinylated goat anti-rabbit secondary antibody and were visualized with streptavidin conjugated to 10 nm colloidal gold.

C) Control. The ultrathin sections were treated with the same procedure as described in **A** and **B** except T7 monoclonal antibody was substituted with 2% BSA in PBS.

T7-AtVTI1a and AtELP are co-localized on the TGN (**D**) and on dense vesicles (**E**).

D and E) Ultrathin sections were incubated with T7 monoclonal antibody followed by rabbit anti-mouse IgG and biotinylated goat anti-rabbit secondary antibody and were visualized with streptavidin conjugated to 10 nm colloidal gold. After the second fixation step (see Materials and Methods), the same sections were incubated with antiserum to AtELP, followed by biotinylated goat anti-rabbit secondary antibody, then visualized with streptavidin conjugated to 5nm colloidal gold.

F) Control section. The same procedures were used as in **D** and **E** except preimmune serum was used in the place of AtELP antiserum.

G: Golgi; arrow: AtVTI1a; arrow head: AtELP; Bar=0.1 μm.

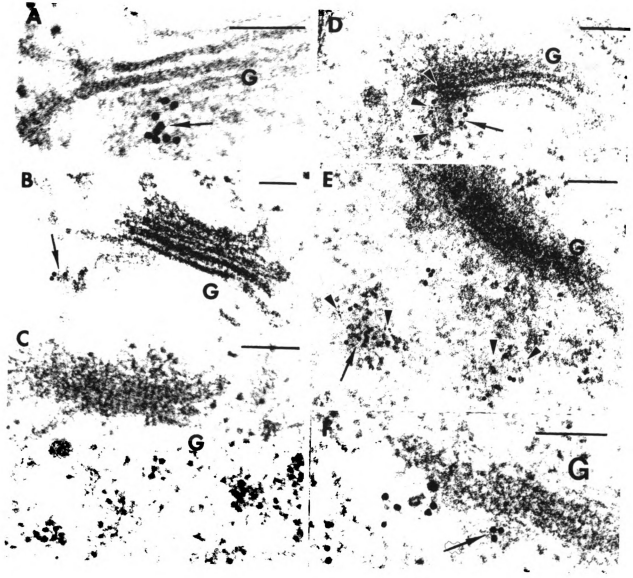
A
G
B
G
C
G
D
G
E
G
F
G

seen in the absence of both primary antisera, but with the secondary antibodies decorated with 5 nm and 10 nm gold (our unpublished results).

We speculate that the electron-dense vesicles labeled with T7-AtVTI1a are PVCs. AtPEP12p is the only known marker on the PVC. Therefore, similar double EM immunocytochemistry was performed to colocalize T7-AtVTI1a and AtPEP12p. For this localization, ultrathin cryosections were employed because AtPEP12p could not be localized using embedment into conventional resin (Conceição *et al.*, 1997). The incubation procedure was similar to that of the T7-AtVTI1a and AtELP double labeling except that AtPEP12p antiserum were used instead of AtELP antiserum. Analysis of sections revealed that T7-AtVTI1a and AtPEP12p colocalized to the structures that are typical for the PVC (Figure 3-9A, B) (Sanderfoot *et al.*, 1998). No staining of the PVC was seen in control experiments (Figure 3-9C). Together with the yeast complementation data, these results strongly support our proposal that AtVTI1a is a v-SNARE involved in traffic between the Golgi and the PVC.

AtVTI1a Interacts with AtPEP12p

To further investigate whether AtVTI1a interacts with a t-SNARE *in vivo*, we attempted to immunoprecipitate AtVTI1a from plant cell extracts and identify the co-immunoprecipitated proteins. Cultured roots of T7-AtVTI1a plants or wild-type plants were homogenized and the extract was clarified by centrifugation at 1000 *g* for 10 min at 4°C. Triton X-100 was added to the supernatant to a final concentration of 1% to solubilize the membrane proteins. These lysates were incubated with T7-antibody conjugated to agarose beads. The beads were

Figure3-9. T7-AtVTI1a and AtPEP12p colocalize on the PVC in cryosections of *Arabidopsis* roots from T7-AtVTI1a transgenic plants.

A and B) Ultrathin sections were incubated with T7 monoclonal antibody followed by rabbit anti-mouse IgG and biotinylated goat anti-rabbit secondary antibody and were visualized with streptavidin conjugated to 10 nm colloidal gold. After the second fixation step (see Materials and Methods), the same sections were incubated with AtPEP12p antiserum, followed by biotinylated goat anti-rabbit IgG, and then detected by streptavidin conjugated to 5 nm gold particles.

C) Control section. The same procedures were used as in **A** and **B** except first antibodies were substituted with 2% BSA in PBS for T7 monoclonal antibody and AtPEP12p preimmune serum for AtPEP12p antiserum.

G, Golgi; arrow: AtVTI1a; arrowhead: AtPEP12p; Bar=0.1 μm.

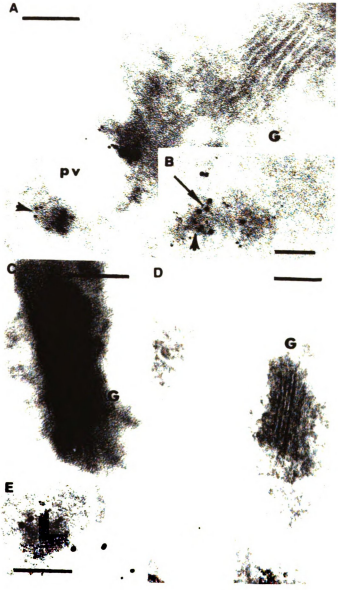
A
G
PV
B
C
D
G
G
E

washed and the bound proteins were eluted. Samples of total extracts, flowthrough, and eluate were separated on SDS-PAGE. The separated proteins were then transferred to a nitrocellulose membrane and blotted by various antibodies. T7-AtVTI1a bound to the T7 antibody agarose with high efficiency (Figure 3-10). Significantly, a fraction of the total AtPEP12p was co-precipitated with T7-AtVTI1a in the eluate. (Figure 3-10, right side) As we expected, in the control experiment where wild-type plant extract was used (Figure 3-10, left side), AtVTI1a did not bind to the T7-antibody. Accordingly, AtPEP12p was not found in the eluate. Thus, our data indicate that AtPEP12p was associated specifically with T7-AtVTI1a. In contrast, AtELP was not co-purified by T7-antibody agarose. These co-immunoprecipitation experiments strongly suggest that AtVTI1a forms a Triton X-100-resistant SNARE complex with AtPEP12p *in vivo*.

Discussion

Several pathways to the vacuole have been identified in yeast. Vti1p, a multifunctional v-SNARE, has been shown to be involved in numerous pathways to the vacuole, including the CPY pathway via the PVC, the ALP alternative pathway, and the CVT pathway for vacuole taking cytosolic proteins such as API (Fischer von Mollard *et al.*, 1997; Holthuis et al, 1998; Fischer von Mollard and Stevens, 1999). We have identified two *Arabidopsis VTI1* homologues. The deduced amino acid sequences of these two genes share significant similarity to Vti1p found in yeast and mammals (Fischer von Mollard *et al.*, 1997; Lupashin *et al.*, 1997; Advani *et al.*, 1998; Fischer von Mollard and Stevens 1998; Li, *et al.*,

Figure 3-10. AtVTI1a associates with AtPEP12p.
Post-nuclear supernatant from three grams of T7-AtVTI1a transgenic or wild-type *Arabidopsis* plants (21 days old) were treated with 1% Triton X-100 to solubilize membrane proteins. An aliquot was saved as total protein. The Triton X-100 solubilized protein extract was then incubated with 100 μl T7-antibody agarose (Novagen, Madison, WI) for 5 hrs. Beads were pelleted and the flowthrough collected. After being washed, proteins associated with the T7-antibody agarose were eluted. Equal volumes of total (T), flowthrough (FT) and elute (E) were separated by SDS-PAGE, followed by immunoblotting with antibodies against AtVTI1a, AtPEP12p or AtELP.

1998). We have found that AtVTI1a and AtVTI1b were able to substitute for yeast Vti1p in different membrane transport pathways. AtVTI1a efficiently suppressed the CPY mistargeting and the growth defect in one set of *vti1* temperature-sensitive mutants and in *vti1* null mutants, suggesting that AtVTI1a could substitute functionally for yeast Vti1p in these pathways. On the other hand, rather than rescuing the CPY missorting phenotype, AtVTI1b was found to restore transport of (1) the vacuolar protein ALP that is transported through the Golgi but bypasses the PVC; and (2) the hydrolase API, which utilizes the CVT pathway from the cytoplasm to the vacuole. By contrast, AtVTI1a does not function in the ALP or API transport pathway in yeast.

Whereas there is only one *VTI1* gene in yeast, two *VTI1*-related genes have been identified in *Arabidopsis*, mouse and human. It is speculated that the existence of two paralogues reflected greater complexity of the endomembrane system in higher organisms compared to yeast. In other words, various members of the Vti1 gene family probably have different functions. This notion is supported by the recent report that the two mouse *VTI1* genes are expressed ubiquitously and the mouse Vti1 proteins may be localized on different compartments (Xu *et al.,* 1998). Whereas the mouse paralogues share only 30% amino acid identity (Lupashin *et al.,* 1997), the plant paralogues are more closely related and share 60% amino acid identity. RNA analysis in plants using gene-specific probes did not detect any expression pattern difference between these two genes, indicating that both genes are expressed in the same cells and do not represent organ-specific isoforms. However, the intracellular location of the

AtVTI1b protein is not yet known. In yeast, the two *Arabidopsis* Vti1 homologues have functionally substituted for yVti1p in different vesicle transport steps. In plants, AtVTI1a most likely functions in a transport pathway analogous to the CPY pathway (see below). Based on yeast complementation data, we propose that AtVTI1b is involved in different vacuolar transport pathways in plants. However, the specific function of the two *VTI1* genes in plants will be revealed only when we are able to investigate their products at the protein level.

In plants, several components of the vacuolar targeting pathway machinery have been identified. AtPEP12p is a t-SNARE that resides on the PVC (Conceição *et al.*, 1997). AtELP is proposed to be a vacuolar protein-sorting receptor. In previous studies it has been demonstrated that AtPEP12p and AtELP colocalize on the PVC; AtELP has also been found in the Golgi and TGN (Sanderfoot *et al.*, 1998). Since it is highly probable that both of these proteins are involved in mediating transport of soluble vacuolar proteins, their intracellular distribution in relation to AtVTI1a was very revealing. Under EM, T7-AtVTI1a was localized on the TGN and on vesicular structures that most likely compose the PVC. By double labeling, AtVTI1a was found to co-localize with AtELP at the TGN and with AtPEP12p at the PVC. The colocalization of these three proteins suggests that AtVTI1a, AtELP, and AtPEP12p are most likely involved in the same pathway, the pathway responsible for the transport of a subset of vacuolar proteins at the step between the TGN and the PVC. Co-immunoprecipitation of AtVTI1a and AtPEP12p strongly support the hypothesis that AtVTI1a, as a v-SNARE, is responsible for the docking of vesicles from the

TGN to the PVC by interacting with AtPEP12p, the PVC t-SNARE. It will be interesting to characterize the vesicles whose fusion is controlled by AtVTI1a and to define the branches of the plant membrane traffic pathways in which AtVTI1a is involved. Further investigations should also reveal the membrane traffic pathways regulated by AtVTI1b.

References

Advani RJ, Bae HR, Bock JB, Chao DS, Doung YC, Prekeris R, Yoo JS, and Scheller RH (1998). Seven novel mammalian SNARE proteins localize to distinct membrane compartments. *J. Biol. Chem.* **273:** 10317-10324.

Ahmed SU, Bar-Peled M, and Raikhel NV (1997). Cloning and subcellular location of an *Arabidopsis* receptor-like protein that shares common features with protein-sorting receptors of eukaryotic cells. *Plant Physiol.* **114:** 325-336.

Altschul SF, Gish W, Miller W, Myers EW, and Lipman DJ (1990). Basic local alignment search tool. *J. Mol. Biol.* **215:** 403-410.

Bar-Peled M, and Raikhel NV (1997). Characterization of AtSEC12 and AtSAR1. Proteins likely involved in endoplasmic reticulum and Golgi transport. *Plant Physiol.* **114:** 315-324.

Bassham DC, and Raikhel NV (1997). Molecular aspects of vacuole biogenesis. *Adv. Bot. Res.* **25:** 43-58.

Bassham DC, Gal S, Conceição AS, and Raikhel NV (1995). An *Arabidopsis* syntaxin homologue isolated by functional complementation of a yeast pep12 mutant. *Proc. Natl. Acad. Sci. USA* **92:** 7262-7266.

Becherer KA, Rieder SE, Emr SD, and Jones EW (1996). Novel syntaxin homologue, Pep12p, required for the sorting of lumenal hydrolases to the lysosome-like vacuole in yeast. *Mol. Biol. Cell* **7:** 579-594.

Bent AF, Kunkel BN, Dahlbeck D, Brown KL, Schmidt R, Giraudat J, Leung J, and Staskawicz BJ (1994). RPS2 of *Arabidopsis thaliana:* a leucine-rich repeat class of plant disease resistance genes. *Science* **265:** 1856-1860.

Bryant NJ, and Stevens TH (1998). Vacuole biogenesis in *Saccharomyces cerevisiae:* protein transport pathways to the yeast vacuole. *Microbiol. Mol. Biol. Rev.* **62:** 230-247.

Calakos N, Bennett MK, Peterson KE, and Scheller RH (1994). Protein-protein interactions contributing to the specificity of intracellular vesicular trafficking. *Science* **263:** 1146-1149.

Conceição SA, Marty-Mazars D, Bassham DC, Sanderfoot AA, Marty F, and Raikhel NV (1997). The syntaxin homolog AtPEP12p resides on a late post-Golgi compartment in plants. *Plant Cell* **9:** 571-582.

Cowles CR, Snyder WB, Burd CG, and Emr SD (1997a). Novel Golgi to vacuole delivery pathway in yeast: identification of a sorting determinant and required transport component. *EMBO J.* **16:** 2769-2782.

Cowles CR, Odorizzi G, Payne GS, and Emr SD (1997b). The AP-3 adaptor complex is essential for cargo-selective transport to the yeast vacuole. *Cell* **91:** 109-118.

Darsow T, Rieder SE, and Emr SD (1997). A multispecificity syntaxin homologue, Vam3p, essential for autophagic and biosynthetic protein transport to the vacuole. *J. Cell Biol.* **138:** 517-529.

Fischer von Mollard G, and Stevens TH (1998). A human homolog can functionally replace the yeast vesicle-associated SNARE Vti1p in two vesicle transport pathways. *J Biol. Chem.* **273,** 2624-2630.

Fischer von Mollard G, and Stevens TH (1999). The *Saccharomyces cerevisiae* v-SNARE Vti1p is required for multiple membrane transport pathways to the vacuole. *Mol. Bio. Cell* **10:** 1719-1732.

Fischer von Mollard G, Nothwehr SF, and Stevens TH (1997). The yeast v-SNARE Vti1p mediates two vesicle transport pathways through interactions with the t-SNAREs Sed5p and Pep12p. *J. Cell Biol.* **137:** 1511-1524.

Gomez L, and Chrispeels MJ (1993). Tonoplast and soluble vacuolar proteins are targeted by different mechanisms. *Plant Cell* **5:** 1113-1124.

Hanson PI, Heuser JE, and Jahn R (1997). Neurotransmitter release—four years of SNARE complexes. *Curr. Opin. Neurobiol.* **7:** 310-315.

Hay JC, and Scheller RH (1997). SNAREs and NSF in targeted membrane fusion. *Curr. Opin. Cell Biol.* **9:** 505-512.

Hayashi T, McMahon H, Yamasaki S, Binz T, Hata Y, Sudhof TC, and Niemann H (1994). Synaptic vesicle membrane fusion complex: Action of clostridial neurotoxins on assembly. *EMBO J.* **13:** 5051-5061.

Holthuis JC, Nichols BJ, Dhruvakumar S, and Pelham HR (1998). Two syntaxin homologues in the TGN/endosomal system of yeast. *EMBO J.* **17:** 113-126.

Jones EW (1977). Proteinase mutants of *Saccharomyces cerevisiae*. *Genetics* **85:** 23-33.

Kirsch T, Paris N, Butler JM, Beevers L, and Rogers JC (1994). Purification and initial characterization of a potential plant vacuolar targeting receptor. *Proc. Natl. Acad. Sci. USA* **91:** 3403-3407.

Kirsch T, Saalbach G, Raikhel NV, and Beevers L (1996). Interaction of a potential vacuolar targeting receptor with amino- and carboxyl-terminal targeting determinants. *Plant Physiol.* **111:** 469-474.

Klionsky DJ (1998). Nonclassical protein sorting to the yeast vacuole. *J. Biol. Chem.* **273:** 10807-10810.

Klionsky DJ, and Emr SD (1989). Membrane protein sorting: biosynthesis, transport and processing of yeast vacuolar alkaline phosphatase. *EMBO J.* **8:** 2241-2250.

Klionsky DJ, Cueva R, and Yaver DS (1992). Aminopeptidase I of *Saccharomyces cerevisiae* is localized to the vacuole independent of the secretory pathway. *J. Cell Biol.* **119:** 287-299.

Kyte J, and Doolittle RF (1982). A simple method for displaying the hydropathic character of a protein. *J. Mol. Biol.* **157:** 105-132.

Li HC, Tahara H, Tsuyama N, and Ide T (1998). A hVti1 homologue: its expression depends on population doubling levels in both normal and SV40-transformed human fibroblasts. *Biochem. Biophys. Res. Commun.* **247:** 70-74.

Lukowitz W, Mayer U, and Jürgens G (1996). Cytokinesis in the *Arabidopsis* embryo involves the syntaxin-related KNOLLE gene product. *Cell* **84:** 61-71.

Lupashin VV, Pokrovskaya ID, McNew JA, and Waters MG (1997). Characterization of a novel yeast SNARE protein implicated in Golgi retrograde traffic. *Mol. Biol. Cell* **8:** 2659-2676.

Maeshima M, and Yoshida S (1989). Purification and properties of vacuolar membrane proton-translocating inorganic pyrophosphatase from mung bean. *J. Biol. Chem.* **264:** 20068-20073.

Maeshima M, Hara-Nishimura I, Takeuchi Y, and Nishimura, M (1994). Accumulation of vacuolar H^+-pyrophosphatase and H^+-ATPase during reformation of the central vacuole in germinating pumpkin seeds. *Plant Physiol.* **106:** 61-69.

Matsuoka K, Bassham DC, Raikhel NV, and Nakamura K (1995). Different sensitivity to wortmannin of two vacuolar sorting signals indicates the presence of distinct sorting machineries in tobacco cells. *J. Cell Biol.* **130:** 1307-1318.

Nothwehr SF, Roberts CJ, and Stevens TH (1993). Membrane protein retention in the yeast Golgi apparatus: dipeptidyl aminopeptidase A is retained by a cytoplasmic signal containing aromatic residues. *J. Cell Biol.* **121:** 1197-1209.

Odorizzi G, Cowles CR, and Emr SD (1998). The AP-3 complex, a coat of many colors. *Trends Cell Biol.* **8:** 282-288.

Piper RC, Bryant NJ, and Stevens TH (1997). The membrane protein alkaline phosphatase is delivered to the vacuole by a route that is distinct from the VPS-dependent pathway. *J. Cell Biol.* **138:** 531-545.

Robinson JS, Klionsky DJ, Banta LM, and Emr SD (1988). Protein sorting in *Saccharomyces cerevisiae*: isolation of mutants defective in the delivery and processing of multiple vacuolar hydrolases. *Mol. Cell Biol.* **8:** 4936-4948.

Sambrook J, Fritsch EF, and Maniatis T (1989). Molecular Cloning, a Laboratory Manual (2nd Edition). Cold Spring Harbor Laboratory Press, Plainview, NY. pp7.37-7.57 .

Sanderfoot AA, Ahmed SU, Marty-Mazars D, Rapoport I, Kirchhausen T, Marty F, and Raikhel NV (1998). A putative vacuolar cargo receptor partially colocalizes with AtPEP12p on a prevacuolar compartment in *Arabidopsis* roots. *Proc. Natl. Acad. Sci. USA* **95:** 9920-9925.

Sato MH, Nakamura N, Ohsumi Y, Kouchi H, Kondo M, Hara-Nishimura I, Nishimura M, and Wada Y (1997). The AtVAM3 encodes a syntaxin-related molecule implicated in the vacuolar assembly in *Arabidopsis thaliana*. *J. Biol. Chem.* **272:** 24530-24535.

Shimada T, Kuroyanagi M, Nishimura M, and Hara-Nishimura I (1997). A pumpkin 72-kDa membrane protein of precursor-accumulating vesicles has characteristics of a vacuolar sorting receptor. *Plant Cell Physiol.* **38:** 1414-1420.

Slot JW, Geuze HJ, Gigengack S, Lienhard GE, and James DE (1991). Immuno-localization of the insulin regulatable glucose transporter in brown adipose tissue of the rat. *J. Cell Biol* **113:** 123-135.

Söllner T, Bennett MK, Whiteheart SW, Scheller RH, and Rothman JE (1993) A protein assembly-disassembly pathway *in vitro* that may correspond to sequential steps of synaptic vesicle docking, activation, and fusion. *Cell* **75:** 409-418.

Srivastava A, and Jopnes EW (1998) Pth1/Vam3p is the syntaxin homolog at the vacuolar membrane of *Saccharomyces cerevisiae* required for the delivery of vacuolar hydrolases. *Genetics* **148:** 85-98.

Stepp J, Huang K, and Lemmon SK (1997). The yeast adaptor protein complex, AP-3, is essential for the efficient delivery of alkaline phosphatase by the alternate pathway to the vacuole. J. Cell Biol. **139:** 1761-1764.

Stevens T, Esmon B, and Schekman R (1982). Early stages in the yeast secretory pathway are required for transport of carboxypeptidase Y to the vacuole. *Cell* **30:** 439-448.

Sutton RB, Fasshauer D, Jahn R, and Brunger AT (1998). Crystal structure of a SNARE complex involved in synaptic exocytosis at 2.4 Å resolution. *Nature* **395:** 347-53.

Tokuyasu KT (1989). Use of poly(vinylpyrrolidone) and poly(vinyl alcohol) for cryoultramicrotomy. *Histochem. J.* **21;** 163-171.

Wada Y, Nakamura N, Ohsumi Y, and Hirata A (1997). Vam3p, a new member of syntaxin related protein, is required for vacuolar assembly in the yeast *Saccharomyces cerevisiae. J. Cell Sci.* **110:** 1299-1306.

Vater C.A., Raymond C.K., Ekena K, Howald-Stevenson I, and Stevens TH (1992). The VPS1 protein, a homolog of dynamin required for vacuolar protein sorting in *Saccharomyces cerevisiae*, is a GTPase with two functionally separable domains. *J. Cell Biol.* **119:** 773-786.

Vernet T, Dignard D, and Thomas DY (1987). A family of yeast expression vectors containing the phage f1 intergenic region. *Gene* **52:** 225-233.

Xu Y, Wong SH, Tang BL, Subramaniam VN, Zhang T, and Hong W (1998). A 29-kilodalton Golgi soluble N-ethylmaleimide-sensitive factor attachment protein receptor (Vti1-rp2) implicated in protein trafficking in the secretory pathway. *J. Biol. Chem.* **273:** 21783-21789.

Zheng H, Bassham DC, Conceição AS, and Raikhel NV (1999). The syntaxin family of proteins in *Arabidopsis*: a new syntaxin homologue shows polymorphism between two ecotypes. *J. Exp. Bot.* **50:** 915-924.

Chapter IV

The Comparison of Two AtVTI1 Proteins and Characterization of *Atvti12*, a T-DNA Insertion Mutant of *AtVTI12*

Abstract

In *Arabidopsis*, SNAREs are frequently encoded by gene families composed of two or more highly homologous genes. This phenomenon may be a reflection of the complexity of the endomembrane system. AtVTI11 and AtVTI12 are about 65% identical at the amino acid sequence level. AtVTI11 has been characterized in detail previously. It is localized on the TGN and the PVC. On the TGN, AtVTI11 co-localizes with AtELP, the NTPP cargo receptor, and sporamin, a vacuolar soluble protein with an NTPP sorting signal. AtVTI11 also forms a SNARE complex with SYP2 and SYP5 at the PVC. AtVTI12, however, is found mostly in the SNARE complex with SYP4 and SYP6. In this chapter, I further compared the difference between these two proteins. Based on density gradients, AtVTI11 and AtVTI12 have different subcellular locations. *Atvti12*, a null mutant of *AtVTI12* has been characterized in detail. This mutant has no obvious phenotype. However, the apparent normal phenotype may be explained by the fact that AtVTI11 was found to form a SNARE complex with SYP4 and SYP6 in the mutant.

Introduction

The plant secretory pathway plays a variety of roles in every step of plant development. This pathway is composed of a series of membrane-bound organelles. Each organelle has its own unique biochemical and physiological features and performs different functions. Thus, it is important to maintain homeostasis of each organelle. Vesicle transport is the major means by which proteins are delivered to and from these organelles. Although it is believed that the basic machinery for operating vesicular transport is well conserved between all eukaryotic cells, the uniqueness of the plant endomembrane system can not be ignored. For instance, in mammals and yeast, each cell has only one type of vacuole whereas in plants, different types of vacuoles frequently co-exist in one cell (Paris *et al.*, 1996; Jauh *et al.*, 1999). For soluble vacuolar proteins, there are at least three separate delivery routes based on the location and peptidal sequence of the sorting signal. Some proteins, represented by sweet potato sporamin and barley aleurain, carry a sorting signal with a typical NPIR motif, *e.g.* an N-terminal propeptide (NTPP) signal, at the N-terminus of the protein (Matsuoka and Nakamura, 1991). These proteins first enter the endomembrane system at the endoplasmic reticulum and are then transported through the Golgi apparatus to the *trans*-Golgi network (TGN). At the TGN, a membrane bound cargo receptor (AtELP is one of the examples, see Ahmed *et al.*, 2000) presumably recognizes the NTPP and directs those proteins into clathrin-coated vesicles (CCV). These vesicles deliver their cargo to the prevacuolar

compartment (PVC), which further fuses with the vacuole. AtVTI11 and SYP21 most likely are involved in this process (Zheng *et al.*, 1999; Bassham *et al.*, 1995; Conceição *et al.*, 1997). On the other hand, some proteins carry their vacuolar sorting signal at the C-terminus of the protein. These signals are called C-terminal propeptides (CTPP). CTPP cargos are delivered through a route completely different from the NTPP pathway (Matsuoka *et al.*, 1995). None of the molecular components involved in this pathway have been identified yet. Very often, different types of sorting signals also determine the destination to a specific vacuole. Most NTPP cargos are delivered into the lytic vacuole, while CTPP cargo is sent to the pH neutral storage vacuoles. Sometimes, the lytic and the protein storage vacuoles fuse to form one central vacuole (Di Sansebastiano *et al.,* 2001). It is possible that this complex vacuolar system requires more sophisticated transport machinery than that used in yeast. Based on genome analysis, there are 21 SNAREs in *Saccharomyces cerevisiae* (Bock *et al.*, 2001). In *Arabidopsis*, there are 55 SNAREs that can be subgrouped into several families (Sanderfoot *et al.*, 2000). These multi-gene families could be the reflection of a more complex endomembrane system.

The VTI1 type SNARE has multiple functions. In yeast, although encoded by a single gene, it can form SNARE complexes with 5 of 8 syntaxins (Lupashin *et al.*, 1997; Fischer von Mollard *et al.*, 1997; Abeliovich *et al.*, 1998; Fischer von Mollard and Stevens, 1999). In mouse and human, there are 2 *VTI1* genes that encode proteins about 30% identical to each other and 25% to 33% to yeast Vti1p (Lupashin *et al.*, 1997; Fischer von Mollard and Stevens 1998). In mouse,

VTI1a is localized to the Golgi and involved in intra-Golgi trafficking. Vti1b is found on Golgi, TGN, and possibly also on the endosome (Xu *et al.*, 1998). These two proteins do not completely co-localize when expressed in mammalian cells (Xu *et al.*, 1998).

In *Arabidopsis*, the *VTI1* family is composed of three closely related members (65% to 75% identical at the amino acid sequence level). They are all about 25% identical to yeast Vti1p and are closer to mammalian VTI1a than to mammalian VTI1b (Sanderfoot *et al.*, 2000). *AtVTI11* and *1 2* are highly expressed, while AtVTI13 produces only very low level of mRNA that can not be detected on northern blot (data not shown). Previously, we have described the characterization of AtVTI11 (AtVTI1a, Zheng *et al.*, 1999). AtVTI11 is localized on the TGN, together with the NTPP cargo receptor AtELP, and on the PVC, together with SYP2 and SYP5 groups of syntaxins (Zheng *et al.*, 1999; Sanderfoot *et al.*, 2001). It also physically interacts with SYP2 and SYP5, as has been shown by co-immunoprecipitation experiments (Zheng *et al.*, 1999; Bassham *et al.*, 2000; Sanderfoot *et al.*, 2001). We suggest that AtVTI11 is involved in vesicle trafficking between the TGN and PVC by forming a SNARE complex with SYP2 and SYP5 groups of syntaxins (Zheng *et al.*, 1999; Sanderfoot *et al.*, 2001). It is possible that AtVTI11 is involved in NTPP cargo transport based on its co-localization with AtELP and sporamin (Zheng *et al.*, 1999; chapter V). AtVTI12, a close relative of AtVTI11 (65% identical at the peptide sequence level), is also expressed in *Arabidopsis* (Zheng *et al.*, 1999).

AtVTI11 and *AtVTI12* are expressed in all the tissues that have been investigated. The expression patterns of these two genes are also similar.

However, there is some evidence supporting the notion that AtVTI11 and AtVTI12 function in different pathways. First, *AtVTI11* and *AtVTI12* complement different yeast *vti1* mutant alleles that block different vacuolar protein transport pathways (Zheng *et al.*, 1999). In plant cells, in contrast to the SNARE complex composed of AtVTI11, SYP2 and SYP5, AtVTI12 forms a SNARE complex with SYP4 and SYP6 groups of syntaxins (Bassham *et al.*, 2000; Sanderfoot *et al.*, 2001). These results indicate that AtVTI12 may play a role in vesicle trafficking different from AtVTI11. However, although there is some indication that AtVTI11 is involved in NTPP cargo transport, no clue has been found about the function of AtVTI12. Thus, we decided to search for individual knockout mutants of *AtVTI11* and *AtVTI12*. Here, I describe a T-DNA insertion mutant in the promoter region of *AtVTI12*. Although AtVTI12 protein is abolished from this mutant, *Atvti12* has a normal phenotype. Co-immunoprecipitation results suggest that the apparent normal phenotype may be due to the presence of AtVTI11. I propose that although AtVTI11 has different functions in the wild type, it could substitute for AtVTI12 in the *Atvti12* mutant.

Materials and Methods

Plasmids, Transgenic Plants and *Arabidopsis* Mutants

For generating glutathione-S-transferase (GST) fusion constructs of AtVTI11 or AtVTI12, the same PCR fragments used to construct His-AtVTI11

(Zheng *et al.*, 1999) or His-AtVTI12 (Bassham *et al.*, 2000) were instead fused with pGEX5x-3.

Arabidopsis plants expressing T7-AtVTI11 were described by Zheng *et al.*, 1999. *Arabidopsis* plants expressing HA-AtVTI12 were described by Bassham *et al.* (2000).

Arabidopsis T-DNA insertion mutant *Atvti12* was identified with the help of Mendel Biotechnology. The details of identification of mutant plants in T-DNA insertion mutant pools were described by Sanderfoot *et al.* (2001).

Antibodies and Columns

The same antigen used to generate anti-AtVTI11 in guinea pig (Zheng *et al.*, 1999) was used to raise rabbit antiserum against AtVTI11. Rabbit antiserum raised against AtVTI12 was described by Bassham *et al.* (2000). AtVTI12 antiserum was further affinity purified against *E. coli* expressed GST-AtVTI12. Recombinant GST-AtVTI12 was over-expressed and purified with the use of glutathione-Sepharose beads (Amersham-Pharmacia Biotech AB). Five mg of overexpressed GST-ATVTI12 was then bound to 1 ml of glutathione-Sepharose 4B and equilibrated with 200 mM boric acid, pH 9.0. Dimethyl pimelimidate was added to reach the final concentration of 4 mg/ml. After incubation at room temperature for 30 min, the cross-linker was quenched with 0.2 M ethanolamine (pH 8.0) and washed with phosphate-buffered saline (PBS). Anti-AtVTI12 crude serum was applied to this column. After washes with 5 ml 0.1 M Tris, pH 8.0, followed by another wash with 5 ml of 0.01 M Tris, pH 8.0, the antibodies bound to the column were eluted with 10 ml 100 mM glycine, pH 2.5. The eluate was

collected in 1-ml fractions. The fractions containing antibodies were pooled and protein concentration determined by the value of $O.D._{280}$. One percent BSA and 0.02% azide was added before storage at 4°C. Antibodies from pre-immune serum or AtVTI11 serum were purified by incubating 1 ml serum with 1.5 ml Protein A Sepharose 6MB (Amersham Pharmacia Biotech AB) for 30 min at room temperature. The beads were washed with 5 ml 0.1 M Tris, pH 8.0, followed by another wash with 5 ml of 0.01 M Tris, pH 8.0. The bound antibody was eluted by 2x2.5 ml 0.1M glycine, pH 2.5, for 10 min each. The two fractions were pooled. The protein concentration was determined by the value of $O.D._{280}$. For the anti-AtVTI12 column, 2 mg of the GST-AtVTI12 affinity purified antibody, were incubated with 1.5 ml protein A 6MB beads for 1 hour at room temperature. For anti-AtVTI11, pre-immune of AtVTI11 or pre-immune of AtVTI12 columns, two mg of the protein A affinity-purified antibodies were incubated with 1.5 ml protein A 6MB beads for one hour at room temperature. After wash with 2x5 ml 200 mM borate acid, pH 9.0, the crosslinker dimethyl pimelimidate was added to reach the final concentration of 5 mg/ml. The reactions were kept at room temperature for 30 min before quenching by 0.2 M ethanolamine (pH 8.0). The beads were stored in PBS with 0.02% azide at 4°C.

Immunoprecipitation

Twenty gm of 21-day-old liquid cultured *Arabidopsis* roots were homogenized on ice with 5 ml Extraction Buffer (50 mM HEPES-KOH, pH 6.5, 10 mM potassium acetate, 100 mM sodium chloride, 5 mM EDTA, 0.4 M sucrose) with Complete™ protease inhibitor tablets (Roche). To prepare the total

membrane, the homogenate was centrifuged at 1000 *g* for 15 min and the supernatant was subjected to 100,000 *g* ultracentrifugation for 3 hours. The pellet was homogenized in 3 ml TBS (Tris balanced buffer; 0.14 M NaCl, 2.7 mM KCl, 25 mM Tris, pH 8.0) with miniComplete™ tablets (Roche). The total membrane was solubilized by adding Triton X-100 to 1%. The solubilized membrane was further cleared by ultracentrifugation at 100,000 *g* for 30 min. The supernatant was incubated with antibody or pre-immune columns for 2 hours. After 5 x washes with 5 ml TBST (TBS + 1% Triton X-100) each, the bound protein was eluted with 4 ml 0.1 M glycine (pH 2.5). The antibody columns were neutralized by washing with 10 ml PBS. The eluted protein was precipitated by 10% trichloroacetic acid. After two acetone washes, the protein pellet was solubilized in 50 μl 2X Laemmli buffer. The protein was separated by SDS-PAGE and different proteins were detected by western blot.

Pulse-Chase Labeling

Fifty mature *Arabidopsis* rosette leaves were cut to thin strips and immersed in 10% cellulase (Onozuka R10), 0.5% macerozyme R10 (Yakult Honsha Co., Ltd Japan) and 0.08% BSA in enzyme solution (0.5 M betaine, 10 mM $CaCl_2$ and 1.5 mM MES, pH 5.7). Vacuum was applied for 30 min to facilitate penetration of the solution to the leaf tissues. After incubation for 3 hours in the dark, the protoplasts were separated from undigested tissues as described in Bednarek and Raikhel (1991). The protoplasts were diluted to a final concentration of 100,000 cells/ml in incubation medium (Gamborg's B5 basal medium with mini organics (Sigma) supplemented with 0.3 M betaine, 0.1 M

glucose, 1 mg/L 2,4-D). The protoplasts were labeled with 100 μCi ^{35}SExpress (Dupont) for four hours. The labeling was stopped by adding 100 μl of chase mix (165 mM methionine and 110 mM cysteine in incubation buffer) to the cells. After 30 min chase, the protoplasts were then separated from the incubation buffer and lysed in TBSE (0.14 M NaCl, 2.7 mM KCl, 25 mM Tris, pH 8.0, 0.5mM EDTA) + 1% Triton-X 100. The lysates were cleared of insoluble debris by brief centrifugation at 10,000 *g* for 30 sec. Protein A beads bound with equal amount of affinity-purified aleurain antibody or pre-immune antibody were added to the lysates and incubated for 2 hours at 4°C. After the beads had been washed 3 times with TBSE + 1% Triton-X 100, 50 μl 2X laemmli loading buffer were added to the beads. The eluted proteins were then separated by 12% SDSA-PAGE and visualized by autofluorography.

Subcellular Fractionation

Twenty-one-day old *Arabidopsis* cultured roots were used to prepare total membrane as described in "Immunoprecipitation". The total membrane was then layered on top of a discontinuous Accudenz® (Accurate chemicals and Scientific Corp., NY) gradient (1.5 ml of each: 2%, 5%, 9%, 12%, 15%, 20% and 30% [w/w] from the top to the bottom). The gradient was then equilibrated by ultracentrifugation at 100,000 *g* for 16 hours. Fractions of 0.5 ml each were taken from the top to the bottom and proteins were separated by SDS-PAGE. Western blots were used to visualize different subcellular markers.

PCR and RT-PCR

Genomic DNA was isolated using the CTAB extraction procedure described in Sanderfoot *et al.* (2001). The following primers were used for screening T-DNA inserted in the gene of *AtVTI12:* 5' end gene-specific primer: 5' TAT TTC CTG GAC GAG TAA TCT TGG TTC TGC 3', 3' end gene-specific primer: 5' TCT GAC GTG ACA GTG GGT CTC CTG CCT GCG 3'. T-DNA left border: 5' CTC ATC TAA GCC CCC ATT TGG ACG TGA ATG 3'. T-DNA left border nested: 5' TTG CTT TCG CCT ATA AAT TAC GAC GGA TCG 3'. T-DNA right border: 5' TGG GAA AAC CTG GCG TTA CCC AAC TTA AT 3'. The PCR reaction condition for amplifications of genomic DNA was the standard condition described in manufacturer's recommendations (Gibco-BRL, Rockville, MD). Reverse transcription reactions for RT-PCR were done using the Superscript II reverse transcriptase system following recommendations from the manufacturer (Gibco-BRL, Rockville, MD). The following gene-specific primers were used to generate first-strand cDNAs: for *AtVTI12*: 5' GAG CCA CGA TTA CCG ATGT 3'; for *NPSN-12*: 5' AGT GTA ATA TGC ACC AAA CC 3'. These reverse primers and forward primers (for AtVTI12: 5' GAA AAT GTC ACT CTG CAT CG 3'; for *NPSP12*: 5' GAG CCT GAA ATA ATC CGG CAG AT 3') were used for PCR amplification of the reverse transcript products with the standard conditions described in the manufacturer's recommendations (Gibco-BRL, Rockville, MD).

Results

The Specificity of Antibodies Raised Against AtVTI11 and AtVTI12.

Instead of being concentrated in certain domains, the similarities between AtVTI11 and AtVTI12 are found throughout the sequence (Zheng *et al.*, 1999).

Thus, it is difficult to generate specific antibodies using a particular peptide sequence. Instead, anti-VTI11 and anti-12 rabbit anti-sera were raised against His-tagged N-terminal part of the proteins just before the transmembrane domain (Zheng *et al.*, 1999; Bassham *et al.*, 2000). Previously, we have shown that when these two antibodies are used on western blots to visualize T7-AtVTI11 or HA-AtVTI12 in total protein extracts from transgenic plants, anti-AtVTI11 specifically recognizes T7-AtVTI11 and anti-AtVTI12 specifically recognizes HA-AtVTI12 (Bassham *et al.*, 2000). However, because the expression levels of T7-AtVTI11 and HA-12 are different in transgenic plants, the quantities of AtVTI11 and AtVTI12 are difficult to control and thus the specificity of the antibodies is still not clearly evaluated. Here, two different approaches were used to address the specificity of these two antibodies. First, cytosolic domains of AtVTI11 and 12 (identical to the part that fused with 6XHis to make antigens) were fused with GST and over-expressed in *E. coli*. The recombinant protein was affinity purified through a glutathione column. The amount of purified proteins was visually determined by Coomassie Brilliant Blue stain after SDS-PAGE. As shown in Figure 4-1A, when equal amounts of GST-AtVTI11 and GST-AtVTI12 were loaded on the gel, western blot indicates that the affinity of anti-AtVTI11 to the GST-AtVTI11 is about 10 times higher than to the GST-AtVTI12. AtVTI12 antibody, however, shows almost equal sensitivity towards GST-AtVTI11 or GST-AtVTI12 proteins.

Figure 4-1. Characterization of the specificity of Anti-AtVTI11 and Anti-AtVTI12. **A)** The GST-fusion of N-terminal AtVTI11 or 12 were purified by glutathoine columns. Equal amount of purified GST-fusion proteins of AtVTI11 and 12 (loading quantities were indicated on the top) were separated by SDS-PAGE. AtVTI11 and 12 antisera were used for western blots. Molecular weight marker is shown at the left. **">"**: the full length GST-fusion protein. **B)** Total membrane from 10 gm of root culture (21-day old) were solubilized by 10% Triton X-100. Equal volumes of these solubilized proteins were passed through anti-AtVTI12, 11 or pre-immune columns. After extensive wash, protein bound to the columns was eluted by 0.1 M glycine (pH 2.5) and precipitated by 10% TCA. 1/10 eluate from anti-AtVTI11 (V11), anti-AtVTI12 (V12), their pre-immune columns (pre) or 1/300 of total membrane protein (T) were separated by SDS-PAGE. Anti-AtVTI11 or 12 were used for western blot. **">"**: AtVTI11, **"*"**: AtVTI12

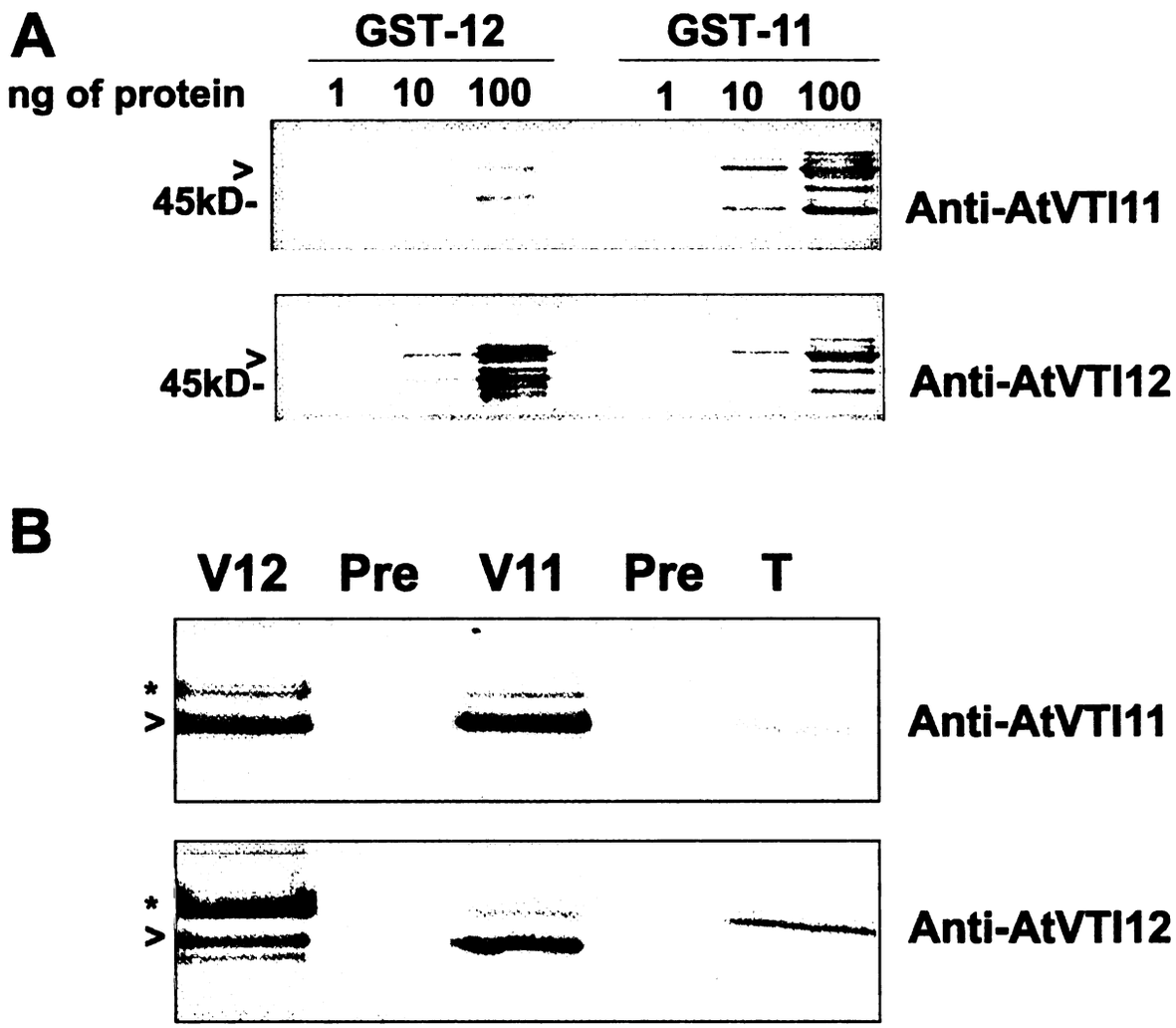
A
GST-12
GST-11
ng of protein
1 10 100
1 10 100
45kD-
Anti-AtVTI11
45kD-
Anti-AtVTI12
B
V12 Pre V11 Pre T
Anti-AtVTI11
Anti-AtVTI12

Because immunoprecipitation is the major means by which we can address the question of SNARE complex composition, the specificities of these two antibodies when used for immunoprecipitation were evaluated. The antibodies from anti-AtVTI11 or pre-immune sera were affinity purified through protein A beads and eluted using 0.1 M glycine (pH 2.5). The amount of eluted antibodies was visually determined by SDS-PAGE followed by Coomassie Brilliant Blue staining. The antibodies were then cross-linked to a Protein A 6MB column by dimethyl pimelimidate with the ratio of 1 mg antibody/1 ml beads. The same procedure was used to generate anti-AtVTI12 column and its pre-immune control column except the anti-AtVTII12 was affinity purified through a GST-AtVTI12 column. Total membrane prepared from 10 gm of 21-day-old *Arabidopsis* cultured roots was used as starting material. The post-nuclear total membranes were solubilized with 1% Triton X-100 and cleared by ultracentrifugation at 100,000 *g* for 30 min before being divided into equal volumes and incubated with pre-immune columns or anti-AtVTI11 or AtVTI12 columns for 2 hours. After washing, the proteins bound to the columns were eluted with 0.1 M glycine, pH 2.5. The total membrane or the eluates from immune or pre-immune columns were separated by SDS-PAGE and western blots were used to detect AtVTI1 proteins. In the lanes where total membrane protein was loaded, AtVTI12 antibody detected two bands, whereas only the lower band was detected by AtVTI11 antisera (Figure 4-1B). Since AtVTI11 anti-sera were more specific than AtVTI12, it was concluded that the lower band detected by both antisera was AtVTI11. The band recognized only by AtVTI12

anti-serum was AtVTI12. Although not easy to distinguish, these two proteins migrated with about 1 to 3 kDa difference on SDS-PAGE. Based on the assumption that AtVTI12 antiserum has equal sensitivity towards both AtVTI11 and 12, there may be more AtVTI12 than AtVTI11 in the total membrane proteins from cultured roots (Figure 4-1B). Although the ratios of these two proteins vary slightly, there were always more AtVT12 proteins than AtVTI11 in all tissues examined (data not shown). When used for immunoprecipitation, AtVTI11 antibody had higher affinity toward AtVTI11 protein than AtVTI12. However, AtVTI12 antibody, although it would not distinguish AtVTI11 and 12, also precipitated more AtVTI12 owing to a larger amount of AtVTI12 in the sample (Figure 4-1B).

In conclusion, when used for western and immunoprecipitation, AtVTI11 and AtVTI12 antibodies are not absolutely specific to one or the other, although AtVTI11 are relatively more specific towards AtVTI11. However, there is a molecular weight difference between the two proteins. When carefully examined, these two proteins can be distinguished on western blots.

AtVTI11 and AtVTI12 Have Different Fractionation Patterns

To further analyze the functional difference between AtVTI11 and AtVTI12, the subcellular localizations of these two proteins were studied. Neither AtVTI11 nor AtVTI12 antibodies work well in immunocytochemistry. Therefore, T7-AtVTI11 and HA-AtVTI12 double transgenic plants were used for EM study. The root tip cells were double labeled with T7- and HA- monoclonal antibodies to

visualize the locations of AtVTI11 and 12. Both AtVTI11 and AtVTI12 were found on the TGN or the PVC membrane. Sometimes these two proteins were co-localized on the same membrane, but at other times, they were localized on separate membranes (Zheng H, Kovaleva V and Raikhel NV, unpublished). To address the question of the relative location of AtVTI11 and AtVTI12 accurately, a discontinuous Accudenz gradient was used to fractionate total microsomes from *Arabidopsis* roots. Post-nuclear supernatant from 21-day-old *Arabidopsis* cultured roots was loaded on top of a step Accudenz gradient (2, 5, 9, 12, 15, 20, and 30% from top to bottom). The gradient was equilibrated by ultracentrifugation at 100,000 *g* for 16 hours at 4°C, and fractions of 0.5 ml were collected from the top to the bottom. These fractions were then analyzed by western blot. As shown in Figure 4-2A, after ultracentrifugation, the gradient became almost linear with a slower slope between 1.075 mg/ml to 1.175 mg/ml. We chose to look at the fractionation patterns of several well-studied markers. Using the experimental conditions described above, microsomes harboring SYP2 (the PVC membrane) and SYP6 (the TGN membrane) can be clearly distinguished. SYP2 fractionated at lower density (around 1.125 mg/ml), whereas SYP6 peaked at the high-density (around 1.175 mg/ml) fractions. AtELP, which labels the TGN and the PVC, and SYP4, which labels TGN by immunocytochemistry, mostly fractionated with SYP6 (AtELP see Figure 4-2, data for SYP4 is not shown). SYP5 co-fractionated with SYP2 (data not shown). AtVTI11 completely co-fractionated with SYP2. However, using AtVTI12 anti-sera, we saw two bands peaked at different

Figure 4-2. Subcellular fractionation of AtVT11 and AtVTI12 by discontinuous Accudenz gradient. Post-nuclear membranes of *Arabidopsis* cultured roots (21-day-old) were loaded on a step Accudenz gradient. After equilibrium by ultracentrifugation at 100,000 *g* for 16 hours, 0.5-ml fractions were collected from the top (1) to the bottom of the gradient. The densities of the fractions were determined by refractometry and plotted in **A**. Equal volumes of even-numbered fractions were loaded on an SDS-PAGE and immunoblotted with anti-sera of interested proteins as shown in **B**.

A

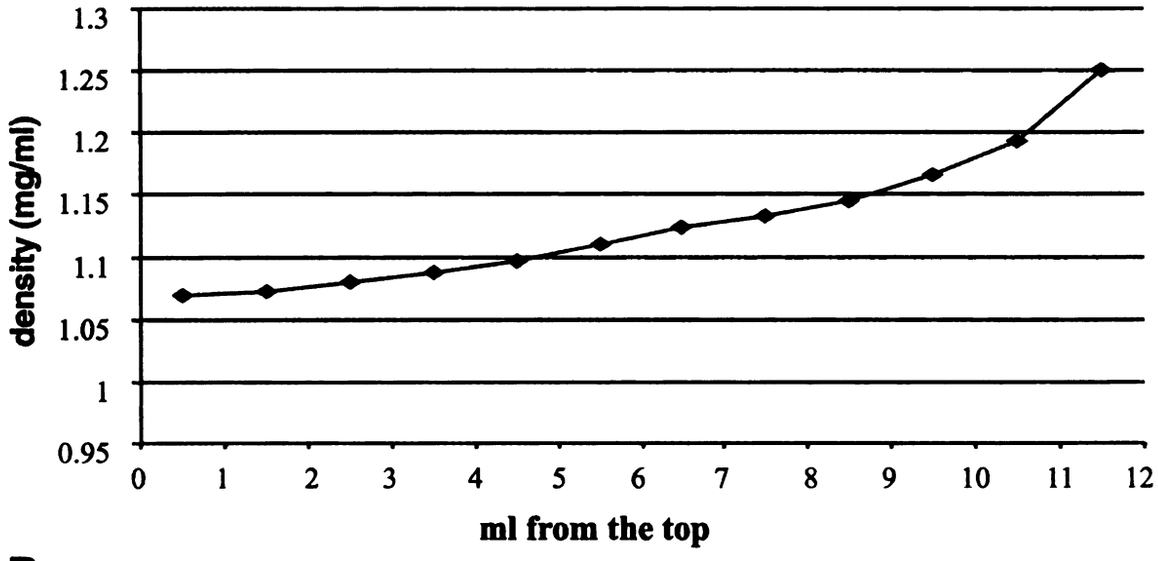
1.3
1.25
1.2
1.15
1.1
1.05
1
0.95
density (mg/ml)
0
1
2
3
4
5
6
7
8
9
10
11
12
ml from the top

B

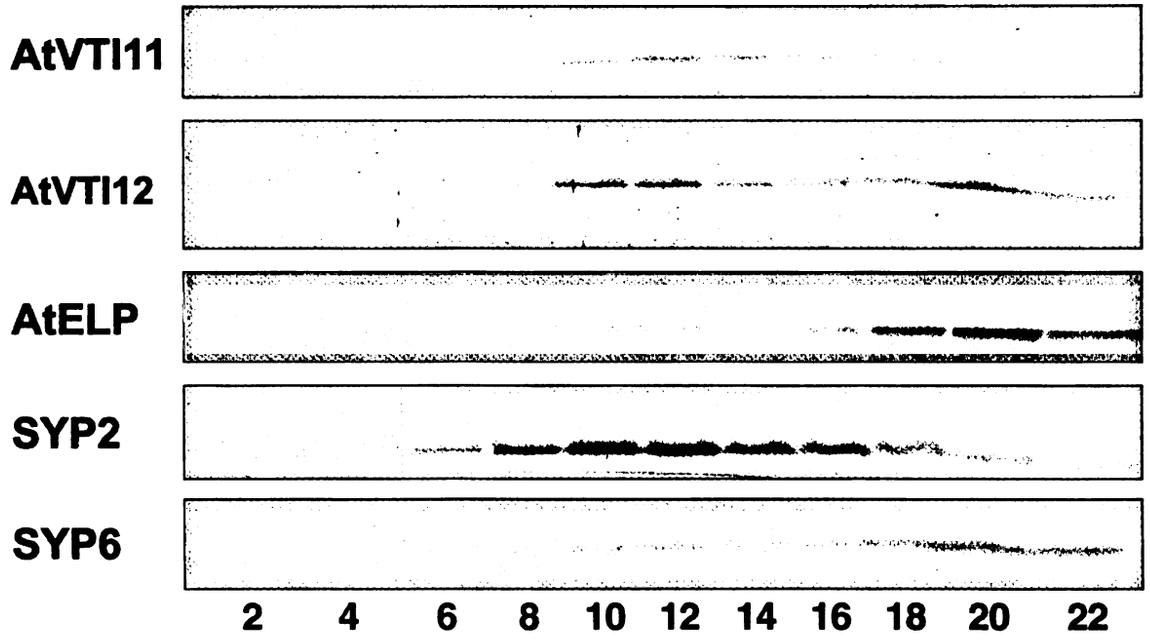
AtVTI11
AtVTI12
AtELP
SYP2
SYP6
2
4
6
8
10
12
14
16
18
20
22

fractions. The band with higher molecular weight co-fractionated with SYP6 and peaked at high-density fractions. This band most likely represented AtVTI12. The lower molecular band has the same molecular weight as the band recognized by anti-AtVTI11 and was found to co-fractionate with SYP2 at relatively lower density. This band is most likely AtVTI11. The Accudenz gradient thus offered the first clear evidence that AtVTI11 and AtVTI12, two very closely related SNAREs, might have different subcellular locations. The different location in the cell may reflect the fact that these two proteins are involved in the formation of different complexes.

Characterization of the Mutant *Atvti12*

A reverse genetics approach was taken to further address the function of AtVTI12. To identify a T-DNA insertion mutant of AtVTI12, pools of *Arabidopsis* Col-*gl* seeds mutagenized with T-DNA were screened using gene-specific primers and T-DNA border primers (see Materials and Methods). One mutant plant with a T-DNA inserted at –76nt upstream of transcription start (Figure 4-3A) was identified at the heterozygous stage. This allele was named at*vti12* for its mutation in *AtVTI12*. The seeds of this plant were collected and the individual plants from the next generation (F1) were examined in detail. Genomic PCR was performed using a 5' gene-specific primer and T-DNA left border primer to detect the insertion; while 5' and 3' gene specific primer pairs were used to detect the intact *AtVTI12* gene without the insertion. Among 42 F1 plants, 12 were homozygous for the T-DNA insertion and 10 were homozygous wild-type plants. The total RNA prepared from a mixture of leaves, stems, and flowers of

Figure 4-3. *Atvti12* is a null mutant for *AtVTI12*. **A)** The diagram of the T-DNA insertion in *Atvti12* gene. T-DNA is inserted at -76 nt upstream from transcription start of *AtVTI12* gene on chromosome I. **B)** RT-PCR of *AtVTI12*. Total RNA from seedlings of wild-type (Col-0), heterozygous plants (20, 39) or homozygous insertion mutant (21, 29) were used as templates. AtVTI12 cDNA was generated by reverse transcription with gene specific primers at the 3' end of the *AtVTI12* mRNA. 5' and 3' primer pairs were used to amplify the cDNA. The amplified DNA was separated by 1% agarose gel and visualized by 1% ethdium bromide. The molecular weight is indicated at the left. **C)** RT-PCR of *NPSN-12* using the same template described in **B** with gene specific primers for *NPSN-12* mRNA. **D)** Western blots of total protein extracted from wild-type (7, 27) or *Atvti12* (21, 29) seedlings. The proteins were separated by SDS-PAGE and immunoblots were used to visualize AtVTI11 or 12. Arrows indicate the AtVTI12 protein band that was missing in *Atvti12* plants.

ram of the T-DN
from transcript
12. Total RNA fr
9) or homozygo
NA was genera
end of the AtVT
The amplified DN
lium bromide Th
12 using the sa
SN-12 mRNA
or Atvti12 (2
mmunoblots we
protein band

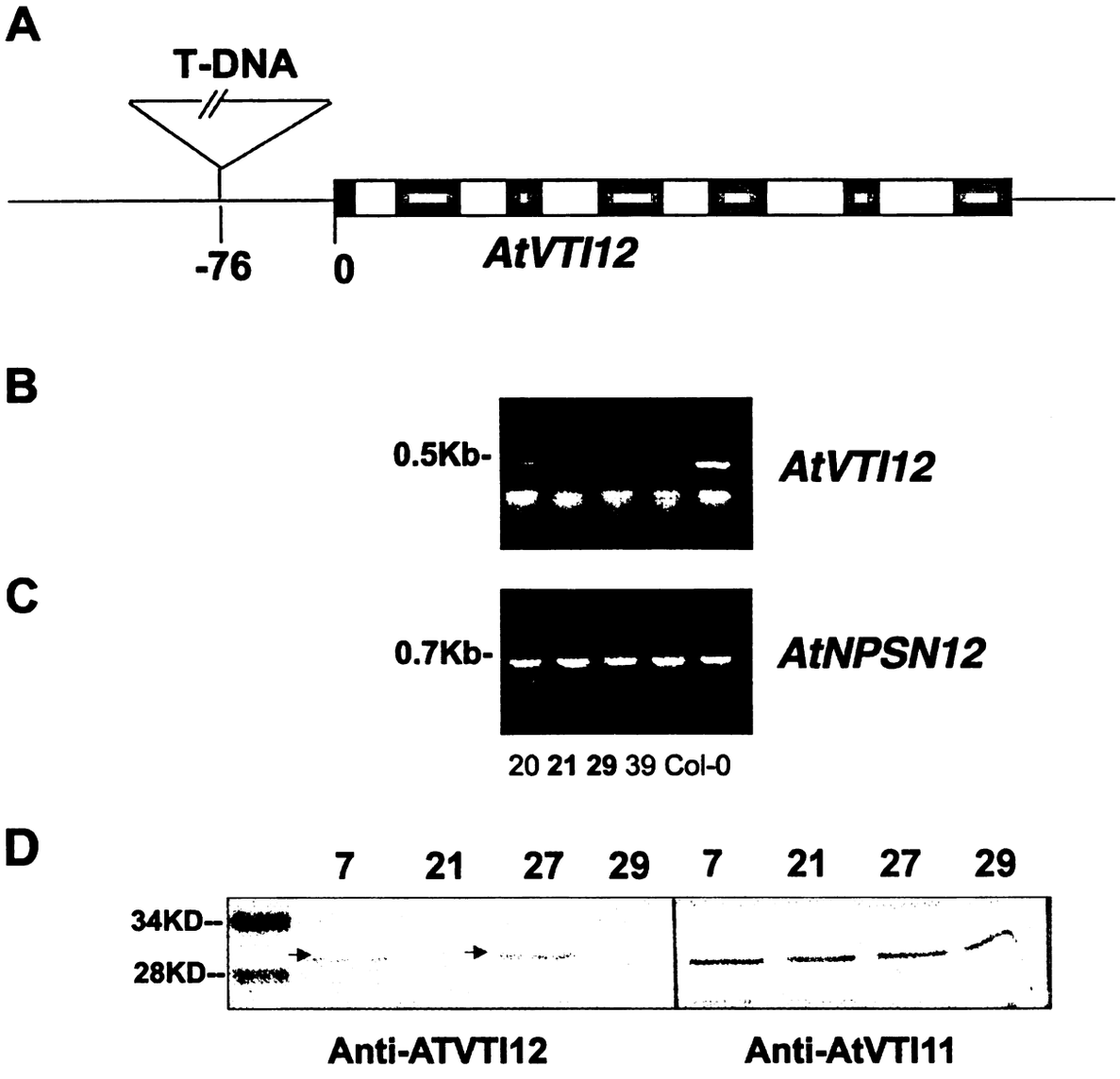

wild-type plants, heterozygous plants (20, 39) and homozygous *Atvti12* plants (21, 29) were used as templates for RT-PCR. The condition of the RT-PCR was designed to detect even very low levels of mRNA (see Materials and Methods). As shown in Figure 4-3B, RT-PCR from RNA of homozygous *Atvti12* plants did not produce a band that represents *AtVTI12* mRNA. In comparison, using RNA from wild type or heterozygous plants, RT-PCR produced a band at around 500bp. This band indicates that *AtVTI12* mRNA was present in the total RNA sample and thus the gene was expressed in those plants. RT-PCR of an unrelated gene (*NPSN12*) using the same RNA samples was used as a control to indicate the quality of the total RNA sample (Figure 4-3C). Two plants with homozygous insertion (21 and 29) and two plants with homozygous wild-type AtVTI12 genes (7 and 27) were chosen for further characterization. Their seeds were germinated on plates containing solid medium. The protein extracts from these seedlings were further analyzed. As shown in Figure 4-3D, on western blot, AtVTI12 antibody recognized a band at around 28 to 30 kDa that was missing from the homozygous *ATVti12* plants but present in wild-type plants. This band is putatively the AtVTI12 protein. In contrast, when AtVTI11 antibody was used for western blot analysis, there was no significant difference between proteins of the wild type and the *Atvti12* homozygous plants. Proteins extracted from other tissues (flowers, mature leaves, and roots) have been analyzed with the same results (data not shown). This experiment indicated that there is no significant amount of AtVT12 protein in *Atvti12* mutant plants. At the same time, the AtVTI11 protein level is not changed between *Atvti12* mutant and wild type plants.

The *Atvti12* plants were then checked for any defect in NTPP vacuolar protein transport. It has been shown that *Arabidopsis* aleurain has a typical NTPP signal and is most likely transported through the route common for NTPP proteins (Ahmed *et al.*, 2000). Thus, the processing of aleurain protein was examined in *Atvti12* plants. When the vacuolar cargo transport routes are blocked, we expect the marker protein is either targeted to the wrong place and degraded (reduced amount) or accumulated in an intermediate compartment (indicated by appearance of higher molecular variants due to lack of processing). In total protein extract, no difference in total amount of mature aleurain was found between wild type or *Atvti12* plants (Figure 4-4A). There is no obvious abnormal accumulation of higher molecular variants of aleurain in the *Atvti12* plants either. To examine the dynamics of aleurain transport, pulse-chase labeling of aleurain was performed. Protoplasts generated from mature leaves of the wild type and the *Atvti12* plants (Number 30 line) were labeled with ^{35}SExpress for 4 hours. The cells were lysed and total proteins were incubated with the pre-immune or anti-aleurain columns (1 mg pre-immune or affinity purified aleurain antibody/ 1 ml protein A 4MB). After washing, the retained proteins were eluted and separated by SDS-PAGE. Since the pre-immune antibody precipitated strong background bands, we have to use the affinity-purified aleurain antibody reveal the purified aleurain. In autofluorographs that were exposed for 20 days, the weak aleurain bands were revealed. However, there was no difference in the amount of precursor or mature protein between the wild type or *Atvti12* plants (Figure 4-4B). The homozygous *Atvti12* plant also had no visible phenotype as

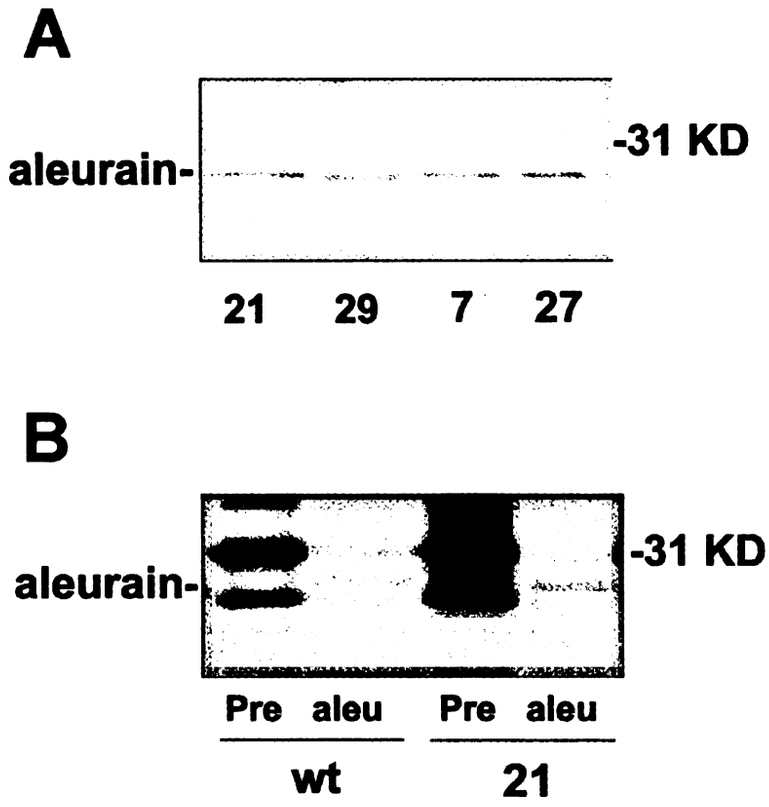

Figure 4-4. Aleurain processing in *Atvti12* cells. **A)** Western blot of aleurain. Total protein extracts from wild type (7, 27) or *atvti12* homozygous mutant (21, 29) seedlings were separated by SDS-PAGE. Aleurain was detected by immuno-blot. Molecular weight marker was marked at the right. **B)** Pulse-chase labeling of aleurain. Protoplasts from wild type (wt) or homozygous *Atvti12* (21) mature leafs were labeled with ^{35}S Express for 4 hours and chased for 30 min with excess cold cysteine and methionine. Pre-immune (Pre) or affinity-purified aleurain (aleu) antibodies were used to immuno-precipitate the radio-labeled proteins. One forth of the precipitated proteins were analyzed by SDS-PAGE followed by autofluorogarphy. The aleurain bands were marked at the left. Molecular weight marker was labeled at the right.

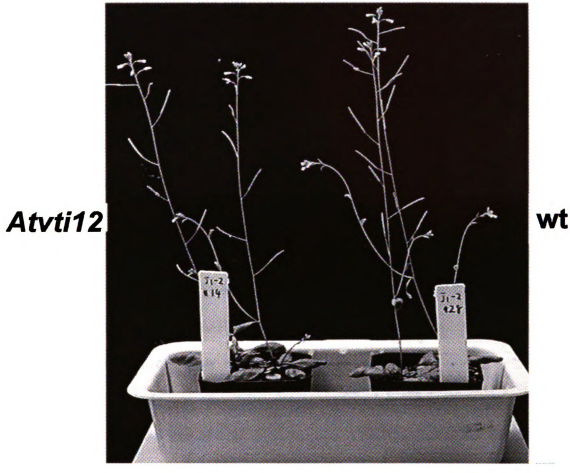

Figure 4-5. Phenotype of *Atvti12*. The plants were grown in standard conditions with 16-hour light/8-hour dark. The picture was taken at 21 days after germination. Number 14 at left is a homozygous *Atvti12* mutant. Number 28 at the right is a plant segregated from the same parental line with homozygous intact *AtVTI12* genes. The *Atvti12* plant has no apparent phenotype.

shown in Figure 4-5. Under various physiological conditions, no difference between the wild type and the *Atvti12* plants was observed (data not shown). In conclusion, *Atvti12* mutant has no obvious phenotype and the absence of AtVTI12 protein caused no obvious defect to the plants.

We have shown that the AtVTI1 family of proteins, although closely related, may form SNARE complexes with different sets of syntaxins (Bassham *et al.*, 2000; Sanderfoot *et al.*, 2001). Thus, they may have functional differences as well. The genes encoding other members of those SNARE complexes, *e.g.* SYP2, SYP5, SYP4, and SYP6 are all absolutely required for the plant; since no homozygous knock-out mutants has been recovered. Thus, it is a surprise to us that the plants lacking AtVTI12 protein do not have any physiological or developmental defect. One hypothesis is that AtVTI11 and AtVTI12 can functionally substitute for each other when one is missing. To evaluate this possibility, I analyzed the SNARE complexes of AtVTI11 in the wild type and *Atvti12* mutant. As shown in Figure 4-6, when AtVTI11 antibody was used for immunoprecipitation, SYP2 and SYP5 families of syntaxins were co-precipitated in both the wild type and *Atvti12* mutant plants. There was no difference in the amount of SYP2 and SYP5 brought down from the wild type or *Atvti12* mutant plants. This observation suggests that AtVTI11 forms a SNARE complex with SYP2 and SYP5 and its ability to perform its functions are not changed when AtVTI12 is missing. However, there was much more SYP4 and SYP6 co-precipitated in *Atvti12* than in the wild-type plants (Figure 4-6). Most likely,

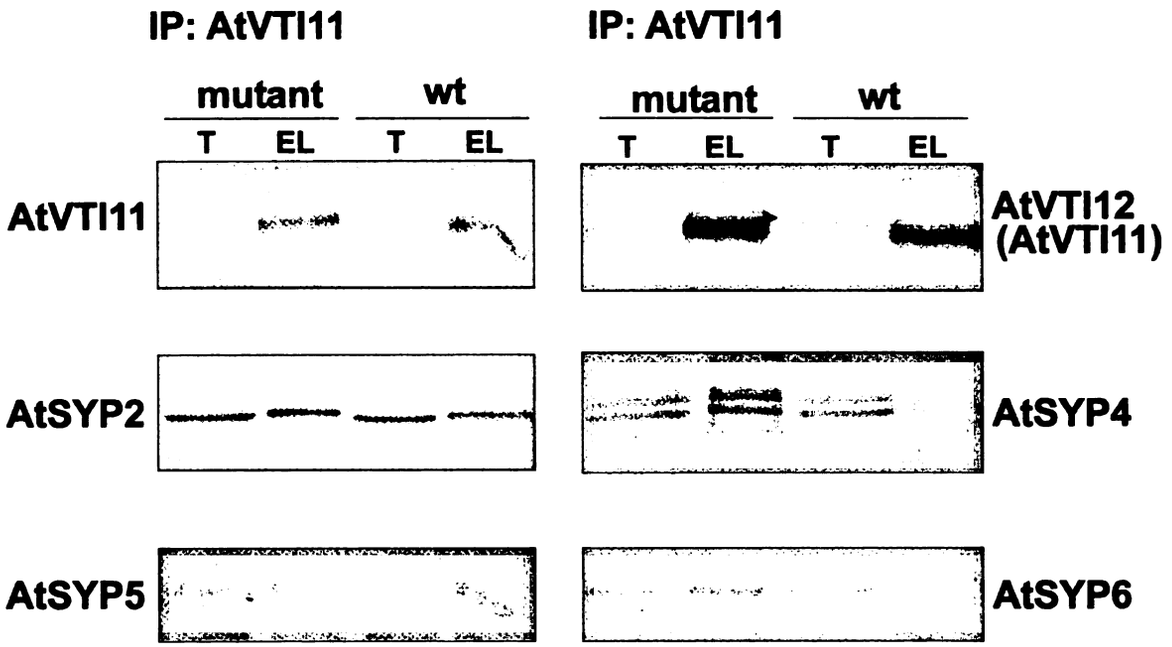

Figure 4-6. Immunoprecipitation of AtVTI11 from wild-type and *Atvti12* mutant plants. Total membarne from 10 gm of 21-day old wild type or *Atvti12* root culture were treated with 1% Triton X-100 to solublize the membrane proteins. An aliquot of 1/300 was saved as total membrane protein samples (T). The Triton X-100 solubilized membarne proteins were then passed through anti-AtVTI12 or pre-immune columns. After extensive wash, the proteins associated with the columns were eluted by 0.1 M Glycine (pH 2.5) and precipitated by 10% TCA. 1/5 of the eluates (EL) or 1/300 of total membarne proteins (T) were separateed by SDS-PAGE. Proteins of interest were visualized by immuno-blotting Arrow head indicates AtVTI12 band in wild-type plants.

AtVTI11 formed a SNARE complex with SYP4 and SYP6 and performed the function of AtVTI12.

Based on the data described above, I propose that in wild type plants, AtVTI11 interacts with SYP2 and SYP5. One function of this SNARE complex might be to facilitate the transport of NTPP vacuolar proteins because AtELP (a vacuolar cargo receptor) also co-localizes with AtVTI11 and SYP2. AtVTI12, however, interacts with SYP4 and SYP6 to form a completely different SNARE complex. The function of this SNARE complex requires further investigation. In the mutant where AtVTI12 is absent, AtVTI11 performs dual functions and forms a noncognate SNARE complex with SYP4 and SYP6 (Figure 4-7) and leads to normal plants.

Discussion

Although the basic machinery for vesicle transport is believed to be well conserved among all eukaryotic organisms, plant secretory pathways are much more complicated than single-celled yeast. Plant cells often have multiple vacuoles that require multiple pathways for vacuolar protein transport. At the whole plant level, different cell types might require cell-specific functions performed by these pathways that may not be necessary for yeast or mammals. For the components of the secretory machinery, it is possible that gene families are developed from one single gene to accommodate the complex duties they face. The AtVTI1 family proteins are proven to be a good example. In yeast, the VTI1 protein is encoded by a single gene but The protein is involved in several SNARE complexes and thus has diverse functions (review see Götte and Fischer

Figure 4-7. Summary of results. AtVTI11 and AtVTI12 are highly homologous SNAREs. Although they are both localized on the TGN and the PVC membranes, Their ratios between two membranes are different and can be separated by biochemical means. Moreover, AtVTI11 forms SNARE complexes with SYP2 and SYP5, whereas AtVTI12 forms complexes with SYP6 and SYP4. In the AtVTI12 mutant *Atvti12*, AtVTI11 forms an additional SNARE complex with SYP4 and SYP6.

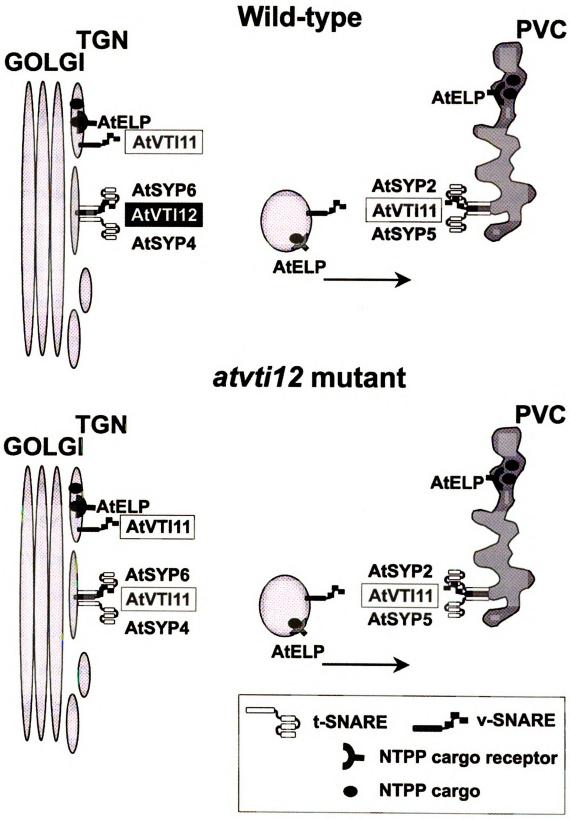
Wild-type
TGN
GOLGI
PVC
AtELP
AtVTI11
AtSYP6
AtVTI12
AtSYP4
AtELP
AtSYP2
AtVTI11
AtSYP5
AtELP
atvti12 mutant
TGN
GOLGI
PVC
AtELP
AtVTI11
AtSYP6
AtVTI11
AtSYP4
AtELP
AtSYP2
AtVTI11
AtSYP5
AtELP
t-SNARE
v-SNARE
NTPP cargo receptor
NTPP cargo

von Mollard, 1998). When expressed in the yeast *vti1* mutant, AtVTI11 facilitates the transport of soluble carboxy-peptidase Y to the vacuole. AtVTI12, however, is more effective in the transport of vacuolar membrane proteins and in the autophagy pathway (Zheng *et al.*, 1999). In plants, AtVTI11 is in a SNARE complex with SYP2 and SYP5, whereas AtVTI12 is in a SNARE complex composed of SYP4 and SYP6. (Bassham *et al.*, 2000; Sanderfoot *et al.*, 2000). SYP2 is localized on the PVC, and SYP4 on the TGN. Using transgenic plants expressing T7- or HA- tagged AtVTI11 or AtVTI12, we have shown by immunocytochemistry that these two proteins are both localized on the TGN and the PVC and sometimes on the same membrane. However, when separated by an Accudenz gradient, AtVTI11 and AtVTI12 membranes are fractionated differently. EM, as a snapshot, reflected that AtVTI11 and AtVTI12 are localized on both the TGN and the PVC. However, density gradient fractionation reflected the ratios of marker proteins on different membranes. AtVTI11 co-fractionated with SYP2 and AtVTI12 with SYP4 and SYP6. It is likely that *in vivo,* after the CCV fuses with the TGN, AtVTI11 spend majority of its time on the PVC before being recycled back. Most AtVTI12 proteins remain on the TGN after mediating the fusion between a yet unknown vesicle with the TGN. SNAREs are localized on the membrane where they function. It thus safe to speculate that AtVTI12 may also play a role in vesicle transport between the TGN and the PVC. However, in *Atvti12* mutant, although AtVTI11 forms a SNARE complex with SYP4 and SYP6, the fractionation pattern of AtVTI11 was still the same as in wild type plants (data not shown). This can be explained by the observation that the subcellular

localization of a SNARE is determined by its transmembrane domain sequence (Rayner and Pelham, 1997; Watson and Pessin, 2001) instead of by SNARE partners it interacts with.

There is no indication about the function of AtVTI12 in plants yet except that when expressed in yeast, it functioned in membrane vacuolar membrane protein transport and the cytoplasm-to-vacuole (Cvt) pathway (Zheng *et al.*, 1999). Although it has been shown that membrane protein vacuolar transport is separated from soluble protein transport, it is a poorly characterized pathway in plants. Except for electron microscopy description of plant autophagy, little is known about the molecular basis of autophagy and the related Cvt pathway. In yeast, besides Vti1p, Tlg2p and Tlg1p are also required for the Cvt pathway and for vacuolar membrane protein transport. SYP4 family of proteins are the homologues of Tlg2p in *Arabidopsis*. SYP6 is a Tlg1 homologue. Thus, it is likely that the transport steps in which SYP4, SYP6 and AtVTI12 play roles are evolved from the membrane vacuolar protein transport or the Cvt pathways in yeast. We hope the study about these *Arabidopsis* SNAREs will shade light on the exact nature and the functions of these pathways in plants.

Reverse genetics is a powerful way to address the question regarding the functions of AtVTI12 and its SNARE complex. However, SYP41, SYP42 and SYP6 mutations have been shown to be lethal to the plants (Sanderfoot *et al.*, 2000). These observations indicate that the AtVTI12-SYP4-SYP6 complex is involved in a function that is critical for the cell. Unfortunately, those SYP mutants are not very helpful for our understanding of the exact nature of this complex.

Surprisingly, the situation of mutation at the *AtVTI12* gene is quite different. In *Atvti12,* where the *AtVTI12* is not expressed, the plant appeared normal. When AtVTI11 SNARE complex was precipitated, we found besides the complex formed with SYP2 and SYP5, AtVTI11 also formed a complex with SYP4 and SYP6. It is likely that AtVTI11 can fully substitute for AtVTI12 in this mutant.

A similar situation is observed in the AtVTI11-SYP2-SYP5 pathway. As previously shown, SYP21 and 22, although closely related, can not functionally substitute for each other. *SYP21* and *SYP22* null mutants are both lethal possibly at as early as the pollen stage (Sanderfoot *et al.*, 2001). Recently, an AtVTI11 null mutant *zig-1* has been identified. The complete absence of AtVTI11 protein causes a shoot gravitropic defect, wrinkled leaves, fragmented vacuoles, and some other light phenotypes (Morita *et al.*, 2001; Kato *et al.*, 2001). It is speculated that the gravitropic defect is a secondary defect caused by certain changes in the physical or chemical environment of the vacuole (Morita *et al.*, 2001). At least in roots, AtVTI12 was found in the complex with SYP21 and SYP22 (Zheng and Raikhel, unpublished data). AtVTI12 seems to take the place of AtVTI11 and generates relatively normal plants.

It seems that SYP2 and SYP4 group of syntaxins, although are composed of closely related family members, in the cell, each member has unique functions and cannot take each other's place. The reason might rely on the dynamic difference between syntaxins and VTI1 type SNAREs. In a cell, the localization of a SNARE reflects its functional site. Syntaxins are SNAREs with less flexible

locations. The subcellular localization of a syntaxin is determined by its transmembrane domain sequence (Rayner and Pelham, 1997; Watson and Pessin, 2001). SYP41 and SYP42 have been localized on different domains of the TGN. Although SYP21 and SYP22 are both localized on the PVC in root tips, SYP22, but not SYP21, has been found on tonoplast of small vacuoles in shoot meristems (Sato *et al.,* 1997) and in vacuole-enriched membranes prepared from suspension cells (Rojo E and Raikhel NV, unpublished data). When one SYP is absent, it is impossible for its homologue to take its place unless the two are localized at the same place. However, the VTI1-type SNAREs are more mobile. Immunocytochemical study localized both AtVTI11 or AtVTI12, on the TGN and the PVC, although their distribution ratios between the TGN and the PVC might be different as reflected by their density gradient fractionation pattern difference. AtVTI11 and AtVTI12 may both shuttle between the TGN and the PVC. When one is missing, the other one has the chance to meet its SNARE partner and to fulfill its functions. Thus, although VTI1-type proteins might have functions critical for the plant, the loss of one is well tolerated. Only in the double mutant, we might have the opportunity to understand the real function of AtVTI1 family of proteins.

The phenomenon that two functionally different SNARE proteins substitute for each other *in vivo* has not been reported before. However, noncognate SNAREs have been shown to form complexes in arbitrary combinations *in vitro* (Fasshauer *et al.*, 1999). It is not difficult to imagine that more closely related AtVTI11 and AtVTI12 could be exchanged in their SNARE complexes *in vitro*. *In*

vivo, this possiblity of substitution also exists because both AtVTI11 and AtVTI12 are localized on the TGN and the PVC membrane (Zheng H, Kovaleva V and Raikhel NV unpublished data). In *Arabidopsis*, there are quite a number of reports of mutated genes causing no phenotype. Normally, this is attributed to gene redundancy. However, when we start to understand the machinery of the plant cell function in more detail, sometimes, the "redundant" genes might be found to have functional differences. This mechanism for related but not redundant proteins to stand in for each other reflects one facet of flexibility of plant cells.

References

Ahmed SU, Rojo E, Kovaleva V, Venkataraman S, Dombrowski JE, Matsuoka K, and Raikhel NV (2000). The plant vacuolar sorting receptor AtELP is involved in the transport of NH2-terminal propeptide-containing vacuolar proteins in *Arabidopsis thaliana*. *J. Cell Biol.* **149:** 1335-1344.

Abeliovich H, Darsow T, and Emr SD (1999). Cytoplasm to vacuole trafficking of aminopeptidase I requires a t-SNARE-Sec1p complex composed of Tlg2p and Vps45p. *EMBO* **18:** 6005-6016.

Bassham DC, Gal S, Conceição AS, and Raikhel NV (1995). An *Arabidopsis* syntaxin homologue isolated by functional complementation of a yeast *pep12* mutant. *Proc. Natl. Acad. Sci. USA* **92:** 7262-7266.

Bassham DC, Sanderfoot AA, Kovaleva V, Zheng H, and Raikhel NV (2000). AtVPS45 complex formation at the *trans*-Golgi network. *Mol. Biol. Cell* **11:** 2251-2265.

Bednarek SY, and Raikhel NV (1991). The barley lectin carboxyl-terminal propeptide is a vacuolar protein sorting determinant in plants. *Plant Cell* **3:** 1195-1206.

Bock JB, Matern HT, Peden AA, and Scheller RH (2001). A genomic presepective on membrane compartment organization. *Nature* **409:** 839-841.

Conceição AS, Marty-Mazars D, Bassham DC, Sanderfoot AA, Marty F, and Raikhel NV (1997). The syntaxin homologue AtPEP12p resides on a late post-Golgi apparatus in plants. *Plant Cell* **9:** 571-582.

Di Sansebastiano GP, Paris N, Marc-Martin S, and Neuhaus JM (2001). Regeneration of a lytic central vacuole and of neutral peripheral vacuoles can be visualized by green fluorescent proteins targeted to either type of vacuoles. *Plant Physiol.* **126:** 78-86.

Fasshauer D, Antonion W, Margittai M, Pabst S, and Jahn R (1999). Mixed and non-cognate SNARE complexes. *J Biol. Chem.* **274:** 15440-15446.

Fischer von Mollard G, and Stevens TH (1998). A human homolog can functionally replace the yeast v-SNARE Vti1p in two vesicle transport pathways *J. Biol Chem.* **273:** 2624-2630.

Fischer von Mollard G, and Stevens, TH (1999). The *Sacchromyces cerevisiae* v-SNARE Vti1p is required for multiple membrane transport pathways to the vacuole. *Mol. Biol. Cell* **10:** 1719-1732.

Fischer von Mollard G, Northwehr SF, and Stevens TH (1997). The yeast v-SNARE Vti1p mediates two vesicle transport pathways through interactions with the t-SNAREs Sed5p and Pep12p. *J. Cell Biol.* **137:** 1511-1524.

Götte M and Fischer von Mollard G (1998). A new beat for the SNARE drum. *Trends Cell Biol.* **8:** 251-218.

Jauh GY, Philips TE, and Rogers JC (1999). Tonoplast intrinsic protein isoforms as markers of vacuolar functions. Plant Cell 11: 1867-1882.

Kato T, Morita MI, Fukaki H, Yoshiro Y, Uehara M, Nihama M, and Tasaka M (2001). SGR2, a phospholipase-like protein, and ZIG/SGR4, a SNARE, are involved in the shoot gravitropism of *Arabidopsis*. Submitted.

Lupashin VV, Pokrovskaya ID, McNew JA, Waters MG (1997). Characterization of a novel yeast SNARE protein implicated in Golgi retrograde traffic. *Mol. Biol. Cell* **8:** 1379-1388.

Matsuoka K, and Nakamura K (1991). Propeptide of a precursor to a plant vacuolar protein required for vacuolar targeting. *Proc. Natl. Acad. Sci USA* **88:** 834-838.

Matsuoka K, Bassham DC, Raikhel NV, and Nakamura K (1995). Different sensitivity to wortmannin of two vacuolar sorting signals indicates the presence of distinct sorting machineries in tobacco cells. *J. Cell Biol.* **130:** 1307-1318.

Morita MT, Kato T, Nagafusa K, Saito C, Ueda T, Nakano A, and Tasaka M (2001). Involvement of the vacuoles of the endodermis in early process of shoot gravitropism in *Arabidopsis*. Submitted

Paris N, Stanley CM, Jones, RL, and Rogers JC (1996). Plant cells contain two functionally distinct vacuolar compartments. *Cell* **85:** 563-572.

Rayner JC, and Pelham HR (1997). Transmembrane domain-dependent sorting of proteins to the ER and plasma membarne in yeast. *EMBO J.* **16:** 1832-1841.

Sanderfoot AA, Assad, FF, and Raikhel NV (2000). The *Arabidopsis* genome. An abundance of soluble N-ethylmaleimide-sensitive factor adaptor protein receptors. *Plant Physiol.* **124:** 1558-1569.

Sanderfoot AA, Pilgrim M, Adam L, and Raikhel NV (2001). Disruption of individual members of *Arabidopsis* syntaxin gene families indicates each has essential functions. *Plant Cell* **12:** 659-666.

Sato MH, Nakamura N, Ohsumi Y, Kouchi H, Kondo M, Hara-Nishimura I, Nishimura K, and Wada Y (1997). The atVAM3 encodes a syntaxin-related

molecule implicated in the vacuolar assembly in *Arabidopsis thaliana*. *J Biol. Chem.* **272:**24530-24535.

Watson RT, and Pessin JE (2001). Transmembrane domain length determines intracellular membarne compartment localization of syntaxins 3, 4, and 5. *Am. J. Physiol. Cell Physiol.* **28:** C215-C223.

Xu Y, Wong SH, Tang BL, Subramaniam VN, Xhang T, and Hong W (1998). A 29-kilodalton Golgi soluble N-ethylmaeimide-sensitive factor attachment protein receptor (Vti1-rp2) implicated in protein trafficking in the secretory pathway. *J. Biol. Chem.* **273:** 21783-21789.

Zheng H, Fischer von Mollard G, Kovaleva V, Stevens TH, and Raikhel NV (1999). The plant vesicle associated SNARE AtVTI1a likely mediates vesicle transport from the *trans*-Golgi network to the prevacuolar compartment. *Mol. Biol. Cell* **10:** 2251-2264.

Chapter V

Characterization of AtVTI1-Containing Vesicles Purified by Immuno-affinity Columns

Abstract

The Pre-vacuolar compartment (PVC) is a recently identified compartment of the endomembrane system in plants which function is still not clear. The syntaxin SYP21 is the only known marker that localizes exclusively in the PVC. Several other membrane proteins, including AtELP, AtVTI11 and 12, have been found on this compartment as well as on the TGN. However, none of the soluble proteins present in the lumen of the PVC have been identified. I have taken a biochemical approach to characterize this organelle and investigate its function. I have purified the PVC based on the presence of AtVTI11 and 12 are localized on it. An affinity column with conjugated anti-AtVTI12 antibodies was used to purify AtVTI1-containing vesicles. Sporamin, an NTPP cargo marker was found to co-purify in the vesicle fraction. This co-localization was confirmed by immuno-electron microscopy. To identify novel cargo, the proteins in the immunopurified fraction were separated by 2-D gel electrophoresis. These proteins will be identified by mass spectrometry techniques.

Introduction

The prevacuolar compartment (PVC) is defined as an intermediate organelle in the vesicular trafficking pathway from the TGN to the vacuole. It is most prominent in cells where new vacuoles are actively formed. It has been extensively characterized morphologically by electron microscopy (Marty, 1978). It was speculated that provacuoles were involved in protein transport to the vacuole both through the biosynthetic pathway and through autophagy (Marty, 1978; Marty, 1980). However, no resident protein of the PVC was known and thus it was hard to study this organelle. Recently it was shown that SYP2 is localized in the PVC. SYP2 is an *Arabidopsis* syntaxin homologue of yeast Pep12p. In yeast Pep12p resides on the prevacuolar compartment (PVC) and is critical for vacuolar transport of carboxy-peptidase Y from the TGN to the vacuole (Becherer *et al.*, 1996). In *Arabidopsis* root tips, SYP2 group proteins decorate a tubular-vesicular electron dense structure between the TGN and the vacuole. AtELP, a vacuolar cargo receptor, can be observed on the TGN and on this compartment but not in the vacuole (Conceição *et al.*, 1997, Sanderfoot *et al.*, 1998). Based on these results, we speculate that this organelle is a PVC that functions as a midstation for protein transport between the TGN and the vacuole and allows recycling of the trafficking machinery before arrival at the lytic vacuole. To characterize the PVC in more detail, we have purified it by biochemical means and analyzed its protein content. The detailed catalog of protein content of this organelle will offer us insight into its traffic dynamics, and

will supply us with more tools to study it by genetic and biochemical means. The identification of the PVC content also will yield clues about the function of SYP2.

The purification methods based on the unique physical features of the organelle have not proved to be very efficient for PVC purification, in contrast to those for vacuole, nuclei or chloroplast isolation. A major constraint is that the PVC is most abundant in vacuolating cells of the meristem which are difficult to harvest and thus tissues with less accumulation of PVCs must be used. Moreover, the PVC has similar physical characteristics as a lot of other organelles and thus it is difficult to separate to high purity (Zheng and Raikhel, unpublished). Therefore, the only available method to obtain highly enriched PVC fractions relies on affinity purification.

AtVTI11and 12 and SYP2 have been found on the PVC by immuno-electron microscopy (Zheng *et al.*, 1999; Zheng, Kovaleva and Raikhel, unpublished data). Moreover, AtVTI11 and 12 are found to co-fractionate with SYP2 on various types of density gradients (Zheng *et al.*, 1999; Sanderfoot and Raikhel, unpublished data). Our results indicate that most of AtVTI11 and 12 is present on the PVC membrane. Thus, it is possible to use AtVTI11 or 12 antibodies to purify the PVC. The AtVTI12 antibody can be purified from other IgGs in the serum with relative ease and it recognizes AtVTI11 ands 12 with similar sensitivity (See chapter IV). I have used this antibody to affinity purify the membranes containing AtVTI1 (AtVTI11 and 12) in large scale. The purified microsomes were eluted with detergent and separated by 2-D gel electrophoresis. The specific spots will be identified using matrix-assisted laser

desorption ionization- time of flight (MALDI-TOF)- or electrospray ionization (ESI)- mass spectrometry (MS). After the proteins have been identified, the interesting ones will be studied further by immunocytochemistry to confirm their localization.

Few vacuolar soluble markers endogenous to *Arabidopsis* have been characterized to date. Exogenous markers like sweet potato sporamin are properly targeted to the vacuole when expressed in *Arabidopsis* (Matsuoka *et al.*, 1991). Recently, it has been shown AtELP specifically interacts with the sporamin NTPP peptide and that AtELP and sporamin co-localize on the same domain of the TGN (Ahmed *et al.*, 2000) indicating that may travel through the PVC, as AtELP, in route to the vacuole. Thus, sporamin can be used as a marker to evaluate the quality of the isolated PVC vesicles. Here, I describe preliminary results in the characterization of the protein content of the PVC.

Materials and Methods:

Arabidopsis Transgenic Lines

The generation of *Arabidopsis* transgenic plants expressing sporamin was described in Matsuoka *et al.*, 1995. The generation of *Arabidopsis* expressing T7-AtVTI11 is described in Zheng *et al.*, 1999.

An *Arabidopsis* plant expressing T7-AtVTI11 was crossed with pollen from a plant expressing sporamin. The F2 generation from the cross was screen for plants stably expressing T7-AtVTI11 and sporamin.

Electron Microscopy

The procedure used to prepare grids for thin plastic sections followed by immunolabeling with the appropriate antibodies was described in Zheng et. al (1999) and Ahmed *et al.* (2001).

Antibody Purification and Preparation of Affinity Columns

The AtVTI12 antibody was subject to affinity purification against *E. coli* over expressed GST-fusion of AtVTI12. Antibody and pre-immune column were made as described in Chapter IV with equal amounts of purified IgG.

AtVTI11 Vesicle Enrichment:

Two hundred grams of *Arabidopsis* cultured roots were homogenized in tissue extraction buffer (50 mM HEPES.KOH pH6.5, 10mM KOAc, 100mM NaCl, 5mM EDTA and 13.7% Sucrose) with complete protease inhibitor cocktail (Roche) using a food processor at high speed 10 sec for three times. The homogenized material was filtered through Miracloth (Calbiochem) and spun at 1000g for 15 min to get rid of the debris. The supernatant was filtered through Miracloth again and total membrane fraction was pelleted by ultracentrifugation at 100,000 *g* for 30 min. The pellet containing total membrane was homogenized by douncing with 16ml tissue extraction buffer. The homogenate was divided into halves and loaded on top of two sucrose gradients (12 ml 24%, 12ml 36%, 3 ml 56% sucrose in tissue extraction buffer). The gradient was spun at 100,000 *g* for two hours in a swing rotor and the interface between 24% and 36% sucrose was collected. The sugar concentration of this AtVTI11 enriched fraction was adjusted to 13-14% by adding 5 volumes of tissue extraction buffer without sucrose.

Affinity Purification

A volume of tissue extraction buffer + 10% BSA was added to the AtVTI11 enriched fraction described above to achieve a BSA concentration of 5%. This membrane fraction was then incubated overnight at 4°C with 1ml protein-A beads conjugated with antibodies that had been pre-incubated two hours with Tissue Extraction Buffer +10% BSA. The beads were then washed with 6X5ml tissue extraction buffer for 10 min each. The protein in the vesicles was eluted with 5ml Tissue Extraction Buffer + 1% Triton X-100. The protein in the eluate was precipitated with trichloroacetic acid (final concentration 10%) and washed with acetone twice. The beads were regenerated by treating with 5ml 0.1M glycine (pH2.5), washed with PBS twice and stored in PBS with 1% azide.

2-D Electrophoresis

The 2-D gel separation procedure was performed as in Peck *et al.* (2001) with minor changes. Detergent eluted proteins from antibody columns were mixed with an equal volume of Tris-buffered phenol, pH 8 (Gibco-BRL, Rockville, MD) and back extracted twice with Back Extraction Buffer (100mn Tris, pH8.4, 20nM KCl, 10mM EDTA and 0.4% β-mercaptoethanol). Two to five volumes of 100mM ammonium acetate in methanol was added to the phenol phase and proteins were precipitated by centrifugation at 10,000 *g* for 30 min at 4°C. After washing the pellet with 80% acetone twice, the protein pellet was resuspened in 370 μl of 2-D loading buffer (7 M urea, 2 M thiourea, 4% CHAPs, 0.5% IPG-Buffer (Amersham-Pharmacia), 2% DTT, and 0.1% bromphenol blue). This loading buffer with solubilized proteins was used to rehydrate the 18cm 3-10NL

IPG strips (Amershan Pharmacia) on IPGphor (Amersham Pharmacia) at 80 V for 12 hours. Subsequently, the isoelectric focusing was performed under the following condition: 500 V for 2 hours, 1000 V for 2 hours, gradient to 5000 V in 12 hours, 5000 V for 12 hours. After isoelectric focusing, IPG strips were equilibrated in the equilibration buffer (50 mM Tris, pH 6.8, 6M urea, 30% glycerol, 1% SDS, and 0.01% bromophenol blue) plus 1% DTT and 15 min in equilibration buffer plus 4.5% iodoacetamide. The strips were then loaded on 12% SDS-PAGE gel (Protean II, Bio-Rad) for separation in the second dimension. Proteins were visualized by silver nitrate staining.

Results

Enrichment of AtVTI1 Vesicles by Sucrose Gradient

The antibody raised against AtVTI12 can be purified from the serum by affinity purification through GST-AtVTI12 columns. The resulting AtVTI12 antibody recognizes both AtVTI11 and 12 as shown in Chapter IV. However, this purified antibody also recognizes other background proteins (Figure 5-1B, line2). The lack of detergents in the buffer required for purification of vesicles increased the background level. Thus, additional purification steps for reduction of the background were implemented. We separated total microsomes on a discontinuous sucrose gradient. After a short spin (100,000g for 3 hours), most microsomes were concentrated at the interphases between the different gradient steps. These microsomes were collected and examined by western. As shown in Figure 5-1, the interphase between 24 and 36% sucrose had the highest amount of AtVTI1. Moreover, the unspecific background was also dramatically reduced.

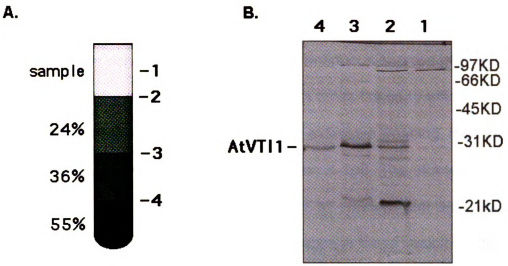

Figure 5-1. AtVTI1 vesicles were enriched though a step sucrose gradient. **A)** Scheme of the sucrose gradient used for enrichment of AtVTI1 vesicles. Total microsome (sample) was loaded on the step gradient with sucrose concentration of 24%, 36% and 55% from top to bottom. The microsomes were separated on the gradient by ultracentrifugation 100,000 *g* for three hours. The top (where the sample was loaded), and interphases between different steps were collected. **B)** Western blot of the fractions taken indicated in **A**. Equal amounts of proteins of different fractions were loaded on the SDS-PAGE. The AtVTI1 was visualized by western blot. Although AtVT12 antibody recognized many background bands as shown in fraction 2, which was from interphase between sample and the 24% gradient. Fraction 3, which was from the interphase of gradient 24% and 36%, enriched majority of the AtVTI1 vesicles with less background bands. Molecular weights are indicated at the right.

This enriched AtVTI1-containing membrane fraction was used as the starting material for affinity purification of AtVTI1 vesicles.

The Characterization of Affinity Purified AtVTI1 Vesicles

The AtVTI1 enriched fraction from the discontinuous sucrose gradient was passed through affinity columns containing beads cross-linked to affinity purified AtVTI12 antibody or pre-immnune antibody. After extensive washing, the vesicles retained on the beads were eluted with 1% Triton X-100. The eluates from the immune or preimmune columns were examined by western blot analysis with antibodies for markers that were expected to localize in those vesicles. Previous evidence suggests that sporamin is recruited by AtELP at the TGN and is transported into the vacuole via the PVC (Ahmed *et al.*, 2000). AtELP has been shown to colocalize with AtVTI11 (Zheng *et al.*, 1999) on the TGN and can also be found on the PVC membrane (Sanderfoot *et al.*, 1998). As shown in Figure 5-2, we detected AtVTI1, AtELP and sporamin in the detergent eluate from immune column but not from pre-immune column, indicating that we had successfully affinity purified AtVTI1 vesicles that contained all three markers. In contrast, Bip, an ER residential chaperone, was not present in the purified vesicle. Although 1% Triton X-100 should not dissociate the bond between the antibody and the antigen, some free AtVTI1 molecules may reside on the same membrane where other AtVTI11 molecules were bound to the antibody and account for the eluted AtVTI1. In the case of sporamin, multiple bands were observed, probably caused by changes in the glycosylation states of the protein. The 28 kDa band in the eluate from immune column is also slightly bigger than reported for mature

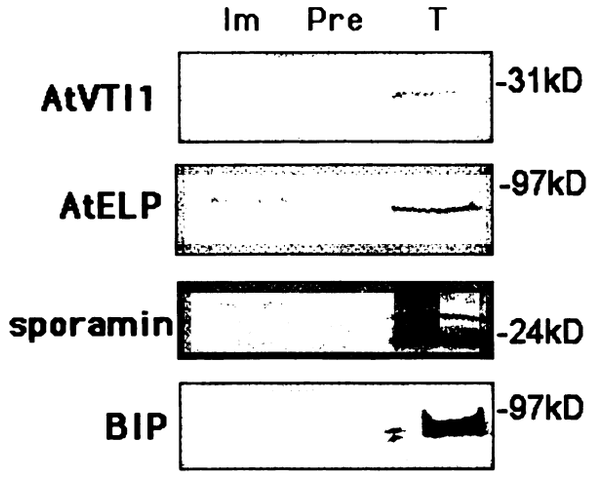

Figure 5-2. Characterization of affinity purified AtVTI1 vesicles. 1/1000 of total AtVTI1 enriched membrane fraction (T), 1/5 of eluate from pre-immune column (Pre) or 1/5 of Triton X-100 eluate from immune column (Im) were separated by SDS-PAGE. Different protein markers were visualized by western blots. Molecular weights were indicated at the right.

sporamin (24 kDa) or its precursor (26 kDa) (Matsuoka *et al.*, 1995b). Conceivably, the TGN or the PVC harbor a particular form of glycosolated sporamin. However, the exact nature of the larger molecular weight of the sporamin band needs to be examined more carefully before any conclusion can reached. The evaluation of the eluates from the immune and pre-immune columns indicated that intact AtVTI1 vesicles were purified using this procedure.

AtVTI11 and Sporamin Colocalize on an Area Close to the Golgi.

The N-terminal propeptide (NTPP) from sporamin has been shown to interact with AtELP *in vitro*. *In vivo*, AtELP and sporamin are found on the same domain of the TGN (Ahmed *et al.*, 2000). AtVTI11 also co-localizes with AtELP on the TGN (Zheng *et al.*, 1999). However, no direct evidence on the colocalization of sporamin and AtVTI11 was available. Here, I show that sporamin is present in purified AtVTI1 vesicles. To confirm the co-localization of sporamin and AtVTI1, an immunocytochemical experiment was performed using an *Arabidopsis* line that expresses both T7-AtVTI11 and sporamin (Figure 5-3). Thin plastic sections of root tips were used to carry out double-labeling experiment. Sections were first labeled with monoclonal anti-T7 antibody (Novagen) and detected with 10 nm gold, Subsequent to a second fixation and blocking step, the sections were incubated with anti-sporamin followed by detection with 5 nm gold. Representative photomicrographs are shown in Figure 5-4A-D. T7-AtVTI11 co- localizes with sporamin at the *trans*-Golgi and in other

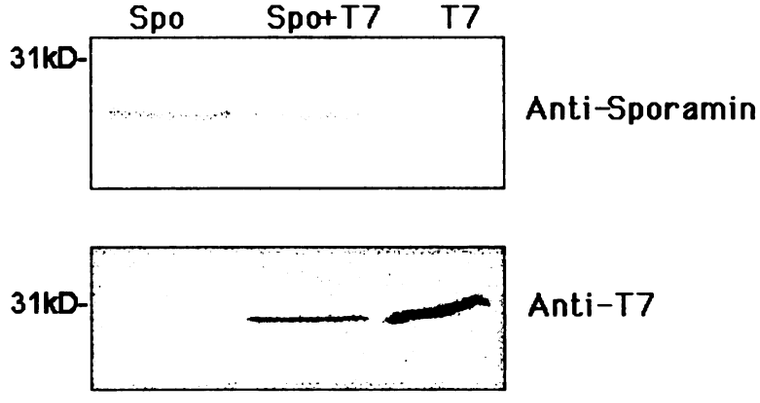

Figure 5-3. The plants crossed between transgeneic plant expressing T7-AtVTI11 and sporamin. Protein extracts from the parental plants expressing T7-AtVTI11 (T7) or sporamin (Spo) or the crossed progeny (Spo + T7) were separated by SDS-PAGE. Antibodies were used to detect T7-AtVTI11 or sporamin by western blots. Molecular weight was indicated at the left.

Figure 5-4. Immuno-localization of T7-AtVTI11 and sporamin on thin sections from *Arabidopsis* roots. Thin sections of root tips from transgenic plant expressing both T7-AtVTI11 and sporamin were first incubated with T7 monoclonal antibody followed by rabbit anti-mouse IgG and biotinylated goat anti-rabbit secondary antibody and were visualized with streptavidin conjugated to 10nm colloidal gold (arrow). After a second fixation step, the same sections were incubated with anti-sproamin antiserum and the bound antibody was visualized with protein-A conjugated to 5 nm colloidal gold (arrowheads). **A-D)** The colocalization of T7-AtVTI11 and sporamin at the structure near the Golgi (G). **E)** The predominant staining of sporamin in the vacuole (V). **F)** Control experiment where first antibodies against T7 or sporamin were omitted in the procedure. Ch: chloroplast. Bars represent 0.1 μm.

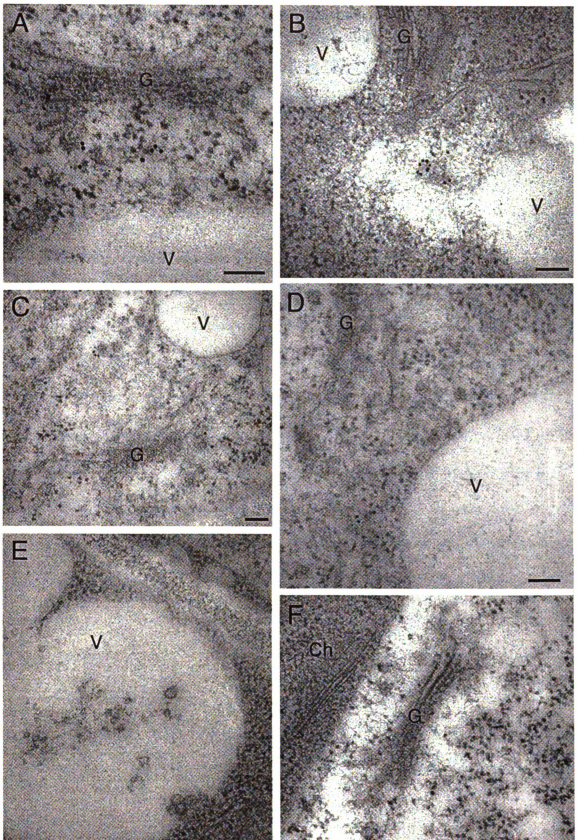
A
G
V
B
V
G
V
C
V
G
D
G
V
E
V
F
Ch
G

Table 5-1. Relative distribution of T7-AtVTI11 and sporamin in intracellular compartments of roots from transgenic *Arabidopsis*.

Outside of vacuole			Vacuole	
Together	Separately		T7-AtVTI11	Sporamin
	T7-AtVTI11	sporamin		
41	7	3	0	56

structures near the vacuole. Those structures resemble the ones where sporamin was found to co-localize with AtELP (Ahmed *et al.*, 2000). Sporamin also accumulates in the vacuole, but AtVTI11 does not reach the vacuolar membrane (Figure 5-4E). The statistics of the double labeling experiment are shown in Table 5-1. These results are consistent with the analysis of the affinity purified AtVTI1 vesicles. Taken together, these data indicates that the AtVTI1 family of proteins is involved in NTPP cargo transport.

Specific Proteins Can be Visualized by 2-D Gel and Silver Staining.

After purification of intact AtVTI1 vesicles from *Arabidopsis*, we undertook the identification of the protein content of those vesicles. The resolving power of SDS-PAGE was proven inadequate (Zheng and Raikhel, unpublished data). Thus, I separated the eluted proteins by 2-Dimensional gel electrophoresis and visualized the proteins by silver nitrate staining. Due to the low yield of the purification, the eluates from 5 isolations were pooled before loading. Comparing eluate from pre-immune and immune column, several spots were reliably determined to be specific to the eluate from the immune column in three different experiments (Figure 5-5). Due to the inherent limitations of the technique, large proteins or highly hydrophobic proteins may have been missed.

Discussion

We have determined the subcellular localization of AtVTI11 and 12, and the complexes they form with other SNAREs (Zheng *et al.*, 1999; Bassham *et al.*, 2000). However, functional data on the AtVTI1 family is still scarce. Here, I found

Figure 5-5. Representative 2-D gels showing protein profiles of affinity-purified AtVTI1 vesicles. From five affinity purification experiments, Triton-X 100 eluate from pre-immune (**A**) or immune (**B**) columns were pooled (about 100 μg protein). Samples were then separated by 2-D gel. Three pairs of gels were compared. The spots reproducibly present in the eluate of immune column but not in pre-immune column are indicated with circles.

rofiles of affinity-purifie
nts, Triton-X 100 elute
pooled (about 100 µ
hree pairs of gels we
of immune column

A:

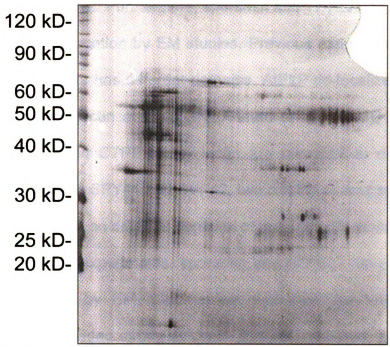

B:

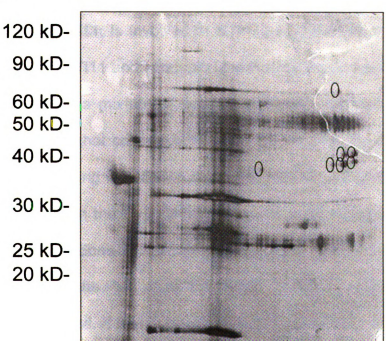

pH3>>>>>>>>>>pH10

that sporamin, an NTPP-containing protein, is present in the affinity purified AtVTI1 vesicles. Furthermore, sporamin and T7-AtVTI11 were found on the same subcellular location by EM studies. Previous experiments have shown that the TGN in plants has different domains. AtELP co-localizes with sporamin but not with barley lectin at the TGN (Ahmed *et al.*, 2000), suggesting that NTPP-sporamin and CTPP-barley lectin are recruited to different domains of the compartment. SPY41 and SYP42, two closely related syntaxin homologues, are also localized on different domains of the TGN (Bassham *et al.*, 2000). Although on separate experiments, sporamin and AtVTI11 have each been co-localized with AtELP by EM, biochemical and immunocytochemical methods taken together provided strong evidence that AtVTI11 also colocalizes with sporamin. These data also support the notion that at least one member of the AtVTI1 family, AtVTI11, is involved in NTPP cargo transport. However, it is not clear whether AtVTI11 and sporamin also co-localize on the PVC. The purified AtVTI1 vesicles are a mixture of vesicles from the TGN, the PVC, and maybe other membranes that contain AtVTI11 or 12. On EM, the PVC can be identified by immunolabeling with SYP2 antibodies. We have found that AtVTI11 and SYP2 co-localize on the PVC. Double labeling experiments with SYP2 and sporamin have to be done to test whether sporamin is transported to the PVC. The presence in the PVC of another NTPP-containing protein, *Arabidopsis* aleurain, will also tested. If that is the case, it will offer direct evidence that the PVC is the midstation for the biosynthetic pathway of NTPP-containing vacuolar cargo transport.

As mentioned above, the PVC contains the marker proteins SYP2, AtELP, AtVTI11, 12 as well as the recently identified syntaxins SYP5 and 6 (Sanderfoot *et al.*, 1998; Zheng *et al.*, 1999; Sanderfoot *et al.*, 2001). However, only SYP2 is exclusively localized in the PVC, whereas the other proteins can also be found on the TGN. Therefore the PVC appears to be closely related to the TGN. To further characterize the PVC and address its function we have undertaken the identification of its protein content. In recent years, great advances have been made in the techniques required for separation and identification of individual proteins in complex protein mixtures. The improved reproducibility of 2-D gel electrophoresis, the development of new mass spectrometry technologies and the complete genome sequence from several model organisms such as *Arabidopsis* allows the identification of proteins in high throughput fashion (review see Mann *et al.*, 2001). It is now possible to characterize all the protein species and their relative quantities within a given organelle at this so-called "proteomic" scale. This proteomic approach will be especially useful when characterizing novel organelles such as the PVC where molecular markers are scarce.

SYP21 is the only marker present exclusively on the PVC. However, the available SYP21 antibodies are not suitable for vesicle purification as the signal to noise ration is low (Sanderfoot and Raikhel, unpublished). Instead, we used AtVTI12 antibodies, which potentially would purify both AtVTI11 and 12 containing vesicles, due to the cross-reactivity of the antibody. The purified vesicles were genuine and intact based on the presence or absence of several

markers from which the intracellular localization is known. However, the identity of these vesicles needs further investigation. Firstly, we must establish whether they are a mixture of AtVTI11 and AtVTI12 vesicles. Secondly, as AtVTI11 and AtVTI12 are localized both on the TGN and the PVC, we need to show the origin of the purified vesicles. Once the proteins in the purified vesicles have been identified, their subcellular location needs to be studied before assigning them to either the TGN or the PVC.

In many cases, the amount of individual protein from purified AtVTI1 vesicles was lower than the limit of detection. When the sensitivity of the identification techniques increases, It may become possible to identify them. Alternatively, a novel approach to purify the PVC could be used. As shown in Figure 5-3, the amount of vesicles purified by the AtVTI1 antibody is low. The low yield may be due to the inherent nature of the antibody or to the conformation of AtVTI1 protein on the membrane that may prevent a higher affinity interaction with the antibody. Raising the scale of the purification would also increase the background level. As an alternative, antibodies against other markers on the PVC, such as SYP5 and SYP6, may be used (Sanderfoot *et al.*, 2001). Ultimately, the purification of the PVC and the characterization of its "proteome" will shed light into the function of this organelle.

References

Ahmed SU, Rojo E, Kovaleva V, Venkatarmam S, Dombrowski JE, Matsuoka K, and Raikhel NV (2000). The plant vacuolar sorting receptor AtELP is involved in the transport of NH2-terminal propeptides-containing vacuolar proteins in *Arabidopsis thaliana*. *J. Cell Biol.* **149:** 1335-1344.

Bassham DC, Sanderfoot AA, Kovaleva V, Zheng H, and Raikhel NV (2000). AtVPS45 complex formation at the *trans*-Golgi network. *Mol. Biol. Cell* **11:** 2251-2265.

Becherer KA, Rieder SE, Emr SD, and Jones EW (1996) Novel syntaxin homologue, Pep12p, required for the sorting of lumenal hydrolasese to the lysosome-like vacuole in yeast. *Mol. Biol. Cell* **7:** 579-594.

Conceição AS, Marty-Mazars D, Bassham DC, Sanderfoot AA, Marty F, and Raikhel NV (1997). The syntaxin homologue AtPEP12p resides on a late post-Golgi apparatus of *Saccharomyces cerevisiae Mol. Biol. Cell* **10:** 2407-2423.

Mann M, Hendrickson RC, and Pandey A (2001). Analysis of proteins and proteomes by mass spectrometry. *Annu. Rev. Biochem.* **70:** 437-473.

Marty F (1978). Cytochemical studies on GERL, provacuoles and vacuoles inroot meristematic cells of *Euphorbia*. Proc. *Nat. Acad. Sci. USA* **75:** 852-856.

Marty F (1980). High voltage electron microscopy of membrane interactions in wheat. *J. Histochemistry and cytochemistry* **28:** 1129-1132.

Matsuoka K, and Nakamura K (1991). Propeptide of a precursor to a plant vacuolar protein required for vacuolar targeting. *Proc. Natl. Acad. Sci USA* **88:** 834-838.

Matsuoka K, Bassham DC, Raikhel NV and Nakamura K (1995). Different sensitivity to wortmannin of two vacuolar sorting signals indicates the presence of distinct sorting machinery in tobacco cells. *J. Cell Biol.* **130:** 1307-1318.

Matsuoka K, Watanabe N, and Nakamura K (1995). O-glycosylation of a precursor to a sweet potato vacuolar protein sporamin, expressed in tobacco cells. *Plant J.* **8:** 877-889.

Peck SC, Nühause TS, Hess D, Iglesias A, Meins F, and Boller T (2001). Directed proteomics identifies a plant-specific protein rapidly phosphorylated in response to bacterial and fungal elicitors. *Plant Cell* **13:** 1467-1475.

Sanderfoot AA, Ahmed SU, Marty Mazars D, Rapopot I, Kirchhausen I, Marty F, and Raikhel NV (1998). A putative vacuolar cargo receptor partially

colocalizes with AtPEP12p on a prevacuolar compartment in *Arabidopsis* Roots. *Proc. Natl. Acad. Sci. USA* **95:** 9920-9925.

Sanderfoot AA, Kovaleva V, Bassham DC, and Raikhel NV (2001). Interactions between syntaxins identify at least five SNARE complexes within the Golgi/prevacuolar system of the *Arabidopsis*. *Mol. Biol. Cell* 12:

Zheng H, Fischer von Mollard G, Kovaleva V, Stevens TH, and Raikhel NV (1999). The plant vesicle associated SNARE AtVTI1a likely mediates vesicle transport from the *trans*-Golgi network to the prevacuolar compartment. *Mol. Biol. Cell* **10:** 2251-2264.

Chapter VI

Conclusions and Future Directions

Endomembrane system is critical for an eukaryotic cell. Vesicle transport is the major means for traffic flows between different membrane bound compartments where SNARE proteins are important players. However, until recently, most of the knowledge regarding the function of this system was acquired by studying single celled yeast or mammalian cell cultures. In vascular plants, the endomembrane system is evolved to suit plant specific challenges. For example, plant cells have developed complex vacuolar system that are composed of different types of vacuoles and multiple pathways to deliver proteins to these vacuoles. Different cells also need specialized membrane system for their particular functions. For example, it is very likely that the vacuolar protein transport system in developing cotyledon will be quite different from the one used by the guard cells. For SNARE genes, one single gene in yeast always found to have evolved into a family of one to five members in *Arabidopsis*. Plants also have novel SNAREs with no homologues in other kingdoms (Sanderfoot *et al.*, 2000). This phenomenon of gene duplications and novel genes reflects the complexity and uniqueness of the plant secretory machinery. The understanding of their specific features will facilitate our understanding of all aspects of plant life.

AtVTI1 is a family of SNARE proteins in *Arabidopsis* that have homologues in yeast and mammals. In yeast, Vti1p is a multi-functional SNARE encoded by a single gene. It has been found to interact with 5 out of 8 of yeast syntaxins (Götte and Fischer van Mollard, 1998). In *Arabidopsis*, VTI1 family is composed of three members. AtVTI13 is expressed in very low level and can not

be detected by northern analysis (data not shown). AtVTI11 and AtVTI12 are highly expressed and present in every tissue examined. Their amino acid sequences share about 65% identity. Cytosolic part of the protein was tagged with 6xHis tag and over-expressed in *E.coli*. These recombinant proteins were used to raise rabbit antisera. When these two anti-sera are carefully evaluated, I found that anti-AtVTI11 has higher affinity towards AtVTI11 protein, while anti-AtVTI12 recognizes both AtVTI11 and AtVTI12 to the same extent (Chapter IV). In addition, these two proteins can be distinguished by a slight molecular weight difference on western blot. Using anti-AtVTI11 in combination with transgenic plants expressing T7-tagged AtVTI11, I characterized AtVTI11 substantially (Chapter III). AtVTI11 is an integral membrane protein associated with several membrane fractions. It is localized on the Golgi, the TGN (*trans*-Golgi network) and the prevacuolar compartment (PVC). It co-localizes with AtELP, the NTPP cargo receptor, at the same domain of the TGN. It also physically interacts with SYP2 and 5 (Chapter II, IV). In a transgenic plant simultaneously expressing T7-AtVTI11 and sporamin, an NTPP vacuolar protein, these two proteins have been co-localized to the same organelles (Chapter V) by EM double immunolabeling. All these data suggest that AtVTI11 is involved in NTPP cargo transport from the TGN to the PVC.

Although *AtVTI11* and *12* are both expressed in most tissues of the plant with similar mRNA tissue distribution of pattern (Chapter III), they differ in several other aspects. When expressed in yeast, AtVTI11 can functionally replace yeast Vti1p in the transport step of carboxy-peptidase Y from the TGN to the PVC. On

the other hand, AtVTI12 is more efficient in facilitating the vacuolar transport of a membrane protein alkaline phosphatase (ALP) and in the cytosol-to-vacuole transport pathway (Chapter III). In plants, AtVTI11 forms complex with SYP2 and SYP5, while AtVTI12 with SYP4 and 6 (Bassham *et al.*, 2000; Sanderfoot *et al.*, 2000; Chapter IV). These two proteins also have distinct subcellular locations based on Accudenz density gradient (Chapter IV). AtVTI11 has been found to co-fractionate with SYP2 and SYP5, while AtVTI12 with SYP4 and SYP6. All these results suggest that these two VTI1 proteins have different functions in plant (summarized in Figure 6-1). A null mutant of *AtVTI12* (*Atvti12*) has been identified and characterized in detail in Chapter IV. Although this mutation caused the absence of AtVTI12, there is no observable phenotype different from wild type plants. This can be explained by the fact that SYP4 and 6 can be co-precipitated with AtVTI11 by anti-AtVTI11 antibody in *Atvti12* but not in the wild-type plant extracts. This substitution of AtVTI12 with 11 allowed the plant to perform its normal function without disturbance (Chapter IV). However, the function of AtVTI12 and the SNARE complex it being a part of remains unclear.

zig-1 (sgr-4) is an *Arabidopsis* shoot gravitropic defect mutant was identified from a pool of fast-neutron treated seeds (Fukaki *et al.*, 1996). Just recently, the gravitropic defect in *sgr-4* has been found to be due to a disruption in *AtVTI11* gene. *zig-1* has a DNA rearrangement that leads to a deletion from the 5th intron to downstream of *AtVTI11* gene. Inflorescence shoots and etiolated hypocotyl of *zig-1* failed to response to gravity and grow in random directions. (Yamauchi *et al.*, 1997; Kato *et al.*, 2001). Except occasional irregular sizes and

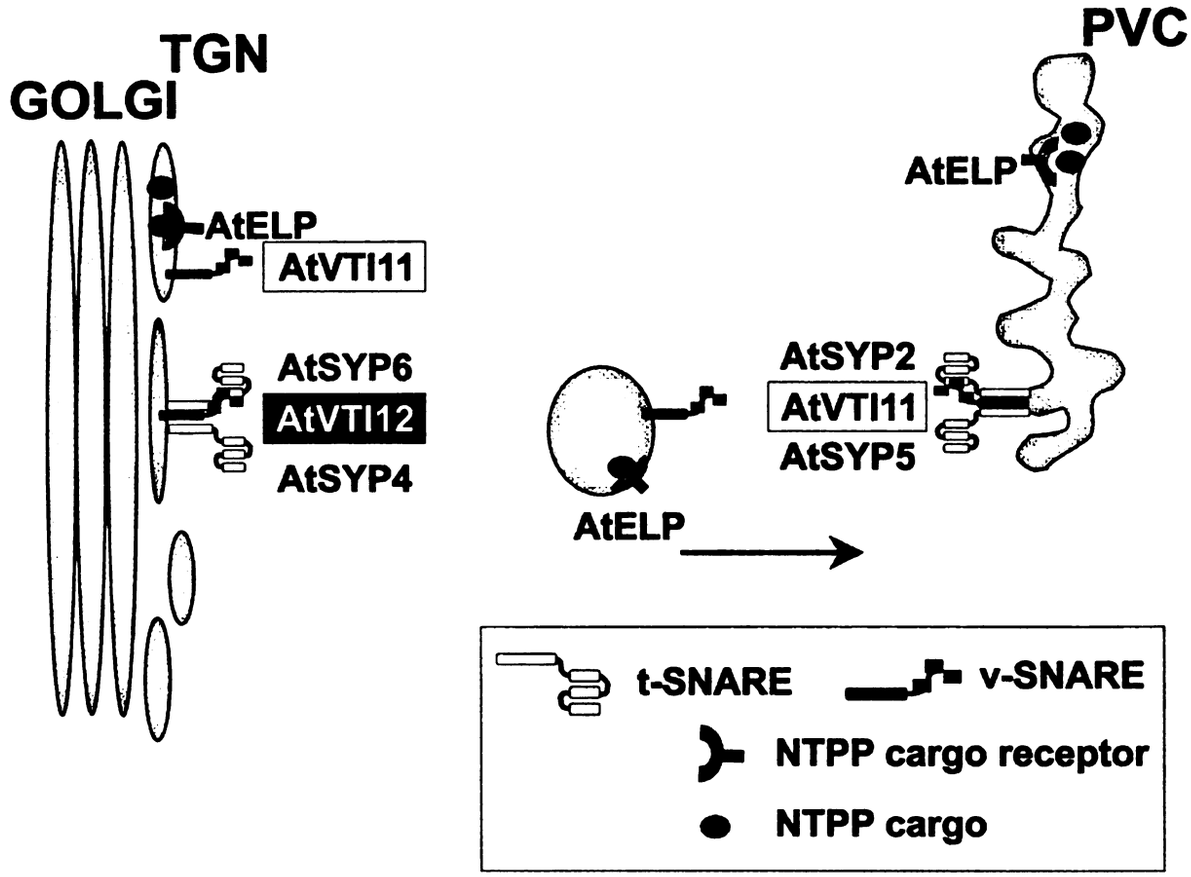

Figure 6-1. Schematic model for the AtVTI1 protein functions in plant cells. A diagram of the late secretory pathway between the Golgi and the PVC is shown. On the TGN, AtVTI11 is packaged into the vesicles together with NTPP cargo and AtELP. Once reach the PVC, AtVTI11 interacts with SYP2 and SYP5 to form a SNARE complex. This complex facilitates the fusion of vesicles and the PVC membrane and the NTPP cargo is delivered to the PVC. AtVTI12 is also found on the TGN. It interacts with SYP6 and SYP4. The significance of this SNARE complex is not clear. Presumably, it is involved in vesicles targeting to the TGN.

shapes of endodermal cells, this mutant has normal tissue organization in the stem with one epidermal cell layer, three cortex layers and one endodermal cell layer arranged in a concentric manner from the outside to the core. The amyloplasts, a special type of plastids containing starch granules, act as statolith for gravity sensing and sediment at the bottom in the direction of gravity (Sack 1997). They are located in Columbia cells of root caps and the endodermis or starch sheets of the shoots. In wild type plants, the amyloplasts are sedimented at the bottom and are able to move downward in response to the change of the gravity stimulation (Konings, 1995; Blancaflor, *et al.*., 1998). However, in *zig-1* mutant, they are localized on the top, the bottom and the side of the endodermal cells in the inflorescent stem and do not respond towards the directional change in gravity. The amyloplasts in Columbia cells of root cap are sedimented correctly, which correlates with the fact that the roots of *zig-1* respond to gravity normally (Kato *et al.*, 2001; Morita *et al.*, 2001). Beside the gravitropic defect, the shoots also elongate in zigzag fashion and the leaves are wrinkled and smaller than wild type plants (Yamauchi *et al.*, 1997). At the cellular level, besides the abnormal amyloplasts position in endodermal cell layers, aberrant vacuolar or vesicular structures are occasionally observed in the cytoplasm (Morita *et al.,* 2001). The fragmented vacuoles are observed in the epidermis of the hypocotyl using γ-TIP-GFP as a tonoplast visual marker (Dr. Morita, personal communication). This array of phenotypic abnormalities are complemented by reintroduction of the genomic fragment containing *AtVTI11* (MUL8.15; Kato *et al.*, 2001). The shoot gravitropic defect, but not the zigzag shape of the stems or

wrinkled and shrunken leaves, are also complemented by *AtVTI11* expressed under control of pSCR, an endodermis specific promoter (Kato et al., 2001). Besides *zig-1*, two other alleles of *zig* are also found to have gravitropic defect. *zig-2* is a complete deletion mutant and *zig-3* is a point mutant with a G151D point mutation. More recently, another shoot gravitropic mutant, *sgr-3*, is found to be attributed by a point mutation in *SYP22* gene (Dr. Tasaka, personal communication). It is likely the vesicle trafficking step of which AtVTI11 and SYP22 are involved in gravity sensing in stems.

The shoot gravitropism defect in *zig-1* may also be a second effect caused by abnormal vacuolar protein trafficking that leads to physical or chemical changes of the vacuole. Thus, the transport of vacuolar marker proteins should also be investigated in *zig-1* mutant. For example, the endogenous NTPP marker aleurain, carboxy-peptidase Y homologue, VPE (vacuolar processing enzymes) and other markers can be pulse-chase labeled in *zig-1* protoplasts to investigate their transport process. GFP-fusion markers for the study of vacuolar protein targeting have been developed rapidly. GFP-AtELP may be used to monitor the dynamics of vesicle transport between the TGN and the PVC. δ-TIP-GFP, a tonoplast marker (Cutler *et al.*, 2000) can be used for observe vacuolar morphology changes and vacuolar membrane protein transport. GFP fused to a C-terminal vacuolar sorting determinant (VSD) from tobacco chitinase A has been shown to be correctly targeted to neutral vacuolar compartment but excluded from lytic vacuoles in tobacco cells (Di Sansebastiano *et al.*, 1998). GFP fused with VSD from barley aleurain (an NTPP containing sequence) is

correctly delivered to the lytic vacuole (Di Sansebastiano, 2001). In tobacco and other species, vacuoles have been shown to regenerate from devacuolated protoplasts (Wu and Tsai 1992). In this system, the GFP fused with C-terminal or N-terminal VSD are targeted correctly to the neutral pH or lytic vacuoles respectively (Di Sansebastiano, 2001). Using this vacuole regeneration system in combination with GFP markers, we can start to study the vacuolar protein targeting in double mutants. From a different approach, vacuoles from *zig-1* should be compared with the ones from wild type plants. Vacuoles have been easily purified by flotation on a Percoll gradient (Gomez L, and Chrispeels MJ, 1993). The difference in metabolite profile can be compared by nuclear-magnet resonance (NMR) or GC (gas chromatography)-mass spectrometry. 2-D gel profiles or isotope-coded affinity tags (ICAT; Gygi *et al.*, 1999) treated samples followed by mass spectrometry can be used to access the vacuolar protein content changes. The phenotype of *zig-1* is not as severe as we assumed based on its role in the vacuolar protein transport. It is unlikely vacuolar proteins are completely blocked from entering vacuole as AtVTI12 is capable to substitute AtVTI11 (Zheng H, and Raikhel NV, unpublished). However, it is possible when both VTI1 proteins are absent, the transport will be dramatically changed. In the double mutant, there might be other phenotypes that are unrelated to gravitropism. In that case, the experiments mentioned above should be also used to evaluate the double mutant. The study in double mutant will yield rich information regarding the role of AtVTI family in the vacuolar protein transport and in the whole plant wellbeing. However, if the functions of AtVTI11 and 12 are

critical for the plant, it is possible that the double mutant will be lethal. In that case, *zig-3*, the point mutant of AtVTI1 should used to cross with *Atvti12*. It is more likely to yield viable plants that allow us to conduct meaningful analysis.

The correlation between vacuolar protein transport and the gravitropic signal perception is significant for us to understand endomembrane system at the whole plant level. The root and shoot gravitropism mechanism is related in the sense that both of them use amyloplasts indicator for gravity. The sedimentation of amyloplasts to the direction of the gravity induced certain unknown chemical signals that lead to redistribution of auxin and asymmetry growth (Sack 1997). Roots grow towards the direction of the gravity and the shoots grow in the opposite direction. If the vacuolar transport or homeostasis defect is related to amyloplasts sedimentation abnormalty and thus gravitropic defects in shoots, it is very likely similar mechanism also exists in roots. However, amyloplasts of *zig-1* roots are still able to sediment according to the direction of gravity and there is no gravitropic defect in roots (Morita *et al.*, 2001). Furthermore, in *zig-1* roots, we failed to find any abnormality in the Golgi and vacuolar morphology or the aleurain transport (Zheng H, Kovaleva V and Raikhel NV, unpublished results). Based on preliminary results, when AtVTI12 was immunoprecipitated from *zig-1* roots but not wild type roots, SYP21 and SYP22 were both co-precipitated. It is likely that AtVTI12 can substitute AtVTI11 in *zig-1* roots and interacts with both SYP21 and SYP22. The apparent normal roots may be the result of this substitution. It is imaginable that when the vacuolar transport in roots is also disturbed, the root gravity response might be reduced or diminished. It is thus

interesting to see the root gravitropism response in double mutant of *zig-1* and *Atvti12*. Of course, it is also possible that the mechanism of gravity perception in roots is different from shoots and does not require AtVTI11 or AtVTI12 functions.

The fact that *Atvti12* resembles the wild type while *zig-1* has abnormal phenotypes worth our investigation. In single mutants, both proteins seem to be able to form SNARE complexes with syntaxins that normally only interacts with the other one. It appears that the AtVTI11 is efficient at forming the complex with SYP4 and SYP6 and resulted in a normal plant in *Atvti12*. On the other hand, at least in stems, the complex AtVTI12 formed with SYP2 and 5 seems not enough for the proper function. One possible explanation is that there are three VTI1 genes in *Arabidopsis*. AtVTI13 is more closely related to AtVTI12 (75% identical) than to AtVTI11 (65% identical). *AtVTI13* expression level is significantly lower than the other two genes, and it can not be detected by anti-AtVTI12 antibody on western (the more general antibody). However, we can not rule out that AtVTI13 is expressed highly in certain cells or the very low level of protein is enough to functionally complement AtVTI12 in *Atvti12*. The gene expression pattern of these three *VTI1* genes should be investigated in more detail. Another explanation about the different phenotypes between *zig-1* and *Atvti12* lies in the difference between SYP2 and 4. SYP41 and 42 both are localized on the TGN but at different domains. It is possible AtVTI12 form complex with SYP41 and 42 to lead different vesicles recycling back to the TGN. As we know, AtVTI11 is localized on both the PVC and the TGN membrane. In *Atvti12*, AtVTI11 still has the opportunity to interacts with both SYP41 and SYP42 and fulfill the functions

of AtVTI12. The situation for SYP2 group syntaxins is different. In root tips, both SYP21 and SYP22 are found on the PVC (Sanderfoot *et al.*, 1999). The interaction between AtVTI11 and SYP2 may help vesicle trafficking from the TGN to the PVC. AtVTI12 is also observed on both the PVC and the TGN membrane in root tips. Thus, in the roots of *zig-1*, AtVTI12 may be able to transport vesicles from the TGN forward to the PVC by interacting with SYP21 and SYP22 and allows the roots grow without defect. However, in shoot meristem, SYP22 has been observed on small vacuolar membranes (Sato *et al.*, 1997). SYP22, but not SYP21, is also found to be enriched in vacuoles prepared from protoplasts of suspension cultured *Arabidposis* cells (Rojo E, and Raikhel NV, unpublished data). Because AtVTI12 does not travel beyond the PVC, it is not able to interact with SYP22 on the vacuole and stand in for AtVTI11 in that step of membrane fusion in shoot tissues of *zig-1*. To see if this model is true, we should consider the plant as truly a multicellular organism with different tissues and organs requiring different specialized cellular functions. Most information regarding the subcellular locations of the SNAREs is acquired by studying root tips. However, the locations of these SNAREs may be different in soil grown plants. Using gradient fractionation or immunocytochemistry, the subcellular localization of AtVTI11, AtVTI12, SYP21, SYP22, SYP41, and SYP42 should be revisited with tissue specificity in mind. Preliminary results indicate that on Accudenz gradient, vacuoles float on top of the gradient. AtVTI11 peak is shifted to lighter fractions in stems compares to the same experiment using root materials (data not shown). SYP21 and SYP22 have identical fractionation pattern in roots, but it will be

interesting to see whether SYP21 and SYP22 are localized differently in stems. To study the tissue specific expression pattern of these SNARE genes, promoter fused with GFP or GUS should also used to tranform *Arabidopsis*.

In our lab, there are several lines of T-DNA mutants of *AtELP* and other *VSR* (Vacuolar sorting receptor) genes. None of those mutants has no obvious phenotype (Avila-Teeguarden E, and Raikhel NV, unpublished results). Since AtELP is in the same pathway with the AtVTI11 in transport of NTPP proteins, it is possible other VSRs also have related functions. Thus, it will be interesting to examine the phenotype of those mutants with *zig-1* or *Atvti12*.

In general, the mutants of AtVTI11 and 12 offer good tools to understand the function of this family of SNAREs. They are also useful in our attempt to understand the roles they play in the endomembrane system and in the development and physiology of plants.

References

Blancaflor EB, fasano JM, and Gilroy S (1998) Mapping the functional roles of cap cells in the response of *Arabidopsis* primary roots to gravity. *Plant Physiol.* **116:** 213-222.

Cutler SR, Ehrhardt DW, Griffitts, JS, and Somerville CR (2001) Random GFP :: cDNA fusions enable visualization of subcellular structures in cells of *Arabidopsis* at high frequency. *Proc. Natl. Acad. Sci. USA* **97:** 3718-3723.

Di Sansebastiano GP, Paris N, Marc-Martin S, and Neuhaus JM (1998) Specific accumulation of GFP in a non-acidic vacuolar compartment via a C-terminal propeptide-mediated sorting pathway. *Plant J.* **15:** 449-457.

Di Sansebastiano GP, Paris N, Marc-Martin S, and Neuhaus JM (2001). Regeneration of a lytic central vacuole and of neutral peripheral vacuoles can be visualized by green fluorescent proteins targeted to either type of vacuoles. *Plant Physiol.* **126:** 78-86.

Fukaki H, Fujisawa H, and Tasaka M (1996) SGR1, SGR2, SGR3: novel genetic loci involved in shoot gravitropism in *Arabidopsis thaliana*. *Plant Physiol.* **110:** 945-955.

Gomez L, and Chrispeels MJ (1993). Tonoplast and soluble vacuolar proteins are targeted by different mechanism. *Plant Cell.* **5:** 1113-1124.

Götte M and Fischer von Mollard G (1998) A new beat for the SNARE drum. *Trends Cell Biol.* **8:** 251-218.

Gygi SP, Rist B, Gerber SA, Turecek F, Gelb MH, and Aebersold R (1999) Quantitative analysis of complex protein mixtures using isotope-coded affinity tags. *Nat Biotechnol* **17:** 994-999.

Kato T, Morita MI, Fukaki H, Yoshiro Y, Uehara M, Nihama M, and Tasaka M (2001) SGR2, a phospholipase-like protein, and ZIG/SGR4, a SNARE, are involved in the shoot gravitropism of *Arabidopsis* (Submitted).

Konings H (1995). Gravitropism of roots, an evaluation of progress during the last three decades. *Acta Bot. Neerl.* **44:** 195-223.

Morita MT, Kato T, Nagafusa K, Saito C, Ueda T, Nakano A and Tasaka M (2001). Involvement of the vacuoles of the endodermis in early process of shoot gravitropism in *Arabidopsis* (Submitted).

Sack FD (1997) Plastides and gravitropic sensing. *Planta* **203:** S63-S68.

Sanderfoot AA, Kovaleva V, Zheng H, and Raikhel NV (1999) The t-SNARE AtVAM3p resides on the prevacuolar compartment in *Arabidopsis* root cells. *Plant Physiol.* **121:** 929-938.

Sanderfoot AA, Assaad, FF, and Raikhel NV (2000), The *Arabidopsis* genome. An abundance of soluble N-ethylmaleimide-sensitive factor adaptor protein receptors. *Plant Physiol.* **124:** 1558-1569.

Sato MH, Nakamura N, Ohsumi Y, Kouchi H, Kondo M, Hara-Nishimura I, Nishimura K, Wada Y (1997). The atVAM3 encodes a syntaxin-related molecule implicated in the vacuolar assembly in *Arabidopsis thaliana*. *J Biol. Chem.* **272:** 24530-24535.

Wu FS, and Tsai YZ (1992) Evacuolation and enucleation of mesophyll protoplasts in self-generating Percoll gradients. *Plant Cell Environ.* **15:** 685-692.

Yamauchi Y, Fukaki H, Fujisawa H and tasaka M (1997). Mutations in the SGR4, SGR5 and SGR6 loci of *Arabidopsis thaliana* alter the shoot gravitropism. *Plant Cell Physiol.* **38:** 530-535.

MICHIGAN STATE LIBRARIES
3 1293 02305 5159